QA: NA

November 2003

Technical Basis Document No. 13: Volcanic Events

Revision 2

Prepared for:
U.S. Department of Energy
Office of Civilian Radioactive Waste Management
Office of Repository Development
1551 Hillshire Drive
Las Vegas, Nevada 89134-6321

Prepared by:
Bechtel SAIC Company, LLC
1180 Town Center Drive
Las Vegas, Nevada 89144

Under Contract Number
DE-AC28-01RW12101

EXECUTIVE SUMMARY

The possibility that volcanic activity could affect a repository at Yucca Mountain has been recognized since the site was identified in the late 1970s. The geologic and hydrologic setting of the southern Great Basin, which has many features that are favorable for waste isolation, is also characterized by ongoing low levels of seismic activity and geologically recent volcanic activity.

Volcanic activity in the Yucca Mountain region peaked between about 13 and 11 million years ago with the eruption and deposition of the silicic volcanic tuffs that form Yucca Mountain from caldera complexes in and near Timber Mountain. Since then, volcanic activity has declined to very low levels, with the last event occurring approximately 80,000 years ago at the Lathrop Wells Cone 18 km south of Yucca Mountain. The potential for future igneous intrusion or volcanic activity has been evaluated through an integrated approach utilizing information from geological, geophysical and geochemical investigations, and an expert elicitation and peer review. The mean probability of a future volcanic event intersecting a repository has been estimated to be on the order of 1.7×10^{-8} per year, or approximately one chance in 6,000 of occurring over the next 10,000 years. The sensitivity of the probability estimate has been tested through the consideration of a variety of alternative models and multiple lines of evidence. The probability estimate has been found to be robust. That is, it is unlikely that new information will lead to a substantive revision of the estimate, because uncertainties associated with the available information and models used to calculate the probability have been incorporated into the analysis.

The potential consequences of volcanic activity have also been evaluated. Although the likely styles of volcanic activity that could occur at Yucca Mountain are small in scale compared to the style and magnitude of events associated with large volcanoes such as Mount St. Helens or Mount Pinatubo, repository performance could be affected if volcanic activity intersected a repository. The physical processes and conditions associated with basaltic volcanism, and the potential effects of such activity on the integrity of the repository, have been evaluated. If basaltic magma intrudes into emplacement drifts, possible consequences could include damage to waste packages leading to eventual release of radionuclides to groundwater. An eruptive event through a repository could incorporate spent nuclear fuel or high-level radioactive waste into the volcanic ash ejected into the atmosphere. These possibilities have been incorporated into total system performance assessment calculations. Analyses to date have indicated that potential releases associated with these “disruptive events” are not likely to affect the repository’s ability to comply with the performance requirements specified in applicable regulations (40 CFR Part 197; 10 CFR Part 63).

INTENTIONALLY LEFT BLANK

CONTENTS

Page

CONTENTS (Continued)

Page

CONTENTS (Continued)

Page

INTENTIONALLY LEFT BLANK

FIGURES

Page

FIGURES (Continued)

Page

TABLES

Page

INTENTIONALLY LEFT BLANK

ACRONYMS AND ABBREVIATIONS

AIN	additional information need
AMR	analysis and model report
DOE	U.S. Department of Energy
IA	Igneous Activity
KTI	Key Technical Issue
LA	license application
NRC	U.S. Nuclear Regulatory Commission
PVHA	*Probabilistic Volcanic Hazard Analysis for Yucca Mountain, Nevada*
RMEI	reasonably maximally exposed individual
TSPA	total system performance assessment
TSPA-LA	total system performance assessment for the license application
TSPA-SR	total system performance assessment for the site recommendation

INTENTIONALLY LEFT BLANK

1. INTRODUCTION

Volcanism studies for the U.S. Department of Energy (DOE) Yucca Mountain Project began in 1979, and researchers from many organizations and universities, particularly Los Alamos National Laboratory, have conducted investigations in the Yucca Mountain region. DOE-sponsored investigations of volcanism in the Yucca Mountain region include: geological mapping; geophysical investigations; physical, petrological, geochemical, and geochronological investigations of the erupted materials; and numerical modeling of magma ascent through dikes and conduits and its eruption onto the surface as pyroclastic material and lava flows. The principal references describing this work are:

- *Yucca Mountain Site Description* (CRWMS M&O 2000a)
- *Probabilistic Volcanic Hazard Analysis for Yucca Mountain, Nevada* (CRWMS M&O 1996)
- *Dike/Drift Interactions* (BSC 2003a)
- *Characterize Eruptive Processes at Yucca Mountain, Nevada* (BSC 2003b)
- *Synthesis of Volcanism Studies for the Yucca Mountain Site Characterization Project* (CRWMS M&O 1998a)
- *Number of Waste Packages Hit by Igneous Intrusion* (BSC 2003c)
- *Igneous Intrusion Impacts on Waste Packages and Waste Forms* (BSC 2003d)
- *Characterize Framework for Igneous Activity at Yucca Mountain, Nevada* (CRWMS M&O 2000b; BSC 2003e).

The purpose of this technical basis document is to review what is known about volcanism in the Yucca Mountain region, and to show how this information has been used in probabilistic volcanic hazard analysis of disruption of the repository by a basaltic volcanic event. Risk is the product of hazard times consequence. Accordingly, the hazard and consequence analyses are used to evaluate the risk of volcanic disruption of the repository.

Note Regarding the Status of Supporting Technical Information–This document was prepared using the most current information available at the time of its development. This technical basis document and its appendices providing Key Technical Issue agreement responses were prepared using preliminary or draft information that reflect the status of the Yucca Mountain Project's scientific and design bases at the time of submittal. In some cases, this involved the use of draft analysis and model reports and other draft references whose contents may change with time. Information that evolves through subsequent revisions of the analysis model reports and other references will be reflected in the license application (LA) as the approved analyses of record at the time of LA submittal. Consequently, the Project will not routinely update either this technical basis document or its Key Technical Issue agreement appendices to reflect changes in the supporting references prior to submittal of the LA.

INTENTIONALLY LEFT BLANK

2. OVERVIEW OF VOLCANISM IN THE YUCCA MOUNTAIN REGION

Two major types of volcanism, explosive silicic volcanism followed by basaltic volcanism, have occurred in the Yucca Mountain region. The early period of Miocene silicic volcanism in the southwestern Nevada volcanic field culminated between 11.8 and 12.4 Ma with the eruption of four voluminous ash-flow tuffs of about 1,000 km^3 each (Sawyer et al. 1994). One of the silicic ash-flow tuffs that erupted from the Timber Mountain caldera complex (Figure 2-1) is the Topopah Spring Tuff, which forms the rock unit that will be used for waste emplacement. Yucca Mountain is a structurally uplifted, erosional remnant of these voluminous ash-flow tuff deposits. The hazards of silicic volcanism are considered to be negligible because of the absence of silicic activity in the Yucca Mountain region during the past 6 to 8 Ma (Crowe, Self et al. 1983, p. 261).

The early caldera-forming, silicic volcanism was approximately coincident with a major period of crustal extension, which occurred primarily between 13 and 9 Ma (Sawyer et al. 1994). The onset of basaltic volcanism in the Yucca Mountain region occurred during the latter part of the caldera-forming period of silicic volcanism, as extension rates waned, and small-volume basaltic volcanism continued into the Quaternary. In terms of eruption volume, the 15-million-year history of volcanism in the Yucca Mountain region is viewed as a magmatic system that peaked between 13 and 11 Ma, with the eruption of over 5,000 km^3 of ash-flow tuffs, and has been in decline since, with relatively minor volumes of basalt erupted since 11 Ma (CRWMS M&O 1998b, Figure 3.9-2). Approximately 99.9 percent of the volume of the southwestern Nevada volcanic field erupted by about 7.5 Ma with the eruption of tuffs from the Stonewall Mountain volcanic center, which is the last active caldera system of the southwestern Nevada volcanic field. The last 0.1 percent of eruptive volume of the volcanic field consists of basalt erupted since 7.5 Ma (CRWMS M&O 1998b, Figure 3.9-5). Considered in terms of total eruption volume and frequency of eruptions, basaltic volcanic activity in the Yucca Mountain region defines one of the least active basaltic volcanic fields in the western United States (e.g., CRWMS M&O 1998a, Chapter 4, Figure 4-2, for post–Miocene basalts of Crater Flat).

The earliest episode of basaltic volcanism in the Yucca Mountain region occurred between approximately 9 and 11 Ma and was closely associated with the waning of silicic, caldera-forming volcanism. Postcaldera basalts in the Yucca Mountain region can be divided into two episodes: Miocene (eruptions between approximately 9 and 7.3 Ma) and post–Miocene (eruptions between approximately 4.8 and 0.08 Ma). The time interval of about 2.5 million years between these episodes is the longest eruptive hiatus of basalt in the Yucca Mountain region during the last 9 million years (CRWMS M&O 1998a, Chapter 3, Table 3.1). This eruptive hiatus also marks a distinct shift in the locus of postcaldera basaltic volcanism in the Yucca Mountain region to the southwest (CRWMS M&O 1998b, Figure 3.9-6). The Miocene basalts and post–Miocene basalts are both temporally and spatially distinct. For assessing the future potential for volcanism, the past 5 million years (and especially the last 1 million years) are most relevant to hazard assessment at Yucca Mountain (CRWMS M&O 1996, Figure 3-62).

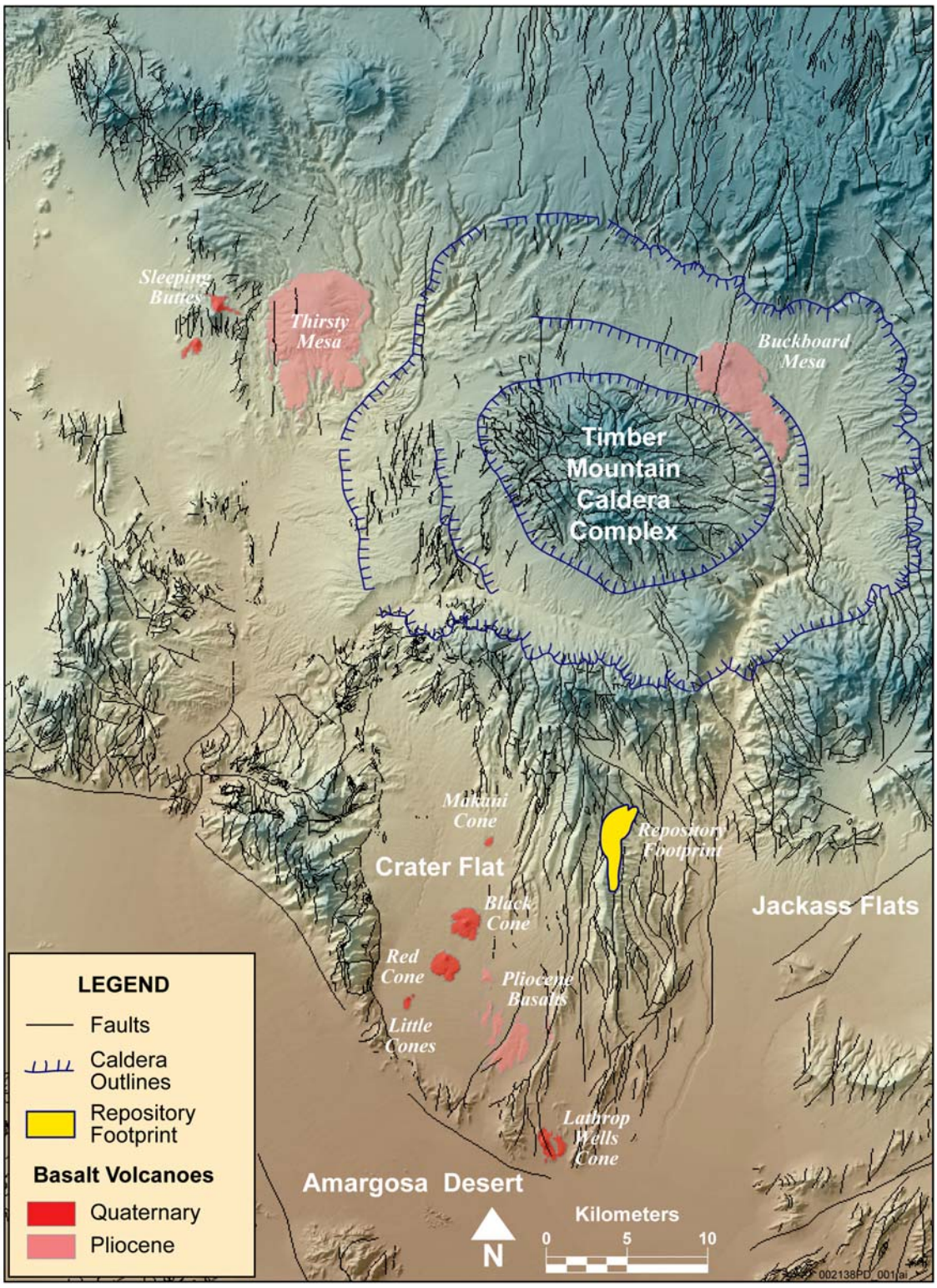

Source: CRWMS M&O 1998a, Chapter 2, Tables 2.B and 2.C; DTNs: LAFP831811AQ97.001; MO0003YMP98126.001 (both are used for reference only).

Figure 2-1. Locations and Ages of Post–Miocene (Less than 5.3 Ma) Volcanoes (or Clusters Where Multiple Volcanoes Have Indistinguishable Ages) in the Yucca Mountain Region

Post–Miocene basalts have erupted at several locations within 50 km of the repository (Figure 2-1). In order of decreasing age, these are the (1) basalt of Thirsty Mesa, (2) Pliocene Crater Flat and Amargosa Valley, (3) Buckboard Mesa, (4) Quaternary Crater Flat (i.e., Makani Cone, Black Cone, Red Cone and Little Cones), (5) Hidden Cone and Little Black Peak (the Sleeping Butte centers), and (6) Lathrop Wells. Three of these basaltic-vent groups are in or near the Crater Flat topographic basin, within 20 km of Yucca Mountain.

Several aeromagnetic anomalies in the Amargosa Valley south of Yucca Mountain have characteristics that indicate buried basaltic volcanic centers (Langenheim et al. 1993, p. 1,840). One of these anomalies (anomaly B of Langenheim et al. 1993) was drilled and basalt cuttings dated at 3.85 Ma using the $^{40}Ar/^{39}Ar$ method (CRWMS M&O 1998a, Chapter 2, Table 2.B). Because of the similarity in age to the 3.75 Ma Pliocene Crater Flat episode, the buried basalts of Amargosa Valley are considered likely to be part of the same episode.

The total eruption volume of the post–Miocene basalts is about 6 km^3. The volume of individual episodes has decreased progressively through time, with the three Pliocene episodes having volumes of approximately 1 to 3 km^3 each and the three Quaternary episodes having a total volume of only approximately 0.5 km^3 (CRWMS M&O 1998b, Figure 3.9-2; Table 3). The Quaternary volcanoes are similar in that they are of small volume (approximately 0.1 km^3 or less, Table 2-1) and typically consist of a single main scoria cone surrounded by a small field of *aa* basalt flows, which commonly extend approximately 1 km from the scoria cone.

The seven Quaternary volcanoes in the Yucca Mountain region (if Little Cones is counted as one volcano) occur to the south, west, and northwest of Yucca Mountain in a roughly linear zone defined as the Crater Flat Volcanic Zone (Crowe and Perry 1990, p. 328). Five of seven Quaternary volcanoes are in or near Crater Flat and lie within 20 km of the Yucca Mountain site (Figure 2-1). Models that attempt to relate volcanism and structural features in the Yucca Mountain region have emphasized the Crater Flat basin because of the volcanic centers within Crater Flat and its proximity to the repository (e.g., Smith, Feuerbach et al. 1990, p. 84; Connor and Hill 1995, p. 10,122).

2.1 STRUCTURAL CONTROLS ON BASALTIC IGNEOUS ACTIVITY

Evaluation of the likelihood of future igneous intrusion or volcanism at a specific location such as the repository requires knowledge of both the timing and the likely locations of potential activity. Basaltic centers in tectonic settings such as the southern Great Basin are fed by dikes that ascend from source regions in the subcontinental lithospheric upper mantle (Crowe, Self et al. 1983, p. 262). As they approach the surface, the dikes are typically 1 to 5 km in length. The location, length, and orientation of the dikes will directly affect the potential that they could intersect a repository.

2.1.1 Influence of the Crater Flat Structural Domain

Post–Miocene volcanoes in the Yucca Mountain region are spatially clustered (Crowe, Perry, Geissman et al. 1995, Chapter 3; Connor and Hill 1995, Figure 2). For probability models that incorporate clustering of volcanoes (Connor and Hill 1995) or specify volcanic source zones based primarily on the location or clustering of volcano centers (CRWMS M&O 1996),

estimation of the hazard to Yucca Mountain is often dominated by the presence of the Crater Flat cluster. This is due to the relatively high frequency and Quaternary age of volcanoes in the Crater Flat structural domain (including Lathrop Wells volcano, which lies within the domain and is the youngest volcano in the Yucca Mountain region) and the proximity of Crater Flat volcanoes to Yucca Mountain, compared to other volcano clusters in the Yucca Mountain region (Figure 2-1).

Table 2-1. Estimated Volumes and $^{40}Ar/^{39}Ar$ Ages of Quaternary Volcanoes in the Yucca Mountain Region

Volcano	Volume (km^3)[a]	Volume (km^3)[b]	Age (m.y.)[d]
Makani Cone	0.006		1.16−1.17
Black Cone	0.105	0.07	0.94−1.10
Red Cone	0.105		0.92−1.08
Little Cones	0.002	>0.01[c]	0.77−1.02
Hidden Cone	0.03		0.32−0.56
Little Black Peak	0.03		0.36−0.39
Lathrop Wells Cone	0.086		0.074−0.084

DTNs: LA0004FP831811.002; LAFP831811AQ97.001 (both are used for reference only).

NOTES: [a] CRWMS M&O 1998a, Chapter 3, Table 3.1, DTN: LA0004FP831811.002, except for Lathrop Wells Cone, from BSC 2003b, Table 9.
[b] Stamatakos et al. 1997, p. 327.
[c] Accounts for volume of buried flows detected by ground magnetic surveys.
[d] Range of ages from CRWMS M&O 1998a, Chapter 2, Table 2.B. Lathrop Wells ages (Heizler et al. 1999, Table 3) represent the range of plateau ages measured, except for sample LW157, a statistical outlier (DTN: LAFP831811AQ97.001).
$^{40}Ar/^{39}Ar$ dates provide the most complete and self-consistent chronology data set for Quaternary volcanoes of the Yucca Mountain region. A full discussion of other chronology methods used to date basaltic rocks in the Yucca Mountain region can be found in *Synthesis of Volcanism Studies for the Yucca Mountain Site Characterization Project* (CRWMS M&O 1998a, Chapter 2). Other chronology methods may not provide consistent or accurate estimates of the time of eruption.

2.1.2 Influence of Regional Stress on Dike Orientation

Together with faulting, magma intrusion is an important component of worldwide crustal extension (Parsons and Thompson 1991). Yucca Mountain lies within the southern Great Basin in the Basin and Range province, which is undergoing active ESE–WNW extension (Zoback and Zoback 1989). The state of stress in the Yucca Mountain region has been investigated using hydraulic-fracturing stress measurements, borehole breakouts, drilling-induced fractures, earthquake focal mechanisms and fault-slip orientations. A review of these data is given by Stock and Healy (1988).

Magma-filled fractures (dikes) will tend to strike orthogonal to the direction of the least compressive horizontal stress, and parallel to the direction of the greatest compressive horizontal stress (Pollard 1987). Most investigations give the orientation of the greatest compressive horizontal stress in the Yucca Mountain region as N30E ±15 degrees. Uncertainty in this orientation results from both inaccuracies in measurement and real variations in stress with depth and location, as observed, in breakout and drilling-induced fracture orientations, which vary by up to 40° in Yucca Mountain boreholes (Stock et al. 1985). By comparison, probabilistic

volcanic hazard analysis (CRWMS M&O 2000b, p. 102; BSC 2003e) suggests that the dike that intersects the repository will be oriented between N35E ± 25°, within the 90 percent confidence interval (between the 5th and 95th percentiles). This range is reasonable given the state of stress at Yucca Mountain and the uncertainty associated with it.

The Crater Flat structural domain as defined by Fridrich (1999, pp. 170 to 178) is a structural basin or graben. It is bounded on the west by the Bare Mountain fault and on the east by structures buried beneath Jackass Flats (Figure 2-2). Seismic reflection surveys show that the Crater Flat basin is deepest to the west (Brocher et al. 1998). It includes the Crater Flat topographic basin on the west and Yucca Mountain near the center of the structural domain (Figure 2-2). Because the repository lies within the Crater Flat structural basin, the structural and geophysical features of the domain, and the degree to which they influence the location of volcanism within the domain, have been key factors in conceptual models of volcanism for assessing hazards to the repository.

The following sections briefly describe the internal structure of the Crater Flat basin, as well as how the probabilistic volcanic hazards assessment (CRWMS M&O 1996) interpreted the influence of structural characteristics of the basin in estimating the locations of future volcanic events. Based largely on work published since 1996, the evidence that the northeastern and southwestern portions of the basin have different extensional histories that may have influenced the location of basaltic volcanism within the basin is summarized below.

2.1.3 Internal Structure and Boundaries of the Crater Flat Structural Domain

The Crater Flat structural domain includes the Crater Flat topographic basin (west of Yucca Mountain), Yucca Mountain, and the western part of Jackass Flats (Fridrich 1999, p. 174). Based on geologic mapping and interpretation of subsurface structures from geophysical surveys, the Crater Flat structural domain appears to be a single, westward-sloping, faulted basin (Figure 2-3). The western boundary of the Crater Flat basin and structural domain coincides with the Bare Mountain fault and its northward extension, which dips steeply (64º near the southern end) and can be imaged by seismic reflection to depths up to 6 km (Brocher et al. 1998). This major fault probably extends to the brittle-ductile transition in the middle crust. The northern boundary consists of a gradational termination of intrabasin structure at the perimeter of the Timber Mountain caldera complex (Fridrich 1999, p. 174).

The eastern and southern margins of the domain are not physiographically distinct but, rather, merge with adjacent portions of the Basin and Range. The eastern margin of the Crater Flat structural domain is probably a buried, down-to-the-west fault known as the Gravity fault (Fridrich 1999). The southern margin is inferred from gravity and magnetic data and from discontinuous outcrops to be a fault structure buried beneath young alluvium. It is typically drawn in a northwestern direction along the Amargosa Valley (Fridrich 1999, p. 176). Fundamental changes in the style, timing, magnitude of extension, and other deformation occur across all of the boundaries of the Crater Flat structural domain.

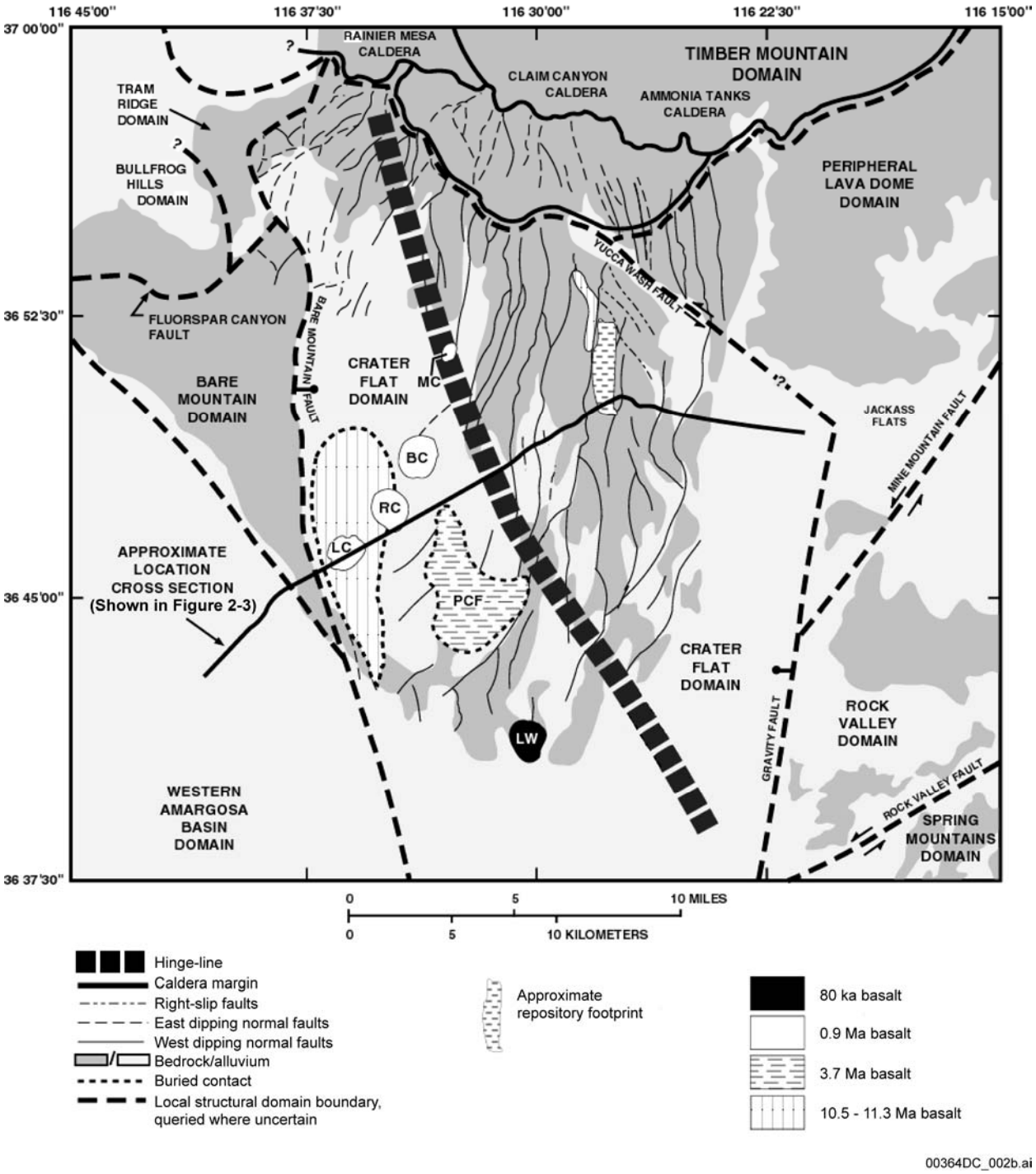

NOTE: Basalts of different ages are shown in relation to basin structure (modified from Fridrich et al. 1999, Figure 1). The 80-ka age of the Lathrop Wells volcano is from Heizler et al. (1999). MC = Makani Cone; BC = Black Cone; RC = Red Cone; LC = Little Cones; LW = Lathrop Wells volcano; PCF = Pliocene Crater Flat.

Figure 2-2. Local Structural Domains and Domain Boundaries of the Yucca Mountain Region and Internal Structures of the Crater Flat Basin and Selected Parts of Adjacent Domains

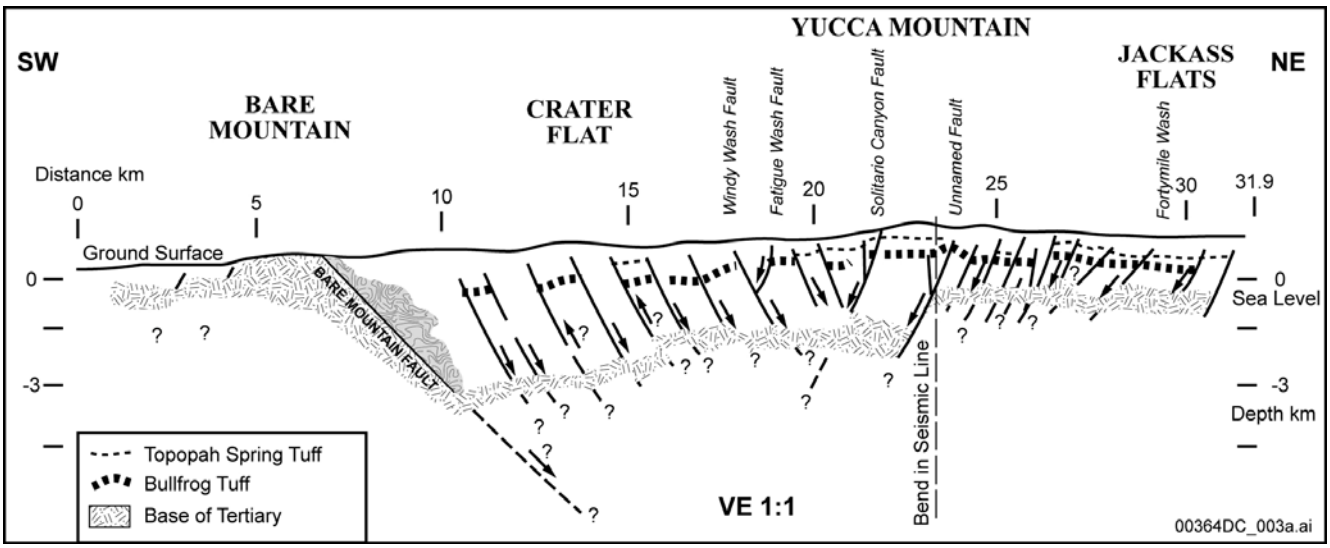

Source: Modified from Brocher et al. 1998.

NOTE: Location of cross section is indicated in Figure 2-2.

Figure 2-3. Schematic Cross Section of the Crater Flat Basin, from Seismic Reflection, Surficial Geology, and Borehole Information

2.1.4 Extensional History of the Crater Flat Structural Domain

Based on the strike directions of faults within the Crater Flat structural domain, a northwest-trending "hinge line" can be defined (Fridrich et al. 1999, p. 208) that separates an area of predominantly north-striking faults on the northeast from an area of predominantly northeast-striking faults on the southwest (Figure 2-2). The hinge line marks the approximate location of (1) the 20° contour of clockwise rotation of the Tiva Canyon Tuff, (2) a subtle yet abrupt decline in elevation to the southwest, and (3) an increase in Quaternary displacement for faults southwest of the hinge line (Fridrich et al. 1999, p. 208; Stamatakos et al. 1997, p. 327). These observations are consistent with a division of the Crater Flat structural domain into two parts, separated at the approximate position of the hinge line (Figure 2-2): (1) a northeastern, less extended part, and (2) a southwestern, more extended part (Fridrich et al. 1999, p. 208; Stamatakos et al. 1997, pp. 327 to 328).

2.1.5 Correlation with Volcanism

Basalts of the past 11 Ma in the Crater Flat basin have erupted in four episodes that together define a trend of progressively declining volume of magma erupted (Fridrich et al. 1999) (Figure 2-4).

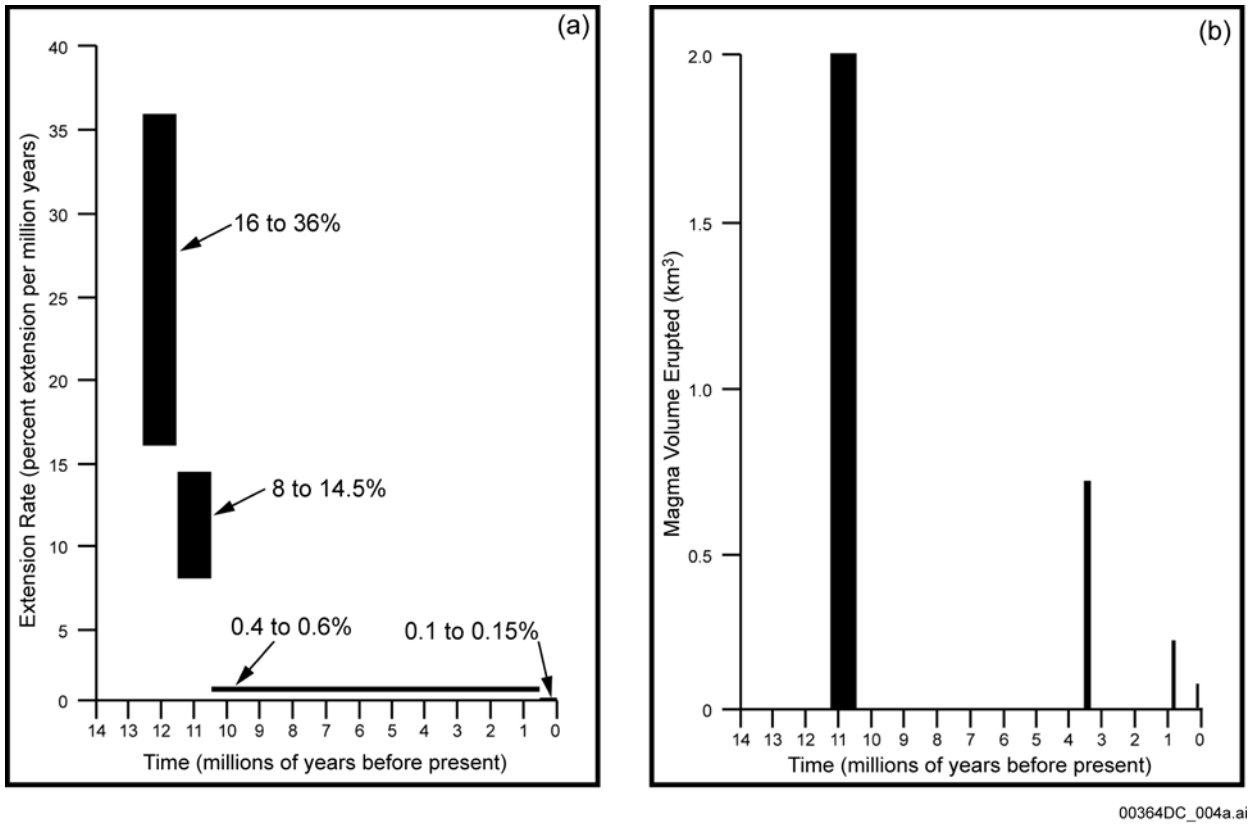

Source: Fridrich et al. 1999.

Figure 2-4. Estimated Extension Rates in Crater Flat Basin as a Function of Time and Magma Volume Erupted as a Function of Time

Vents for these eruptions form a northwest-trending belt across the southwest part of the basin, coincident with the strongest transtensional (lateral and extensional) deformation in the basin, suggesting that ascent of basalt through the crust is structurally controlled. The rates of extension and volcanism in the Crater Flat basin include initial peaks in the Miocene, followed by strongly declining patterns to the present. The similarity and approximate synchroneity of these trends suggest that they are reflections of a single phenomenon—a tectonic system that, at its peak, must have been among the most active zones of tectonism in the Great Basin, comparable to Death Valley today. The Crater Flat basin remains tectonically active, but is now in an advanced stage of decline. Existing data suggest that, within the overall declining pattern, extensional faulting has been cyclical, and that it has varied partly in concert with episodic volcanism in the Crater Flat basin (Fridrich et al. 1999).

The youngest volcano in the Crater Flat basin, the 80-ka Lathrop Wells volcano, lies between the southern ends of the Windy Wash and Stagecoach Road faults, the most active site of late Quaternary faulting in the Crater Flat basin (Fridrich et al. 1999, p. 211). There is a close spatial and temporal relationship between sites of extension and volcanism throughout the Crater Flat basin (Fridrich et al. 1999, p. 211). The occurrence of the three episodes of post–Miocene volcanism in the more extended, southwestern part of the Crater Flat basin suggests that volcanism is less likely to occur at Yucca Mountain, which lies outside of the transtensional zone, in an area where no post-Miocene volcanism has occurred (Fridrich et al. 1999). Other

geologic and geophysical studies provide corroborative evidence that areas of maximum extension in the southwestern Crater Flat basin correspond closely to volcanic source zones (CRWMS M&O 1996; Stamatakos et al. 1997; Brocher et al. 1998; Fridrich et al. 1999).

2.1.6 Relationship of Volcanic Source Zones to Crater Flat Structural Features and the Probability of Dike Intersection

The correlation between the structurally active part of the Crater Flat structural domain and sites of volcanism within the active part of the domain indicate that Yucca Mountain is near, but not within, a local volcanic zone that may produce small volumes of basaltic magma in the future (CRWMS M&O 1996, Appendix E, expert zone maps). Although the PVHA experts (Section 2.2) chose local volcanic source zones (Figure 2-5) based largely on the location of past volcanic events (CRWMS M&O 1996), the zones also correspond to the areas of highest cumulative extension and most active faulting in the Crater Flat basin (Fridrich et al. 1999). This association was recognized by several of the PVHA experts (CRWMS M&O 1996, pp. RC-5, BC-12, AM-3-5, GT-2). In the cases in which local zones were defined, they were limited to the southwestern portion of the Crater Flat basin, or were elongated, northwest-trending belts that included the southwestern portion. The local volcanic source zones excluded the northeastern portion of the Crater Flat basin, in which the repository is located. Given the close association of volcanism and extension, the eastern boundaries of local volcanic source zones separate more tectonically active and less tectonically active portions of the Crater Flat structural domain and are, therefore, reasonable predictors of the eastern extent of volcanism expected in the future.

In summary, the areas of greatest likelihood for future volcanic activity in the region are those where previous volcanism has occurred, and where extensional deformation has been and continues to be greatest, (i.e., the southwestern part of the Crater Flat structural domain) (Figure 2-5) (CRWMS M&O 1996, pp. RC-5, BC-12, AM-5, MS-2, GT-2, and expert zone maps). Analysis by the U.S. Nuclear Regulatory Commission (NRC) also indicates that the highest likelihood of future volcanic activity is in southwestern Crater Flat (Reamer 1999, Sections 4.1.5.4 and 4.1.6.3.3; Figure 28). The southern and southwestern part of the Crater Flat basin is the most extended (Ferrill et al. 1996; Stamatakos et al. 1997; Fridrich et al. 1999) and is the locus of post-Miocene volcanism (Fridrich et al. 1999; Reamer 1999, p. 47). Therefore, the volcanic source zones defined in the PVHA (CRWMS M&O 1996) (Figure 2-5) are consistent with the tectonic history and structural features of the Crater Flat structural domain.

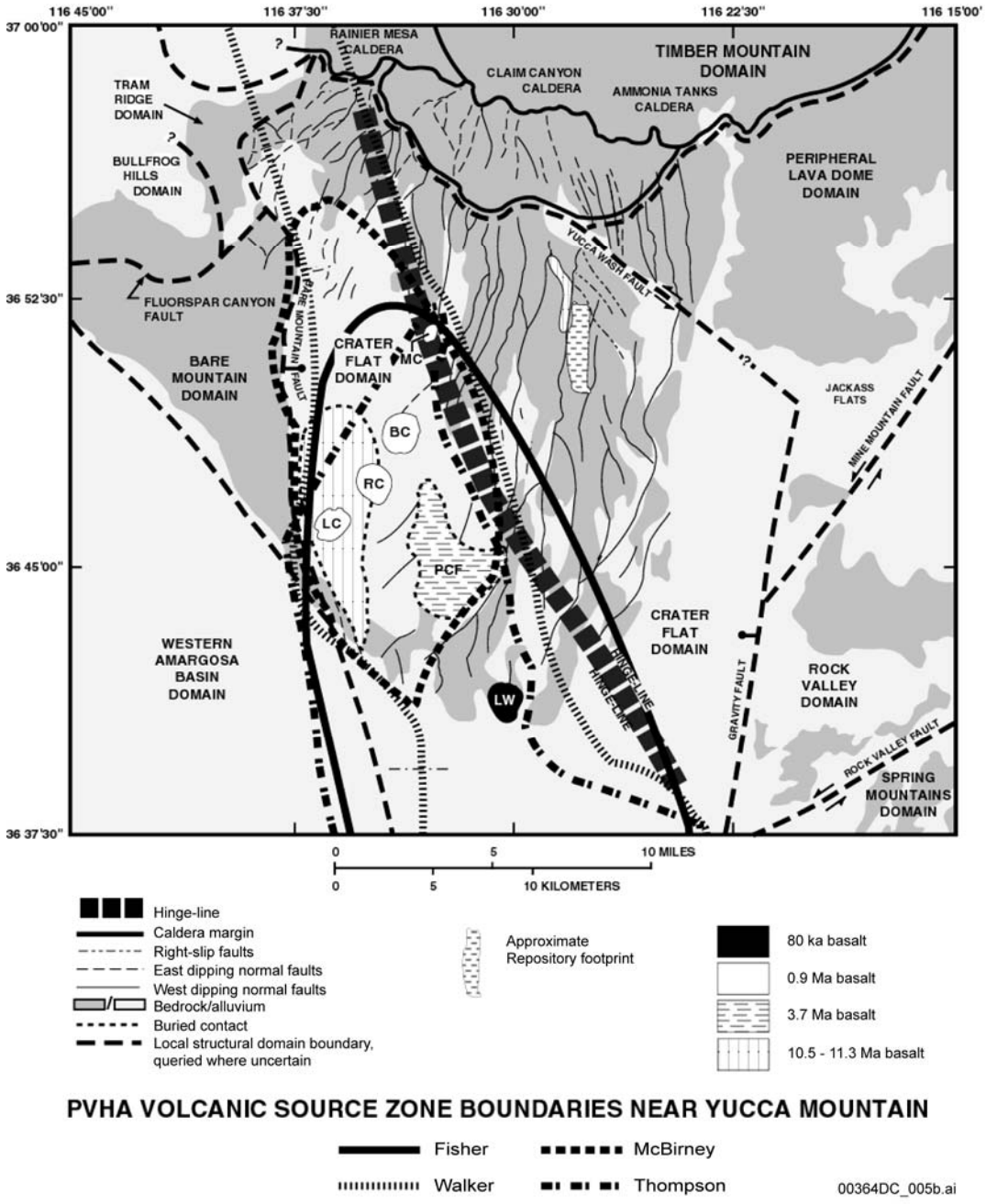

Source: DTN: MO0002PVHA0082.000 (for zone boundaries only).

NOTE: Superimposed on the Fridrich et al. (1999, Figure 1) map are boundaries of selected volcanic source zones (locally homogeneous spatial and temporal model, CRWMS M&O 1996, Section 3.13) that lie within the Crater Flat basin as defined by the PVHA experts (CRWMS M&O 1996, Appendix E). Other experts (not shown for clarity) used similar source-zone boundaries. MC = Makani Cone; BC = Black Cone; RC = Red Cone; LC = Little Cones; LW = Lathrop Wells volcano; PCF = Pliocene Crater Flat.

Figure 2-5. Local Structural Domains and Volcanic Source Zones of the Yucca Mountain Region

2.2 PROBABILISTIC VOLCANIC HAZARD ASSESSMENT

Volcanic hazard analyses have been conducted throughout the Yucca Mountain Project volcanism data-collection process (Crowe, Perry, Geissman et al. 1995; Crowe, Johnson et al. 1982; CRWMS M&O 1996). Results described in the volcanism synthesis report (CRWMS M&O 1998a, p. 6-14) show that 75 percent of Pliocene and Quaternary volcanic centers in the Yucca Mountain region occur in alluvial basins, 12.5 percent occur along range fronts, and 12.5 percent occur in range interiors (CRWMS M&O 1998a, Table 6.3). The distribution of past events indicates that a future volcanic event in the Yucca Mountain region is about six times more likely to occur in an alluvial valley or along a range edge than in a range interior such as the repository location in Yucca Mountain. Early analyses were preliminary assessments of disruption probabilities for the repository, and they also served to focus subsequent data collection toward information with greatest importance to the hazard assessment. The volcanic hazard assessment of Crowe, Perry, Geissman et al. (1995) provided a systematic, comparative analysis of published hazard models and methodologies; presented a range of possible results based on current knowledge and methods; and provided valuable insights into the sensitivities that the various approaches, models, and input parameters would have in the calculated results.

In 1995 and 1996, the DOE sponsored a probabilistic volcanic hazard analysis to assess the probability of a future volcanic event intersecting the repository at Yucca Mountain, and to explicitly characterize the uncertainties in the hazard analysis (CRWMS M&O 1996). This specific probabilistic volcanic hazard analysis is known as the PVHA. The analysis considered the data and insights from previous hazard assessments. To ensure that a wide range of approaches was considered in the analysis, 10 experts were selected. The use of multiple experts was part of an attempt to fully characterize uncertainties. Each expert played the role of an informed technical evaluator of data, rather than a proponent of a particular interpretation. On occasion, however, some experts were asked to present particular interpretations to facilitate discussion and the consideration of alternative interpretations. During the PVHA process, it was made clear that the purpose of the PVHA was to identify and understand uncertainty, not to eliminate it. It was also emphasized that the purpose was not necessarily to achieve consensus. Instead, disagreement was expected and accepted. The experts provided weighted alternative models and parameters, expressing their degree of belief that these were appropriate models and values. The panel included individuals with expertise in geology, geochemistry, and geophysics, and representing government agencies, universities and private industry. Following a series of workshops, field excursions, and other structured interactions between February and December 1995, the experts' evaluations were gathered in a deliberate elicitation process. Their evaluations were then combined to produce an integrated assessment of the volcanic hazard, an assessment representing the range of alternative scientific interpretations and uncertainties from the informed scientific community. The analysis expressed the volcanic hazard as the annual probability of intersection of the repository by a basaltic dike. This result, in turn, provides input to the assessment of volcanic risk, which is the product of hazard and consequence.

2.2.1 The Fundamental Basis of Volcanic Hazard Assessment

A principal assumption in the volcanic hazards analyses sponsored by DOE, including the 1996 PVHA, is that "the recent geologic past is the key to the future" (CRWMS M&O 1996). This

means that the record of volcanism, as revealed by geological and geophysical data from the area of interest and the geologic time period of interest, is the basis for assessing the probability of future volcanism. A validation of this paradigm was provided in the *Final Report of the Igneous Consequences Peer Review Panel* (Detournay et al. 2003, p. 10).

2.2.2 Temporal and Spatial Aspects of Probability Models

The uncertainty in modeling the spatial and temporal distribution of future volcanic events in the region surrounding Yucca Mountain was incorporated in the probabilistic volcanic hazards analysis using a logic tree methodology. Temporal models describe the frequency of occurrence of volcanic activity and include homogeneous and nonhomogeneous models. Many of the PVHA experts used homogeneous Poisson models to define the temporal occurrence of volcanic events, which assumes a uniform rate of volcanism based on the number of volcanic events that occurred during various periods in the past. Nonhomogeneous models were used by some experts to consider the possibility that volcanic events are clustered in time or to describe the possible waning or waxing of volcanic activity in the region during the period of time the experts considered to be relevant to hazard analysis.

Spatial models describe the spatial distribution (location) of future volcanic activity. The models most commonly used by the PVHA experts considered the future occurrence of volcanoes to be homogeneous within particular defined regions or "source zones" (CRWMS M&O 1996, Figure 3-62). Source zones were defined based on several criteria: the spatial distribution of observed volcanoes, especially post–5 Ma volcanoes; structurally controlled regions; and regions defined based on geochemical affinities, tectonic provinces, and other criteria. Nonhomogeneous parametric spatial distributions of future volcano occurrences were also modeled, (e.g., that the location of future volcanoes will follow a bivariate Gaussian distribution based on the location of volcanoes in Crater Flat). Finally, nonhomogeneous, nonparametric spatial-density models were used by some experts to assess the spatial distribution of future volcanoes. These models make use of a kernel density function and smoothing parameter based on locations of existing centers to obtain the spatial distribution for location of future volcanoes.

2.2.3 Probabilistic Volcanic Hazards Analysis Results and Uncertainty

The product of the PVHA was a quantitative assessment of the probability of a volcanic event intersecting the repository and the uncertainty associated with the assessment (CRWMS M&O 1996, Figure 4-32). Specifically, a probability distribution of the annual frequency of intersection of a basaltic dike with the repository footprint was defined. The contributions to uncertainty from each of the probabilistic volcanic hazards analysis components are described in the PVHA (CRWMS M&O 1996) and are shown in Figure 2-6. The analysis results indicated that the statistical uncertainty in estimating the event rate was the largest component of intra-expert uncertainty. The next largest uncertainty was uncertainty in the appropriate spatial model. Another important spatial uncertainty was the spatial smoothing distance. The temporal issues of importance included the time period of interest, event counts for Crater Flat, and the frequency of hidden events (buried volcanic events, or intrusive events that never reached the surface). Additional discussion of the potential effects of buried or hidden events is presented in Section 2.3.11.3. The variance for frequency of intersection defined by the composite distribution was disaggregated to identify the contributions from each of the sources of

uncertainty, including variability between the experts' interpretations (Figure 2-6). Most of the uncertainty in characterizing the hazard arose from uncertainty in an individual expert's assessment of the hazard (e.g., the likelihood that an event could occur at a given location or time), rather than differences in scientific interpretation between the experts (CRWMS M&O 1996).

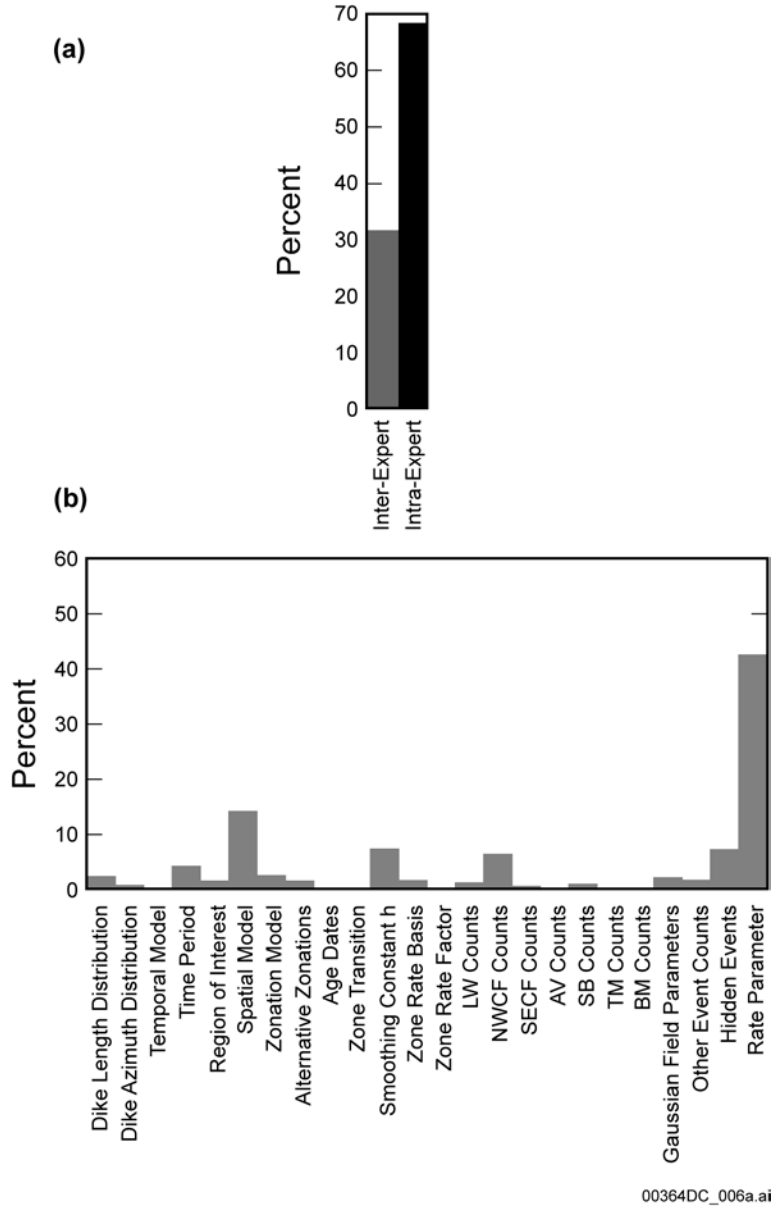

Source: CRWMS M&O 1996, Figure 4-33.

NOTE: (a) Comparison of inter-expert and intra-expert components, and (b) breakdown of intra-expert components of variance. LW = Lathrop Wells; NWCF = Northwest Crater Flat; SECF = Southeast Crater Flat; AV = Amargosa Valley; SB = Sleeping Buttes; TM = Timber Mountain; BM = Buckboard Mesa.

Figure 2-6. Relative Contribution of Uncertainty in Various Components of the Aggregate Probabilistic Volcanic Hazards Analysis Model to the Total Variance in Annual Frequency of Intersection

For the annual frequency of intersection of the repository footprint by a dike, each of the 10 experts independently arrived at a probability distribution that typically spanned approximately 2 orders of magnitude (CRWMS M&O 1996, Figure 4-31). From these individual probability distributions, an aggregate probability distribution for the annual frequency of intersection of the repository footprint by a dike was computed, reflecting the uncertainty across the entire expert panel. The individual expert's distributions were combined using equal weights to obtain the aggregate probability distribution (Figure 2-7).

The computed mean annual frequency of intersection of the repository footprint by a dike is 1.7×10^{-8} for the LA footprint as compared to 1.5×10^{-8} obtained in the PVHA (CRWMS M&O 1996, p. 4-10). The change is due to the revised size and configuration of the repository. The computed 5th and 95th percentiles of the uncertainty distribution for frequency of intersection are 7.4×10^{-10} to 5.5×10^{-8} (BSC 2003e, Section 6.5.3.1), respectively, as compared to 5.4×10^{-10} and 4.9×10^{-8} obtained in the PVHA (CRWMS M&O 1996, p. 4-10). The composite distribution spanned about three orders of magnitude for intersection frequency. The range in the mean frequencies of intersection for the individual expert's interpretations spanned about one order of magnitude (CRWMS M&O 1996).

The probability distribution arrived at in the PVHA accounted for hidden events by using a hidden-event factor ranging from 1 to 5 times the number of observed events, with most estimates in the range of 1.1 to 1.5 (CRWMS M&O 1996, Figure 3-62).

2.2.4 Consideration of Alternative Conceptual Models

The PVHA was an exercise in combining multiple alternative conceptual models into a single distribution, and expressed the uncertainty in the experts' conceptual models of volcanism in the Yucca Mountain region. The PVHA experts were also informed of alternative conceptual models during workshops and other structured interactions, and these were considered by the experts in formulating their own temporal and spatial models of volcanism. No single, principal conceptual model is appropriate in the area of volcanism, because the interplay of physical processes that control the precise timing and location of volcanic events within a particular region is not well constrained. The complexity of the processes and features that can influence volcanic events, and the relatively small number of events available for study, make characterization of the future hazard intrinsically uncertain.

Several alternative models not considered in the PVHA have emerged since the analysis was completed in 1996. These models are listed in Table 2-2 and their key assumptions and assessments of their impact on the results of the analysis are described. None of the alternative conceptual models identified would result in significant change in the PVHA results.

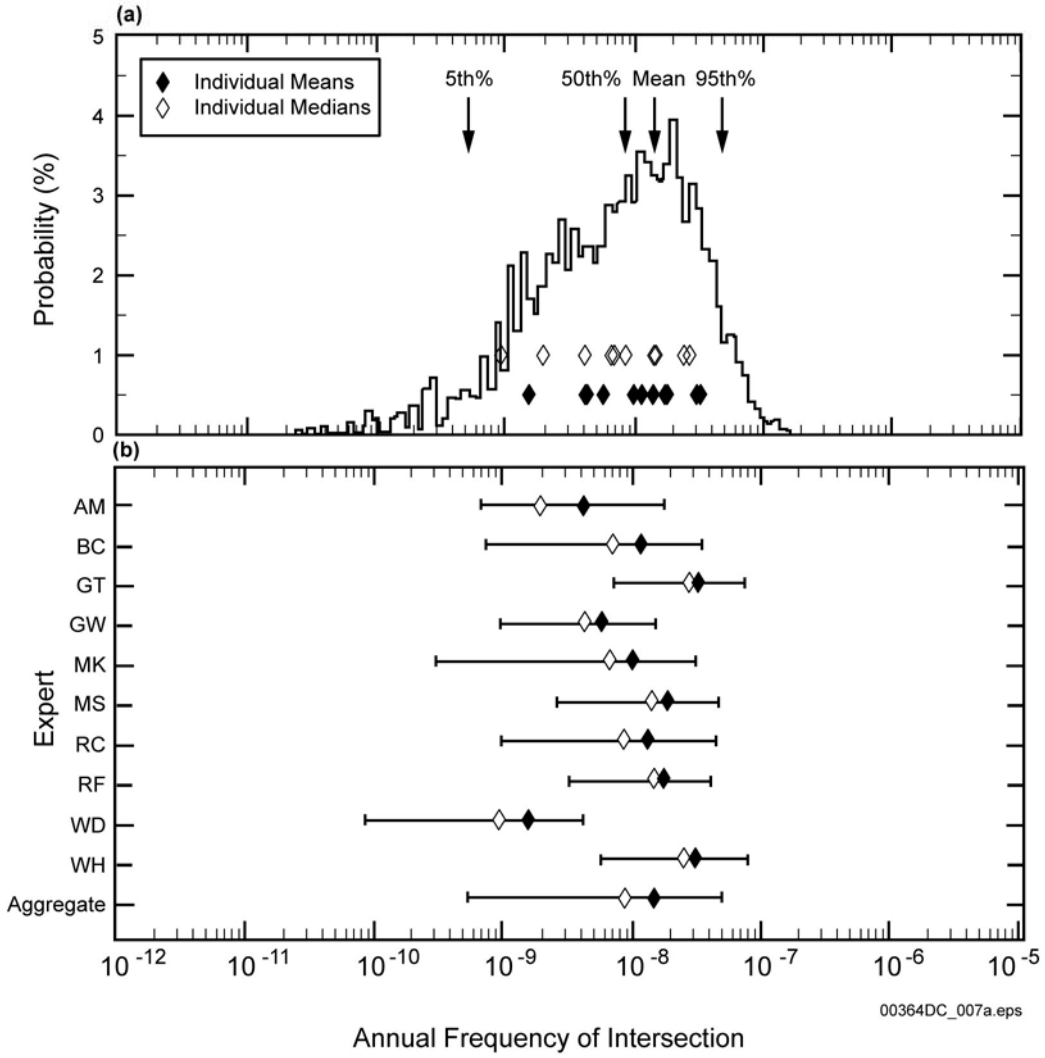

Source: CRWMS M&O 1996, Figure 4-32.

NOTE: (a) Aggregate distribution for frequency of intersection. (b) Individual and aggregate means, medians, and 90-percent confidence intervals (horizontal bars).

Figure 2-7. Aggregate Results for Frequency of Intersecting the Repository Footprint by a Volcanic Event

Table 2-2. Alternative Conceptual Models Not Considered in the Probabilistic Volcanic Hazards Analysis

Alternative Models	Key Assumptions	Assessment
Anomalous strain rate in the Yucca Mountain region (Wernicke et al. 1998)	Anomalously high current strain rate based on GPS measurements indicates volcanic event rate may be underestimated by factor of 10.	Not considered plausible based on later measurements from Savage et al. (1999) that show low strain rate as well as questionable assumptions about links between strain rate and volcanic event rate.
Mantle hotspot beneath the Yucca Mountain region (Smith, Keenan et al. 2002)	Anomalously high mantle basalt source temperatures lead to underestimation of future volcanic event rate.	Not considered plausible based on weight of documented scientific opinion showing that a mantle hotspot is not present beneath Yucca Mountain region; not consistent with waning Yucca Mountain region volcanism.
Tectonically weighted probability models (Connor, Stamatakos, Ferrill, Hill, Ofoegbu et al. 2000, p. 427)	Weighting of certain tectonic elements in probability models lead to probability estimates as high as 10^{-7}.	Not considered plausible based on observation that tectonically weighted probability models are poor predictors of location of volcanism in Yucca Mountain region.
Significant number of buried or undetected volcanic centers in the Yucca Mountain region (Hill and Stamatakos 2002)	Aeromagnetic anomalies suggest that significant number of volcanic events were unaccounted for in the probabilistic volcanic hazards analysis, underestimating the volcanic hazard.	Sensitivity studies documented in this report (see Section 2.2.5) show that the most conservative assumptions about event counts produce only a 40% increase in the mean annual frequency of intersection.

NOTE: See BSC 2003e for detailed discussion of assessments.

2.2.5 Significance of Buried Volcanic Centers on Probabilistic Volcanic Hazards Analysis Results

The event or recurrence rate is one of the fundamental parameters needed to estimate the volcanic hazard or the frequency of intersection of the repository by a future volcanic event. A key parameter for estimating event rates is an estimate of the number of volcanic events that have occurred in the Yucca Mountain region, particularly since the Miocene. The uncertainty in the event rate accounted for about 40 percent of the total intra-expert uncertainty (Figure 2-6) (CRWMS M&O 1996, Figure 4-33). The event rate depends on the number of events estimated for a particular time period and for a particular source zone, and can be expressed as events per year per square kilometer (CRWMS M&O 1996, p. 3-2). Since all post–Miocene volcanic centers having surface expression in the Yucca Mountain region have been identified, the only factor that could significantly change analysis results would be evidence not considered by the PVHA expert-panel members of a significant number of previously unidentified buried volcanic centers or intrusions. The significance of such buried volcanic centers on the probability of repository intersection by a basaltic dike would depend, in turn, upon (1) the geologic age of the buried event, because different weights are assigned to different time periods with more recent events being more heavily weighted; and (2) the distance and location relative to the repository, because basaltic dikes are assigned weighted lengths and azimuths and not all dikes will reach the repository.

Langenheim et al. (1993) presented data for aeromagnetic anomalies in Amargosa Valley and interpreted them as shallowly buried basaltic volcanic centers. Anomaly B was drilled, basalt was found in the drill cuttings, and the cuttings were dated at about 3.85 Ma (CRWMS

M&O 1998a, Table 2.1, sample well 25-1-BMC, and pp. 2-22 to 2-23). These data and interpretations were used by the PVHA experts (CRWMS M&O 1996, p. B-4).

The most common assessment among the PVHA experts of the number of volcanic events represented by the aeromagnetic anomalies in Amargosa Valley was 5, with slightly less weight assigned to 3, 4, and 6 events (CRWMS M&O 1996, Figure 3-63). The experts also applied a hidden-event multiplier, typically 1.1 to 1.5 times the number of volcanic events, to incorporate the possibility of undetected events; i.e., events not accounted for in the aeromagnetic data and the surface geology. The hidden-event multiplier typically resulted in an increase of 10 to 50 percent in the number of volcanic events over that computed from the observed or inferred volcanoes. This information is incorporated in the mean annual frequency of intersection obtained in the PVHA.

New data that could potentially change the assessment of the number of volcanic events in the analysis include ground magnetic surveys of aeromagnetic anomalies (Connor, Stamatakos, Ferrill, Hill, Magsino et al. 1996; Magsino et al. 1998). These magnetic data include surveys of 14 selected aeromagnetic anomalies located in the vicinity of the repository site (Magsino et al. 1998, Figure 1-1). Collectively, these surveys are a comprehensive assessment of aeromagnetic anomalies nearest the repository site and lend confidence that the geologic record of basaltic volcanism near Yucca Mountain is adequately understood. Of the 14 surveys, seven provide no evidence of buried basalt and three were conducted over areas with known surface exposures of basalt and partly to enhance understanding of the relationship between volcanism and geologic structure (Magsino et al. 1998, Section 4). Four of the 14 surveys provide evidence of buried volcanic centers. Two of these anomalies were known to the PVHA experts as possible buried basaltic volcanic centers (from the data of Langenheim et al. 1993; and Crowe, Perry, Geissman et al. 1995), but the data presented by Connor, Stamatakos, Ferrill, Hill, Magsino et al. (1996) and Magsino et al. (1998) provide increased detail and confidence in their volcanic origin. Of the two remaining surveys, anomalies in the Steve's Pass area on the southwest margin of Crater Flat are interpreted as buried basalt. Interpretation of a buried, reversely magnetized body of rock southwest of Northern (or Makani) Cone is less certain and may be either a basalt body or Miocene-age tuff (Magsino et al. 1998). Each of the four anomalies representing probable buried volcanic centers occur within volcanic source zones previously specified in the PVHA (CRWMS M&O 1996, Appendix E), except for the anomalies in the Steve's Pass area, which lie to the southwest of most volcanic source zones in a direction away from Yucca Mountain.

On the basis of evidence for buried volcanic centers presented by Connor, Stamatakos, Ferrill, Hill, Magsino et al. (1996), Brocoum (1997) described sensitivity analyses to assess the potential impact on the analysis results of increased event counts in Amargosa Valley and Crater Flat. Considering the PVHA method for assessment of event counts, particularly for northeast alignments of vents (as in the case of Amargosa anomaly F/G), the mean value for the number of buried volcanic centers was increased from the original PVHA value of 4.7 events to 6.1 events (Brocoum 1997). The mean annual frequency of intersection of a dike with the repository footprint was recalculated using the revised event count distributions, resulting in an increase in the mean annual frequency of intersection of 4 percent (Brocoum 1997). Given the uncertainty factored into the PVHA by assessment of alternative event counts and hidden-event factors, small changes in the event counts have an insignificant impact on the annual frequency of

intersection distribution derived from the analysis. A later sensitivity analysis (CRWMS M&O 1998a, Chapter 6, pp. 6-83 and 6-84) conservatively assumed that all known aeromagnetic anomalies in Crater Flat and Amargosa Valley were of Quaternary age (less than or equal to 1.8 Ma), rather than Pliocene. Using this assumption, the most likely number of Quaternary volcanic events near Yucca Mountain based on event counts was increased from 3.8 to 8 events. This increase in the Quaternary event count resulted in a disruption probability of approximately 2.5×10^{-8} per year (CRWMS M&O 1998a, Chapter 6, p. 6-84), a result not significantly different from the mean PVHA result of 1.5×10^{-8} per year (CRWMS M&O 1996, pp. 4-10, 4-14).

Four anomalies east of Yucca Mountain (Magsino et al. 1998, Figure 1-1) show no evidence of buried volcanic centers. This provides corroborative evidence that the volcanic source zones specified by the experts to the south and west of Yucca Mountain are a valid representation of the spatial distribution of post–Miocene volcanism in the Yucca Mountain region.

In 1999, the U.S. Geological Survey conducted a regional aeromagnetic survey for the purpose of assessing potential hydrologic pathways in the Yucca Mountain/Death Valley region (Blakely et al. 2000). Subsequent interpretation of these data indicated that as many as 20 to 24 aeromagnetic anomalies present to the west and south of Yucca Mountain could potentially represent buried basalt (O'Leary et al. 2002; Hill and Stamatakos 2002). Eight of these anomalies were recognized at the time of the PVHA (CRWMS M&O 1996). The effect of these potential buried volcanic centers on the results of the analysis was assessed and is described in Section 2.2.6.

2.2.6 Impact of 1999 Aeromagnetic Data on Frequency of Intersection

Anomalies observed in aeromagnetic and ground magnetic data gathered by the U.S. Geological Survey and the Center for Nuclear Waste Regulatory Analyses, respectively, since completion of the PVHA suggest that a number of basaltic volcanic centers could be buried beneath alluvium in Crater Flat and the northern Amargosa Desert (Blakely et al. 2000; O'Leary et al. 2002; Hill and Stamatakos 2002). Interpretation of these data indicates that 20 to 24 magnetic anomalies occur within Crater Flat and the northern Amargosa Desert that could represent buried basaltic volcanoes (O'Leary et al. 2002; Hill and Stamatakos 2002). Of these anomalies, eight were known at the time of the PVHA (CRWMS M&O 1996) from previous surveys and were considered as possible volcanic events as part of the analysis (Figure 2-8).

The effect of potential buried volcanic centers on the results of the analysis was evaluated using estimates of the ages of possible buried centers and an assessment of the likelihood that anomalies or groups of anomalies represent buried basaltic volcanic centers (BSC 2003e, pp. 113 to 118). The probable age range of potential buried volcanic centers was estimated using a range of calculated sedimentation rates in Crater Flat and the Amargosa Valley and the modeled depth of anomalies from O'Leary et al. (2002). Consideration of magnetic-polarity data adds another constraint. This approach leads to probable ages for the anomalies that range from 2.6 to 6.3 Ma (BSC 2003e, p. 114). All age ranges represent minimum ages and are therefore conservative for the purposes of volcanic hazard assessment.

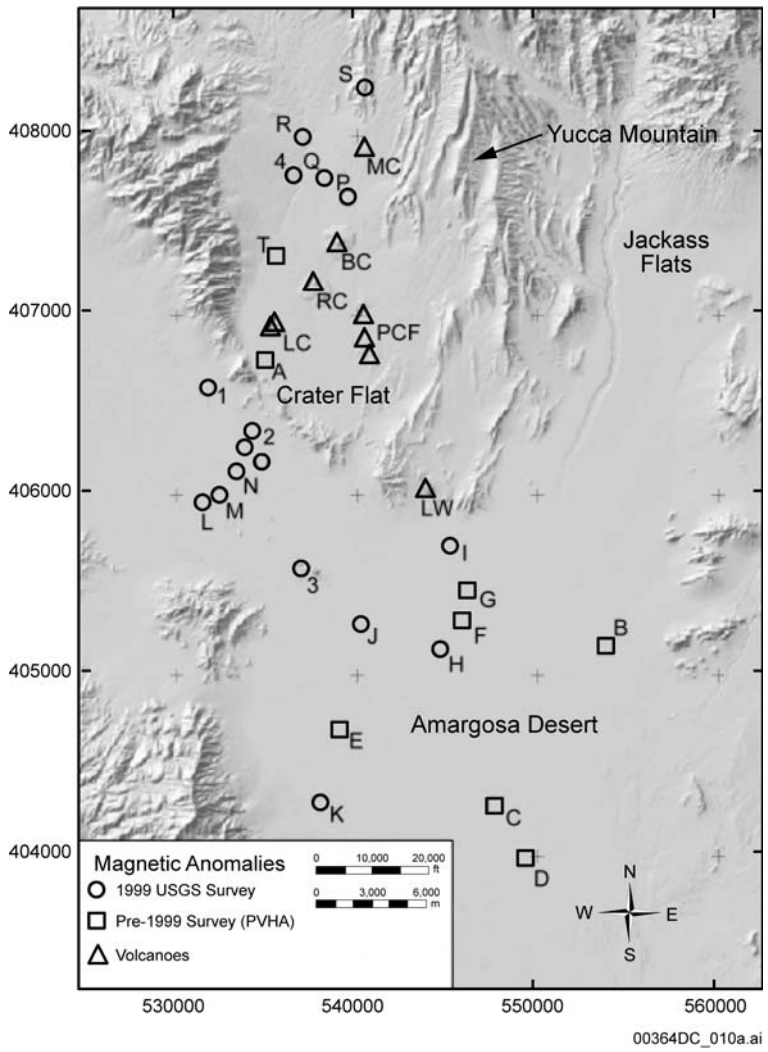

Source: BSC 2003e, Figure 24; coordinates from Hill and Stamatakos 2002.

NOTE: MC: Makani Cone, BC: Black Cone, RC: Red Cone, LC: Little Cones, LW: Lathrop Wells volcano. PCF: Pliocene Crater Flat. Magnetic Anomaly designations are from Hill and Stamatakos 2002

Figure 2-8. Locations of Potential Buried Basalt Inferred from Aeromagnetic Data

The potential impact of the aeromagnetic and ground magnetic data on the probability of igneous disruption of the repository was assessed by developing distributions for the number of volcanic events represented by the anomalies, assigning these events to the Crater Flat and Amargosa Valley volcanic source zones defined in the 1996 PVHA, assigning ages to the events, and calculating the annual frequency of intersection of the repository footprint (BSC 2003e, pp. 115 to 119). The distributions for the number of volcanic events were developed using the tendency of each expert to group aligned anomalies into single or multiple volcanic events. Two cases were developed. Case 1 is consistent with the PVHA approach, and factors the likelihood that the anomalies represent buried volcanic centers into the assessment of the number of volcanic events that have occurred. The distributions for the number of volcanic events represented by the magnetic anomalies for Case 1 were developed using the qualitative likelihoods that the anomalies represent buried volcanic centers and using each expert's tendency for including

anomalies with various levels of confidence into their distributions for volcanic events. In Case 2, all anomalies were assumed to be buried volcanic centers, and the distributions for the number of volcanic events were developed on the basis of each expert's tendency for grouping aligned volcanic centers into events.

In Table 2-3, the volcanic-event-count distributions developed for sensitivity Case 1 result in a 22 percent increase in the mean annual frequency of intersection, and those for sensitivity Case 2 result in a 40 percent increase. The increase in the frequency of intersection is less than the increase in the mean number of volcanic events because the additional events are located in the volcanic source zone to the west of the site.

Table 2-3. Summary of Computed Frequency of Intersection from Sensitivity Cases 1 and 2 for 70,000-MTU No-Backfill Repository Layout

Input Parameters	Annual Frequency of Intersection			
	5th percentile	50th percentile	Mean	95th percentile
1996 Probabilistic Volcanic Hazards Analysis	7.9×10^{-10}	9.8×10^{-9}	1.6×10^{-8}	5.2×10^{-8}
Sensitivity Case 1	7.8×10^{-10}	1.0×10^{-8}	1.9×10^{-8}	6.5×10^{-8}
Sensitivity Case 2	7.9×10^{-10}	1.1×10^{-8}	2.2×10^{-8}	7.6×10^{-8}

Source: BSC 2003e, Table 21.

NOTE: The repository layout used in this calculation includes both primary and contingency blocks of a preliminary design different from the LA footprint used in calculation presented in Table 2-5.

2.2.7 Alternative Estimates of the Intersection Probability

Several alternative estimates of the intersection probability (the annual probability of a volcanic event intersecting the repository footprint) were presented between 1982 and 1998 (Table 2-4). Volcanic events in hazard calculations have been represented as both points and lines. For point events, volcanic source zone areas or the repository area have generally been increased to account for the fact that volcanic events have dimension due to the length of associated dikes. Calculations that incorporate dike length become more comparable to calculations representing volcanic events as points, as dike lengths decrease. Intersection probabilities near 10^{-7} intersections per year (Ho and Smith 1998, pp. 507 to 508; Reamer 1999, p. 61) reflect unusually small volcanic source zone areas or unusually long event lengths.

Most of the published intersection probabilities, including the mean intersection probability estimated in the PVHA (CRWMS M&O 1996), cluster at values slightly greater than 10^{-8} per year, indicating that this probability estimate is robust, given the range of alternative temporal and spatial models and event geometries considered in the probability calculations.

Table 2-4. Published Estimates of the Probability of Intersection of the Repository at Yucca Mountain by a Volcanic Event

Reference	Intersection Probability (per year)	Comment	Event Representation
Crowe, Johnson et al. 1982, pp. 184 to 185	3.3×10^{-10} to 4.7×10^{-8}	Range of alternative probability calculations	point
Crowe, Perry, Valentine et al. 1993, p. 188	2.6×10^{-8}	Median value of probability distribution	point
Connor and Hill 1995, pp. 10, 121	$1–5 \times 10^{-8}$	Range of 3 alternative models	point
Crowe, Perry, Geissman et al. 1995, Table 7.22	1.8×10^{-8}	Median value of 22 alternative probability models	point
Ho and Smith 1998, pp. 507 to 508	(1) 1.5×10^{-8}, (2) 1.09×10^{-8}, 2.83×10^{-8}, (3) 3.14×10^{-7}	3 alternative models; 3rd model assumes a spatial intersection ratio (using a Bayesian prior) of 8/75 or 0.11, approximately one order of magnitude higher than other published estimates, because volcanic events are forced to occur within a small zone enclosing Yucca Mountain	point
CRWMS M&O 1998a, Chapter 6, p. 6-84	2.5×10^{-8}	Sensitivity analysis that conservatively assumes all aeromagnetic anomalies in Amargosa Valley are Quaternary age	point
Connor, Stamatakos, Ferrill, Hill, Ofoegbu et al. 2000, p. 427	10^{-8} to 10^{-7}	Value of 10^{-7} assumes maximum event length of 20 km, regional recurrence rates of 5 events/m.y., and that crustal density variations contribute to event location.	line

Source: BSC 2003e, Table 13.

2.2.8 Definitions and Parameters of a Volcanic Event and Implications for Probability Calculations

An important issue in the PVHA and in alternative volcanic hazard assessments of the repository is the definition of a "volcanic event." The definition of a volcanic event can affect the outcome of probability calculations and must be clearly understood to meaningfully compare the results of alternative probability calculations. The PVHA experts defined a volcanic event to be a spatially and temporally distinct batch of magma ascending from the mantle through the crust as a dike or system of dikes (CRWMS M&O 1996, Appendix E). The physical manifestation of a volcanic event includes the dike or dike system, and any surface eruption deposits. For the purposes of probability models here, a volcanic event is defined as a point in space representing the expected midpoint of the dike system involved in the magma ascent. The dike system associated with the volcanic event is represented in the probability model by a line element defined in terms of a length, azimuth and location relative to the point event (Figure 2-9). The term 'dike length' used in the PVHA and in this report when discussing volcanic events refers to the total length of the dike system associated with the volcanic event. The phrase 'intersection of the repository footprint by a dike' refers to intersection of the emplacement area of the repository by the line element representing the dike system associated with the volcanic event. The possibility that a dike system has width or consists of multiple parallel dikes does not significantly affect the intersection probability and is not part of the hazard calculations. The width of the dikes and the number of parallel dikes does affect the consequences of an intersection, is incorporated into the igneous intrusion scenario presented in *Number of Waste Packages Hit by Igneous Intrusion*

(BSC 2003c), and is discussed in Sections 5.2 through 5.4. Although the PVHA analysis considered volcanic events to have both an extrusive and intrusive component (volcano and dike), the output of the PVHA was the annual frequency of intersection of the repository by an intrusive basaltic dike (CRWMS M&O 1996). The PVHA analysis did not calculate the conditional probability that a dike intersecting the repository would result in an extrusive volcanic eruption through the repository.

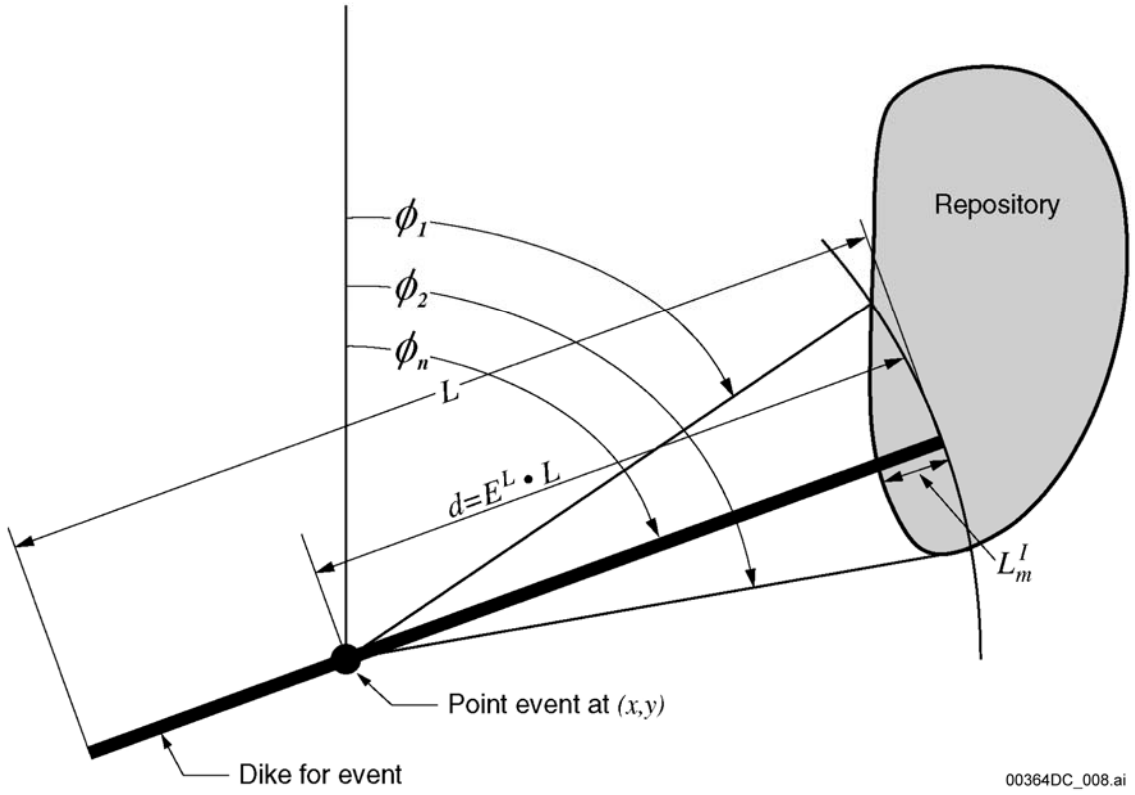

Source: BSC 2003e, Figure 12.

NOTE: L is dike length, L^I and Φ are the length and azimuth, respectively, for that portion of an intersecting dike within the repository footprint; L^i_m and Φ_n are specific bins of intersection length and azimuth; Φ_1 and Φ_2 define the range of azimuths over which a dike extending distance d from a volcanic event at (x,y) will intersect the repository footprint

Figure 2-9. Definition of Parameters Used to Compute the Probability of Intersection of the Repository Footprint by a Volcanic Event

The PVHA represented volcanic events as having both length and orientation. Typical dike dimensions assigned by the experts were a dike width of 1 m and a dike length (the total length of the dike system associated with a volcanic event) of 1 to 5 km (CRWMS M&O 1996, Appendix E, Figure 4). The most likely values for maximum dike lengths were estimated to be in the range of 17 to 22 km (CRWMS M&O 1996, Figure 3-62). The values of maximum dike length represent tails of distributions that have a small impact on the probability of dike intersection. The aggregate dike-length distribution derived from the PVHA has 5th-percentile, mean, and 95th-percentile values of 0.6, 4.0, and 10.1 km, respectively (Figure 2-10). The most commonly assigned dike orientation centers around N30°E (CRWMS M&O 1996, Figure 3-62).

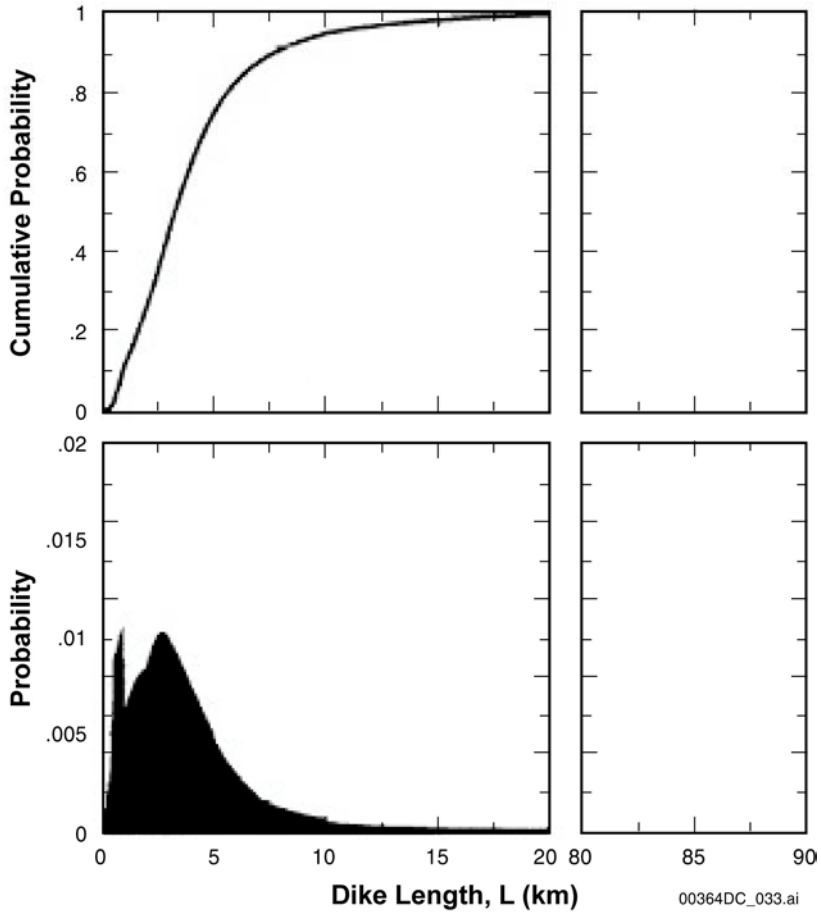

Source: CRWMS M&O 1996; DTN: LA0009FP831811.001.

NOTE: The 5th-percentile, mean, and 95th-percentile values are 0.6, 4.0, and 10.1 km, respectively. The distribution contains a very long upper tail extending to 86 km. The irregular shape of the probability mass function in the lower plot reflects the variation in the distributions defined by the individual experts.

Figure 2-10. Composite Distribution for Dike Length Averaged across All Ten Probabilistic Volcanic Hazards Analysis Experts

2.2.9 Intrusive Versus Extrusive Events: Evidence from the Yucca Mountain Region and Analog Sites

In the PVHA (CRWMS M&O 1996) definition of a volcanic event, the definition requires an intrusive event and allows an extrusive event. A volcanic event is a dike or dike system, together with its associated eruptive products. Dikes that ascend to depths of less than about a kilometer are thought to erupt at some point along the length of the dike, mainly because of volatile exsolution from basaltic magma.

An appropriate analog in the Yucca Mountain region for understanding the relationship between intrusive and extrusive components of a volcanic event is the Paiute Ridge intrusive/extrusive center (Byers and Barnes 1967) on the northeastern margin of the Nevada Test Site. Paiute Ridge is a small-volume Miocene volcanic center comparable in volume and composition to Quaternary volcanoes near Yucca Mountain (CRWMS M&O 1998a, Chapter 5, p. 5-29). Paleomagnetic, geochronologic, and geochemical data indicate that the entire intrusive/extrusive complex formed during a brief magmatic pulse and, thus, represents a single volcanic event (Ratcliff et al. 1994; CRWMS M&O 1998a, p. 5-29). The vents and associated dike system formed within an NNW-trending extensional graben, and excellent exposures of the system include remnants of surface lava flows, volcanic conduits, and dikes and sills intruded into tuff country rock at depths up to 300 m (CRWMS M&O 1998a, p. 5-27 through 5-41). There is evidence of shallow structural control of dike emplacement at Paiute Ridge, including dike emplacement along fault planes (Byers and Barnes 1967; CRWMS M&O 1998a, Chapter 5, pp. 5-27 through 5-28). Dike lengths at Paiute Ridge range from less than 1 to 5 km (CRWMS M&O 1998a, Chapter 5, p. 5-31), comparable to the range estimated for post–Miocene volcanism near Yucca Mountain (Figure 2-10). Field observations at Paiute Ridge clearly show that, while some parts of individual dikes stagnated within about 100 m of the surface without erupting, other parts of the same dike did erupt, as evidenced by associated lava flows and volcanic conduits (Byers and Barnes 1967; CRWMS M&O 1998a, p. 5-29 to 5-33).

In the San Rafael dike swarm on the western Colorado Plateau, Delaney and Gartner (1997, p. 1180) estimate that 174 dikes are represented where an extensive system of shallowly intruded dikes is well exposed. Breccias are present along portions of 45 of these dikes, which are interpreted to represent the subsurface beneath eruptive centers (Delaney and Gartner 1997). No attempt is made by Delaney and Gartner (1997) to estimate the frequency of temporally discrete intrusive versus eruptive events. They suggest only that at least 45 dikes show evidence of eruption along some segment of a dike; other parts of the same dike, or other parts of the same dike system, may have erupted, as is observed at Paiute Ridge. Given the Paiute Ridge analogy and the Delaney and Gartner (1997) interpretation that the San Rafael swarm likely represents the subsurface beneath a large volcanic field that was active for about a million years, it is likely that many individual intrusive/extrusive events are represented at San Rafael, with some part of a dike system erupting during each event, and other parts of the same dike system not erupting. The ratio of intrusive to extrusive events is close to 1, an interpretation that is consistent with the Paiute Ridge analog site and the results of the PVHA (CRWMS M&O 1996).

2.2.10 Event Lengths: Evidence from the Yucca Mountain Region and Analog Sites

The length of dikes or vent alignments can significantly affect intersection probabilities, because volcanic events occurring at some distance from the repository must have sufficient length to intersect the repository, and longer event lengths will result in higher intersection probabilities. Nearer to the repository, volcanic events with shorter lengths are able to intersect the repository with higher frequency.

The mean dike length associated with a volcanic event in the Yucca Mountain region is 4 km, and 95 percent of dikes are shorter than 10.1 km (Figure 2-10). These values are consistent with observed volcanic features in the Yucca Mountain region. For instance, the maximum aligned-vent spacing in the Yucca Mountain region is 5.4 km between Black and Makani Cones, and volcanic-vent alignment lengths are typically in the range of 2 to 5 km (e.g., Hidden Cone-Little Black Peak, Amargosa Aeromagnetic Anomaly A, Red Cone-Black Cone). The longest proposed vent alignment in the Yucca Mountain region, assuming it represents one volcanic event, is the Quaternary Crater Flat alignment with a length of about 11 km (Figure 2-1). Dikes, such as those at Paiute Ridge, range in length from less than 1 to 5 km. Dike and vent alignments of the 3.7 Ma basalts in southeast Crater Flat are no more than 4 km in length (see Figure 2-11).

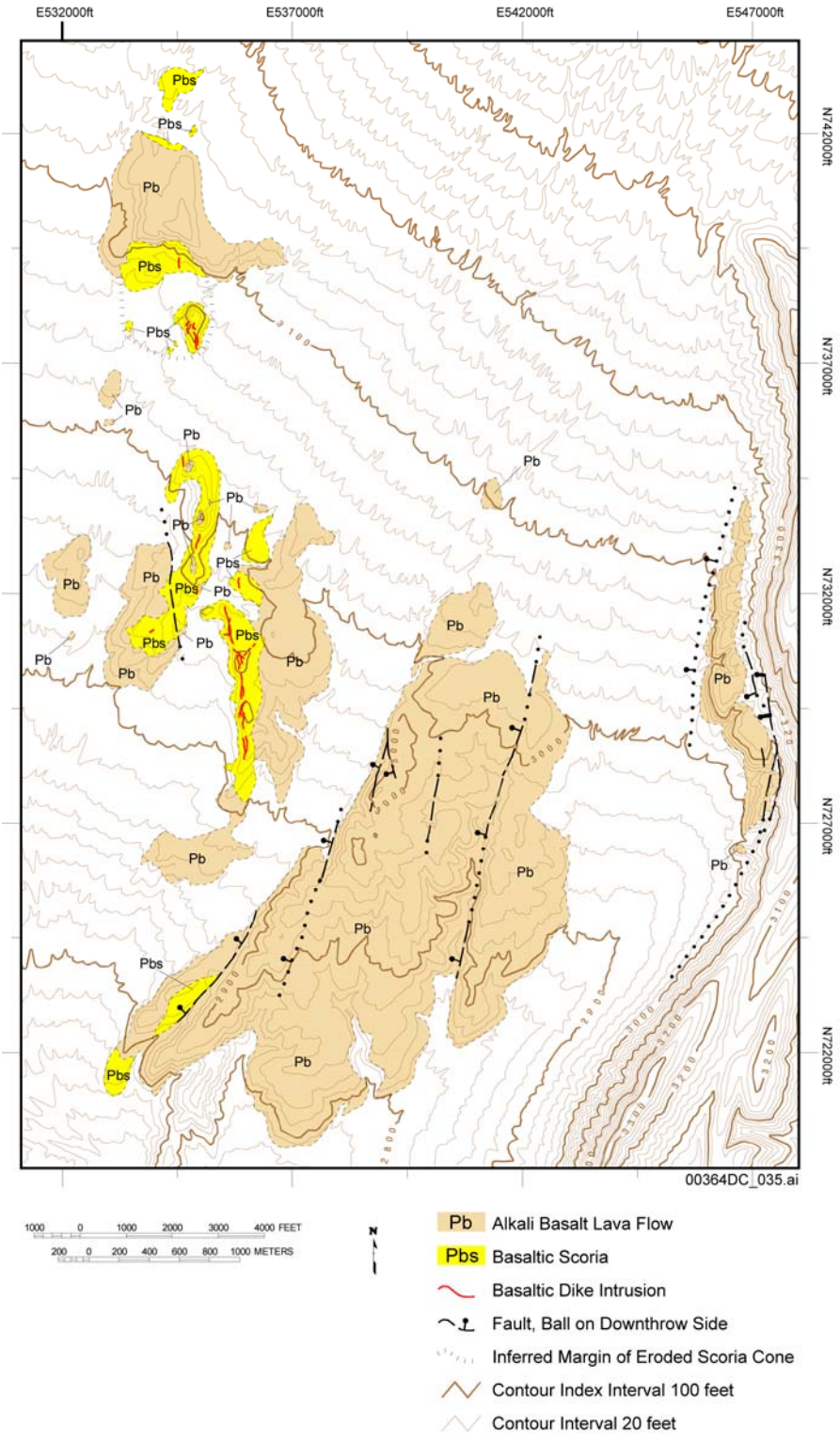

Source: Vaniman and Crowe 1981, Figures 4, 6, 8; CRWMS M&O 1998a, Figure 2.7; Perry et al. 1998.

Figure 2-11. Geologic Map of the Pliocene Basalt of Crater Flat

About 97 percent of the 174 dike lengths measured in the San Rafael volcanic field (discussed above) have total lengths less than 5 km (Delaney and Gartner 1997, Figure 4). The median of the length distribution at San Rafael is approximately 1.1 km, and the maximum dike length is 8 to 9 km (Delaney and Gartner 1997, Figure 4), a distribution similar to that used in the PVHA (Figure 2-10).

A measure comparable to dike half-length, the distance from the end of the dike nearest the repository to the point of origin (the midpoint) of the volcanic event, can be derived from information elicited in the PVHA. This distribution has 5th-percentile, mean, and 95th-percentile values of 0.2, 2, and 5.6 km, which, given the previous discussions of observed dike lengths, vent spacings, and maximum observed half-length vent alignment of 5.6 km, is in excellent agreement with observed volcanic-event features in the Yucca Mountain region.

2.2.11 Conceptual Models of Volcanism and Formulation of Probability Models

In the analysis of volcanic hazard for the repository, the conceptual model of volcanism—how and where magmas form and what processes control the timing and location of magma ascent through the crust to form volcanoes—has a fundamental impact on how probability models are formulated and the consequent results of probability models (e.g., Smith, Feuerbach et al. 1990; CRWMS M&O 1996; Reamer 1999).

The PVHA experts viewed the Yucca Mountain region as part of the same extensional tectonic and volcanic regime as the rest of the southern Great Basin portion of the Basin and Range province, and several members of the panel noted the possible additional influence on volcanism of the Walker-Lane structural zone (CRWMS M&O 1996, Appendix E, e.g., pp. WD-1, WH-1). The Walker Lane Fault Zone is a major tectonic system located at the boundary of the Sierra Nevada and the Basin and Range, that includes several major fault systems. The Walker Lane region, which extends from near Las Vegas to south-central Oregon, is being deformed by both extensional and lateral fault movement. The smaller volumes of basalt erupted in the Yucca Mountain region since the Miocene reflects waning of both tectonism and magmatism in this part of the Basin and Range Province (CRWMS M&O 1996, Appendix E, e.g., pp. RC-1, BC-3, WD-2, RF-3, WH-1, MK-1, AM-3).

Some experts distinguished between deep (mantle source) and shallow (upper crustal structure and stress field) processes when considering different scales (regional and local) of spatial control on volcanism (CRWMS M&O 1996, Appendix E, e.g., pp. MK-2, AM-1). In the PVHA, volcanism in the Yucca Mountain region was viewed as a regional-scale phenomenon, involving melting processes in the upper lithospheric mantle that produce small volumes of alkali basalt, which is a basalt type generated by relatively small percentages of mantle melting compared to other basalt types (CRWMS M&O 1998a, Chapter 4, p. 4-4). The exact mechanism of mantle melting in the Yucca Mountain region is poorly understood but may be controlled by a combination of processes. These include the effect of residual heat in the lithospheric mantle from previous episodes of volcanism and the presence of a former plate-subduction system, local variations in volatile (water) content, variations in mantle mineralogy and chemistry, and the effect of regional lithospheric extension (CRWMS M&O 1996, Appendix E). Researchers who have analyzed magmatic processes in the Yucca Mountain region generally agree that the magnitude of mantle melting has decreased greatly since the middle Miocene and that all melts

in the past few million years have been generated within relatively cool (compared to asthenospheric mantle) ancient lithospheric mantle, a factor that may contribute to the relatively small and decreasing volume of basaltic melt erupted in the Yucca Mountain region since the Miocene (Farmer et al. 1989; Yogodzinski and Smith 1995; CRWMS M&O 1996, Appendix E; Reamer 1999, pp. 17 and 47).

2.2.12 Current Volcanic Hazard Estimate

In terms of probability calculations, the volcanic source zones defined in the PVHA represent local regions of higher event frequency (southwestern part of the Crater Flat structural domain), whereas the northeastern part of the Crater Flat structural domain (including Yucca Mountain) falls within a regional background source zone of lower event frequency (BSC 2003e, p. 63, Figure 17a). According to the intersection probability models used, two mechanisms could generate a disruptive event at Yucca Mountain. Either a volcanic event is generated within a local source zone (higher probability event) to the west of Yucca Mountain and has the appropriate location and dike characteristics (length and azimuth) to intersect the repository, or a volcanic event is generated with a regional background zone (lower probability event) and intersects the repository. Because the total probability of intersection of a volcanic event with the repository includes components of both mechanisms, the intersection probability estimated for the repository should reflect spatial event frequencies that lie between local source zone values and regional background values. This is consistent with the results of the PVHA, and is appropriate for a site that lies outside of a local volcanic source zone but near enough to possibly be affected by dikes generated within that source zone. To compute the consequences of an intersection, information is also needed on the length and orientation of the intersecting dike and the probability that an eruptive center (a surface vent fed by the dike) may form within the footprint. The result of the PVHA (CRWMS M&O 1996) has been recalculated to account for the repository footprint and extended to include the probability of an eruption within the repository footprint, conditional on a dike intersection (Table 2-5). The annual frequency of intersection of the repository footprint by a dike or dike system associated with a volcanic event, and the annual frequency of a volcanic event producing one or more eruptive centers within the repository have been recalculated, based on the current repository footprint. These results are summarized below and shown in Table 2-5.

The volcanic hazard recalculated using the LA footprint (BSC 2003c, Section 4.1) is not significantly different from the PVHA estimate. These updated analyses will be used as the technical basis for probability weighted dose calculations in the LA. The studies of the sensitivity of the PVHA hazard estimate were consistent with NRC guidance on the use of expert elicitation (NUREG-1563, Kotra et al. 1996).

Table 2-5. Summary Frequencies of Disruptive Volcanic Events for the License Application Repository Footprint

Annual Frequency of Intersection of Repository by a Volcanic Event	Composite Conditional Probability of At Least One Eruptive Center	Annual Frequency of Occurrence of One or More Eruptive Centers within Repository
7.4×10^{-10} (5th percentile)	0.75	5.6×10^{-10}
1.7×10^{-8} (mean)	0.78	1.3×10^{-8}
5.5×10^{-8} (95th percentile)	0.77	4.3×10^{-8}

Source: DTN: LA0307BY831811.001.

NOTE: Results presented in this table were rounded to two significant digits after calculation.

2.2.12.1 Length and Azimuth of an Intersecting Dike

The hazard computation gives the overall frequency of a dike intersecting a repository. However, to compute the consequences of an intersection, the distribution for length and orientation of the intersecting dikes is needed. This distribution is developed by breaking down (disaggregating) the total frequency into frequencies for specific values of intersecting dike length and dike azimuth (BSC 2003e, Section 6.5.1.2, paragraph 1, p. 72). The process involves computing the spatial disaggregation of the frequency of intersection into the contributions from each location (x_i,y_j) in the spatial grid around the repository. At each point, the conditional probability of intersection is the probability that dikes of all lengths and azimuths will intersect the repository. The conditional probability of intersection is divided into probabilities for intersection from dikes with specific lengths and azimuths. As a result, the frequency of intersection from volcanic events at point (x_i,y_j) is divided into the frequency of intersection from volcanic events at point (x_i,y_j) that produce specific values of length and azimuth within the repository footprint. Summing these frequencies over all locations gives the frequency of intersection with a specific value of length and azimuth from all volcanic events. Dividing this frequency by the total frequency of intersection gives the conditional probability that an intersecting dike will produce a specific value of length and azimuth within the repository.

2.2.12.2 Conditional Distributions for the Number of Eruptive Centers within the Repository Footprint

The mathematical formulation for assessing the conditional distribution for the number of eruptive centers within the footprint of the repository is based on the concept that eruptive centers will occur at uncertain locations along the length of the dike associated with a volcanic event (BSC 2003e, Section 6.5.1.3, paragraph 1, p. 77). The length of intersection within the repository footprint compared to the total length of the dike, the number of eruptive centers per volcanic event, and the spatial distribution of eruptive centers along the length of the dike provide the bases for assessing the likelihood that one or more eruptive centers will occur within the repository footprint. The total length of the dike and the length of intersection within the repository are completely defined by the PVHA experts' interpretations (BSC 2003e, Section 6.5.1.3, paragraph 1, p. 77). The number of eruptive centers per volcanic event and the spatial distribution of eruptive centers along the length of a dike were not defined as part of the

expert elicitation. However, with a limited set of assumptions (described in the next paragraph), these can be derived from the experts' interpretations. There are alternative ways that these assumptions can be applied. In keeping with the concept of uncertainty characterization employed in the probabilistic volcanic hazards analysis, alternative assessments were developed of the conditional distribution for the number of eruptive centers within the repository footprint. To produce a composite distribution, these assessments were then combined using the relative weights assigned to each alternative assessment.

Two approaches for assessing the number of eruptive centers per volcanic event are considered. The first uses the number of mapped volcanoes in the Yucca Mountain region to derive empirical distributions for the number of eruptive centers per volcanic event independent of any assessment of the length of the dike associated with the volcanic event. In this approach, volcanic events can have from 1 to 5 eruptive centers, the range of individual volcanoes that was associated with a single volcanic event by the PVHA experts. The second approach uses the number and location of the mapped volcanoes to derive empirical distributions for the average spacing between eruptive centers. This distribution, together with the length of the dike associated with a volcanic event, determines the number of eruptive centers for a given volcanic event (BSC 2003e, Section 6.5.1.3, paragraph 2, p. 77).

3. ERUPTIVE PROCESSES AND CHARACTERISTICS OF BASALTIC MAGMA

The behavior of basaltic magmas that could intrude or erupt through a repository provides important constraints on the consequences associated with igneous or volcanic activity. This section describes the properties of basaltic magmas and the mechanisms that determine the style and energy of intrusive or extrusive events. It provides a physical and technical basis for the consequence analysis presented in Section 5.

3.1 GENERAL CONCEPTUAL MODEL OF BASALTIC VOLCANISM IN THE YUCCA MOUNTAIN REGION

The general conceptual model is shown in Figure 3-1. It depicts the key features and processes involved in the formation and construction of the small volcanic centers typical of the Yucca Mountain region. It shows the dikes that feed lava flows and Strombolian eruptions, as well as the ash clouds that deposit air-fall ash (tephra) downwind of the cone.

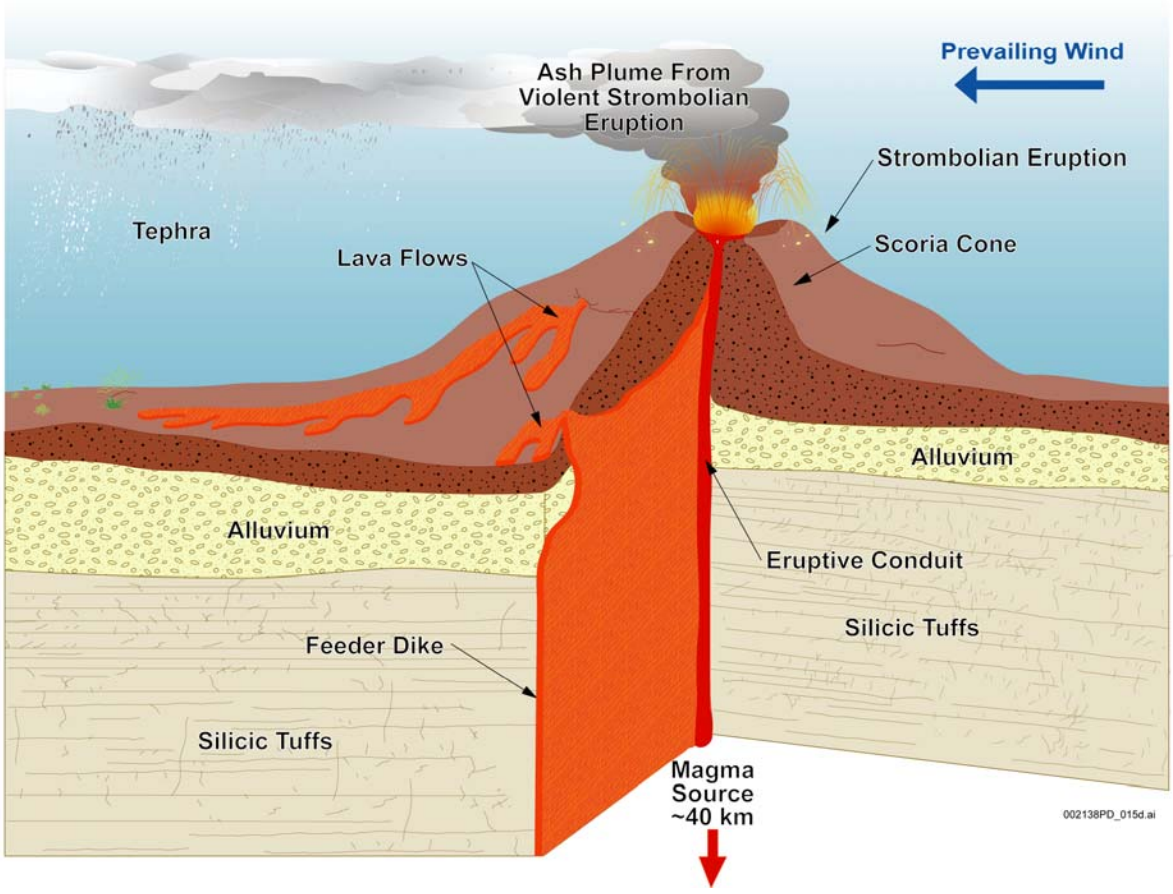

Figure 3-1. General Conceptual Model of Basaltic Volcanism in the Yucca Mountain Region

Alkali-basaltic magma is generated by partial melting of ancient lithospheric mantle beneath the Yucca Mountain region. Driven by buoyancy, the magma ascends through the lithosphere and continental crust of the southern Great Basin. In the brittle crust above approximately 15 km depth, batches of melt ascend as magma-filled cracks or dikes. The dikes are intruded with

azimuths approximately N30E, a direction that is perpendicular to the direction of least compressive stress in the upper crust of the Yucca Mountain region. Within a few hundred meters of the surface, dikes in the Yucca Mountain region are generally 1 to 2 m thick, average 4 km in length, and nearly always erupt to form basaltic volcanoes. As dikes reach the surface, fissure eruptions are focused into central vents within hours or days. The conduits feeding such vents are estimated to be tens of meters in diameter. Conduits may shift in location and change in their subsurface configuration, vent locations may correspondingly change during the course of an eruption, multiple vents may be simultaneously active, and single vents may simultaneously produce lava and tephra.

The petrographic features of the erupted lava and experimental data on similar magma compositions indicate eruption temperatures near 1,170°C, the presence of 2 to 4 weight percent water as the dominant volatile constituent and viscosity of approximately 10^2 poise. Experimental and theoretical data indicate that alkali basaltic magma of the Yucca Mountain region will begin to exsolve gas at about 6 to 7 km depth. Volatile exsolution is a continuous process during the ascent of magma through the upper crust. The resulting volume expansion is a significant factor in driving the basaltic dikes upward through the final kilometer or so of brittle, fractured rock. The inception of basaltic volcanism is typically characterized by pyroclastic eruptions of gas-rich magma.

Based on geologic observations in the Yucca Mountain region, future volcanism in the Yucca Mountain region is expected to produce small, monogenetic basaltic centers, each with a total erupted volume of 0.01 to 0.1 km^3. The dominant style of volcanism is Strombolian, involving the construction of basaltic scoria cones and the effusion of lava flows. Violent Strombolian eruptions may also occur, involving sustained, vertical eruption columns that eject volcanic ash to heights of 3 to 5 km above the scoria cone. Subsequent wind-borne dispersal of the fine tephra may form ash sheets up to approximately 15 km from the vents. The volumes of the ash sheets are estimated to be two to four times the volumes of the associated scoria cones.

The unsaturated zone beneath Yucca Mountain is approximately 550 m deep. Together with magma properties, the high permeability and unsaturated condition of the tuffaceous host rocks of the repository play a major role in determining the style and dynamics of volcanic eruptions and the nature of potential interaction between basaltic magma and the repository drifts. Hydrovolcanism is uncommon in the Yucca Mountain region geologic record due to the deep water table and paucity of surface or perched water. Future hydrovolcanism is unlikely at Yucca Mountain because of the elevated terrain, the great depth of the water table, and the high permeability and low porosity of the unsaturated host tuffs.

Based on historical observations of similar eruptions in analog regions, the duration of single igneous events in the Yucca Mountain region is estimated to have been weeks, months, or perhaps a few years. The estimated durations and volumes of the small basalt volcanic centers in the Yucca Mountain region suggest peak Strombolian mass-eruption rates of 10^4 to 10^5 kg/s, with average rates of approximately 10^3 kg/s. Maximum rates of approximately 10^6 kg/s are possible during violent Strombolian phases of basaltic volcanism in the Yucca Mountain region.

Crustal extension in the Yucca Mountain region is accommodated through a combination of faulting and magma intrusion. There is a strong tendency for basaltic dikes of the Yucca

Mountain region to preferentially ascend and erupt through upper crust that is undergoing extension. The southwestern part of the Crater Flat structural domain, which closely corresponds to Crater Flat, a topographic basin to the west and southwest of Yucca Mountain, is an area of Quaternary faulting and basaltic volcanism in the Yucca Mountain region. Crater Flat is the location of most of the Quaternary volcanoes in the Yucca Mountain region and is identified as the major volcanic source zone that may impact the repository. The most probable scenario for disruption of the repository is the intersection of repository drifts by a basaltic dike, associated with a volcanic event in Crater Flat. If a dike intersects the repository drifts, magma will flow into them as pyroclastic material or gas-poor lava.

3.2 COMPOSITION AND PROPERTIES OF BASALTIC MAGMA IN THE YUCCA MOUNTAIN REGION

Magma is a mixture of silicate melt, crystals (phenocrysts and xenocrysts), and volatiles (present as dissolved constituents in the melt or as exsolved vapor bubbles in the melt). In magmatic systems where explosive interaction with external groundwater or surface water (hydrovolcanism or phreatomagmatic volcanism) plays no role, the viscosity and volatile content of the melt play a fundamental role in the eruption energetics, expressed as volcanic style. Magma viscosity is primarily influenced by melt composition and temperature. In comparison with other types of magma, basaltic magma is relatively fluid and is poor in dissolved gas. Eruptions from basaltic volcanoes, therefore, tend to be less explosive than eruptions of silicic magma.

General information on basaltic magma composition and properties in the Yucca Mountain region is given here, based on the more detailed data, calculations and tables of magma properties found in *Characterize Eruptive Processes at Yucca Mountain, Nevada* (BSC 2001; BSC 2003b) and *Final Report of the Igneous Consequences Peer Review Panel* (Detournay et al. 2003).

3.2.1 Magma Composition

Magma-chemistry data are used to determine parameters for important variables such as magma viscosity, temperature, and density. The magma composition of the Lathrop Wells volcano is adopted to represent the composition of future Yucca Mountain region volcanoes. The Lathrop Wells composition is selected because it represents the most recent eruption in the Yucca Mountain region, and emphasizes the composition that produced more violent explosive eruptions compared to other Yucca Mountain region volcanoes (as inferred from Perry et al. 1998, Chapter 2). The major-element composition for Lathrop Wells is based upon 45 chemical analyses (DTN: LA000000000099.002). Mean values for selected major-element constituents are (weight percent) $SiO_2 = 48.50$; $TiO_2 = 1.93$; $Al_2O_3 = 16.74$; $Fe_2O_3T = 11.63$, $MgO = 5.83$; $CaO = 8.60$; $Na_2O = 3.53$; $K_2O = 1.84$; $P_2O_5 = 1.22$. These values indicate that the magma is a variety of alkali basalt.

3.2.2 Water Content of Primary Basaltic Magma

Eruptive styles in the Yucca Mountain region are inferred to have ranged from violent Strombolian on one end of the spectrum to quiescent *aa* lava on the other (Perry et al. 1998, Chapter 2). Eruption style was primarily controlled by volatile content (which is dominated by

water with subordinate CO_2) and the rate at which volatiles were exsolved from the magma. The eruptive products of the Crater Flat and Lathrop Wells volcanoes indicate a large range in volatile contents and, hence, water content of Yucca Mountain region magmas.

Mineralogical and geochemical data indicate that primary magmatic water contents ranged up to as much as 4 weight percent. Amphibole, possibly of magmatic origin, is found as a rare and sparse phase in some Quaternary Crater Flat basalts. Knutson and Green (1975, Figure 1, p. 126), performing experiments on material similar in composition to Yucca Mountain region basalts, observed that magmatic amphibole was stabilized at water contents of between 2 and 5 weight percent. Baker and Eggler (1983, p. 387) showed that at 2 kbar pressure, water content in excess of 4.5 weight percent is required to stabilize amphibole in high-alumina basalt similar to Yucca Mountain region basalts. Sisson and Grove (1993, p. 167) note that low-Mg basalts with high alumina content cannot erupt as liquids with water content in excess of 4 weight percent because they will exsolve liquid and rapidly crystallize to form phenocryst-rich magmas as they approach the surface. Based on mineralogical and petrologic arguments (BSC 2003b, Section 6.3.2), 4 weight percent water is used as an upper bound on initial dissolved-water content, and zero percent magmatic water has a zero probability of occurrence. The most likely range of water contents for alkali-basaltic magma in the Yucca Mountain region is 1 to 3 weight percent. Direct measurements of water in mafic (low silica) magmas or magmatic products from a range of tectonic settings also support these recommended values (BSC 2001).

3.2.3 Mole Percent of Constituents in Volcanic Gas

Because there is no ongoing volcanism in the Yucca Mountain region, gas composition cannot be directly observed. Therefore, a survey of data from the literature, including volcanoes from various tectonic settings, has been used to constrain the relative proportions of major gas constituents in Yucca Mountain region basalts. Three types of data exist in the literature: (1) measurements of emitted volcanic gases, (2) measurements of gases trapped in volcanic glass or melt inclusions, and (3) experiments on gas solubilities in silicate melts. The values used for gas constituents in Yucca Mountain region mafic magmas are (mol percent): $H_2O = 75$, $CO_2 = 15$, $SO_2 = 9$, $H_2 = 1$ (BSC 2001, simplified from Table 7).

3.2.4 Magmatic Temperatures, Viscosities, and Densities

Experimental results are used to constrain magmatic temperatures for magmas with elevated water content. Table 3-1 gives several properties calculated for Lathrop Wells magma (see BSC 2001, pp. 63 to 65 for details of the calculations). Yucca Mountain region basaltic lavas are generally aphyric to sparsely porphyritic (Perry and Straub 1996, p. 6), which indicates that they erupted at near-liquidus or superliquidus temperatures (liquidus temperature is the temperature at which crystallization begins).

Table 3-1. Calculated Saturation Pressures, Liquidus Temperatures, Viscosities, and Densities as a Function of Water Content for Lathrop Wells Basaltic Magma

Water Content (wt%)	Saturation Pressure (Pa)	Liquidus Temperature (°C)	Viscosity (log poise)	Density (kg/m^3)
0	1×10^5	1169	2.678	2663
0.5	9.0×10^6	1153	2.572	2633
1	2.4×10^7	1137	2.472	2605
2	6.5×10^7	1106	2.284	2556
3	1.2×10^8	1076	2.112	2512
4	1.7×10^8	1046	1.957	2474

NOTE: Derived using mean Lathrop Wells compositions.

A review of relevant experimental data reveals that these values are reasonable. The liquidus temperature for a mildly alkalic basalt similar in composition to the mean Lathrop Wells lava composition is between 1,174 and 1,188°C (Mahood and Baker 1986). The Mahood and Baker (1986) temperature calculations are close to temperatures reported by Knutson and Green (1975, Figure 1) for a hawaiite that is also similar in composition to Lathrop Wells basalt. Yoder and Tilley (1962, Figure 28) published results on the water-saturated liquidus for a high-alumina basalt. At 1.75×10^8 Pa water pressure, the liquidus was more than 100°C cooler than the 10^5 Pa liquidus temperature. Thus, the calculated parameter values are consistent with a well-established body of experimental data.

3.3 PHYSICAL VOLCANOLOGY OF BASALT VOLCANOES IN THE YUCCA MOUNTAIN REGION

Figures 2-11 and 3-2 show geologic maps of selected Quaternary and Pliocene volcanoes near Yucca Mountain (Vaniman and Crowe 1981; CRWMS M&O 1998a; Perry et al. 1998). The deposits consist of scoriaceous tephra cones, with associated *aa* lava flows. Exposed deposits at most of the centers cover less than 2 square km. The cones are typical scoria cones of 300 to 700 m basal diameter and up to 220 m but generally less than 100 m in height, composed predominantly of frothy bombs and lapilli that were produced during Strombolian eruptions. For a number of the centers, several conduits were apparently active along a fissure or set of eruptive fissures, as at Red Cone. Most of the cones produced *aa* lava flows from their flanks or bases. The eruptive products of the 1-Ma Crater Flat volcanoes are deeply eroded and are in places covered by alluvial and eolian deposits, particularly the lava flows, but the proportion of lava to cone tephra deduced from mapping and interpretation of associated aeromagnetic anomalies appears to be generally greater than 1. The tephra-fall deposits from these eruptive centers have been largely removed by erosion or buried by younger sediments and are therefore unmappable. Even at the 80-ka Lathrop Wells volcano, primary tephra-fall deposits are not found at distances greater than about 2.5 km from the vent (BSC 2003b, p. 120).

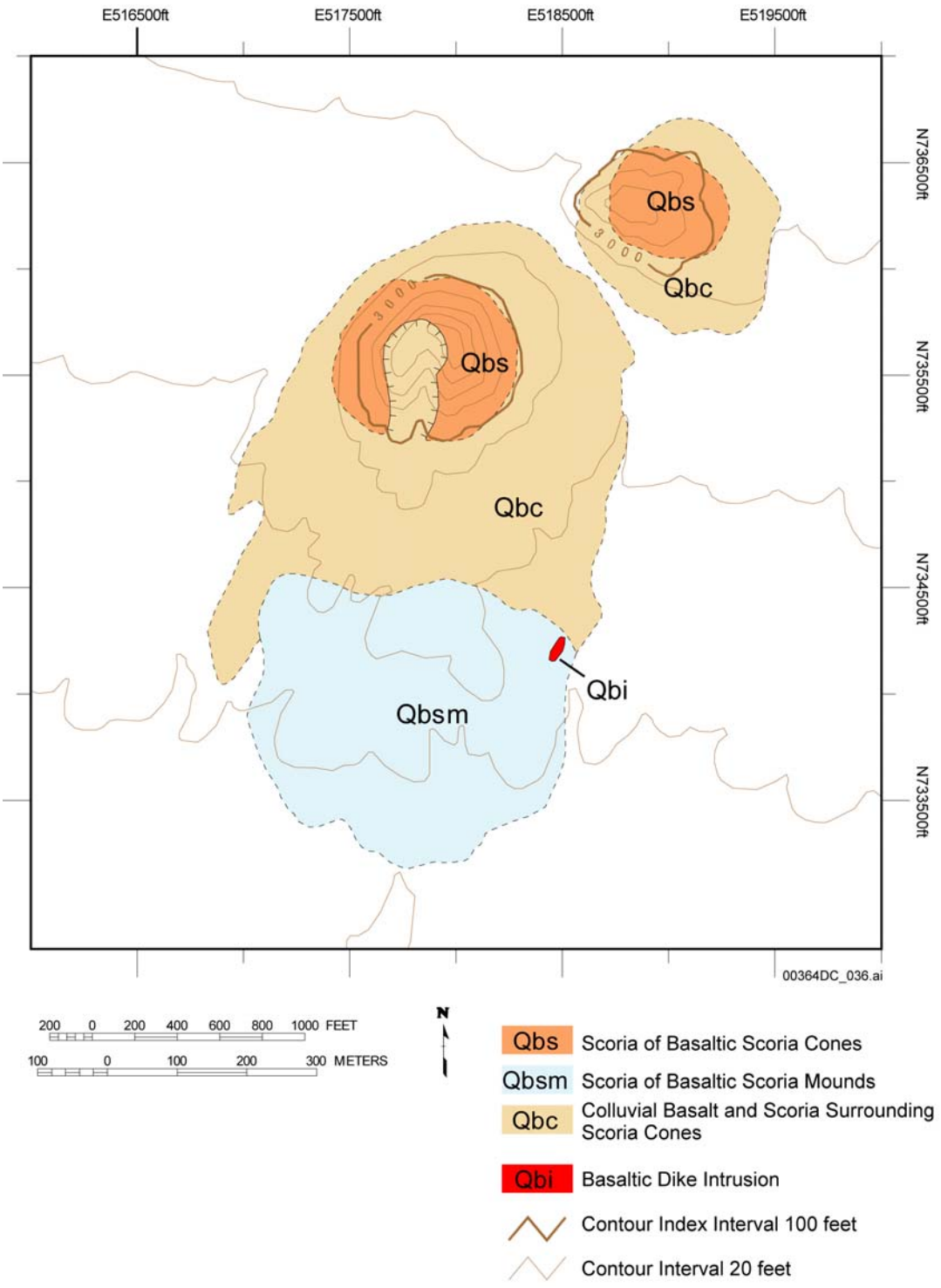

Source: Perry et al. 1998.

Figure 3-2. Geologic Map of Little Cones in Crater Flat

More than half of the ejecta during Strombolian eruptions fall within 500 m of the vent, and cones are usually built rapidly during initial high rates of eruption. During such eruptions, the rapid expansion of dissolved gas leads to the formation of bubbly clots. The largest clots and those rising in the core of the fountain remain fluid during their brief flight and coalesce near the vent into rootless lava flows or lava ponds. Others are quenched by entrained air and are deposited as chilled, individual clasts on the cone flanks or within the summit crater. Dilute convective plumes of volcanic gas, aerosols and ash are inferred to have formed above the Crater Flat vents, although the tephra-fall deposits of such plumes are not well preserved, having been removed by erosion or covered by surficial deposits (BSC 2003b, Section 6.4.2). Observations of historical Strombolian and Hawaiian eruptions indicate that these plumes contain less than 0.17 percent of the total mass fraction of lava erupted and rarely penetrate the tropopause (Vergniolle and Mangan 2000, p. 452), or upper atmosphere.

At the location of the Pliocene basaltic centers of southeastern Crater Flat (Figure 2-11), most of the cone-building scoria deposits have been eroded, exposing the shallow feeder systems of these volcanic centers. Sinuous dike segments of 50 to 300 m length occur in close association with remnants of welded scoria or as rootless lava ponds or intrusions into alluvial deposits. Dike widths are generally less than 2 m but in places the dikes swell into pluglike lava masses of approximately 5 m width.

3.4 PHYSICAL VOLCANOLOGY OF THE LATHROP WELLS CONE

Because of its relative youth, exposure, composition, and position in the sequence of basaltic eruptive events in the Yucca Mountain region, the Quaternary Lathrop Wells volcano is an appropriate example of the type of eruptive event that could disrupt the repository (Figures 3-3 and 3-4). An exception to this generalization is the occurrence of hydrovolcanic tephra deposits from the early and late stages of eruption at Lathrop Wells volcano, reflecting the interaction of basaltic magma with shallow groundwater, perhaps contained in near-surface alluvial deposits. Such magma-water interaction would not be expected during a future eruption through the repository, because the repository is located in the unsaturated zone, the saturated zone is located several hundred meters beneath the repository, and the low porosity and unsaturated condition of the repository tuff would not permit the water inflow needed to maintain continuous hydrovolcanism (Crowe, Self et al. 1983, p. 268).

The Lathrop Wells lava flows have an eruption age of approximately 77.3 ± 6.0 ka, based on seventeen $^{40}Ar/^{39}Ar$ ages on the stratigraphically oldest lava flow. An age of 80,000 years is used, based on the discussion of Perry et al. (1998) and the detailed geochronology studies of Heizler et al. (1999). The most probable interpretation for the Lathrop Wells eruptive center is that of a complex monogenetic volcanic center producing a cone, lava flows, and tephra-fall deposit erupted within a span of a few months or years, but the center also exhibits some features that support other interpretations of age and eruptive history (Perry et al. 1998).

The Lathrop Wells volcano consists of lava flows with an estimated volume of 0.029 km^3, a scoria cone of 0.018 km^3, and a tephra-fall deposit of 0.039 km^3, for a total erupted volume of 0.086 km^3 (BSC 2003b).

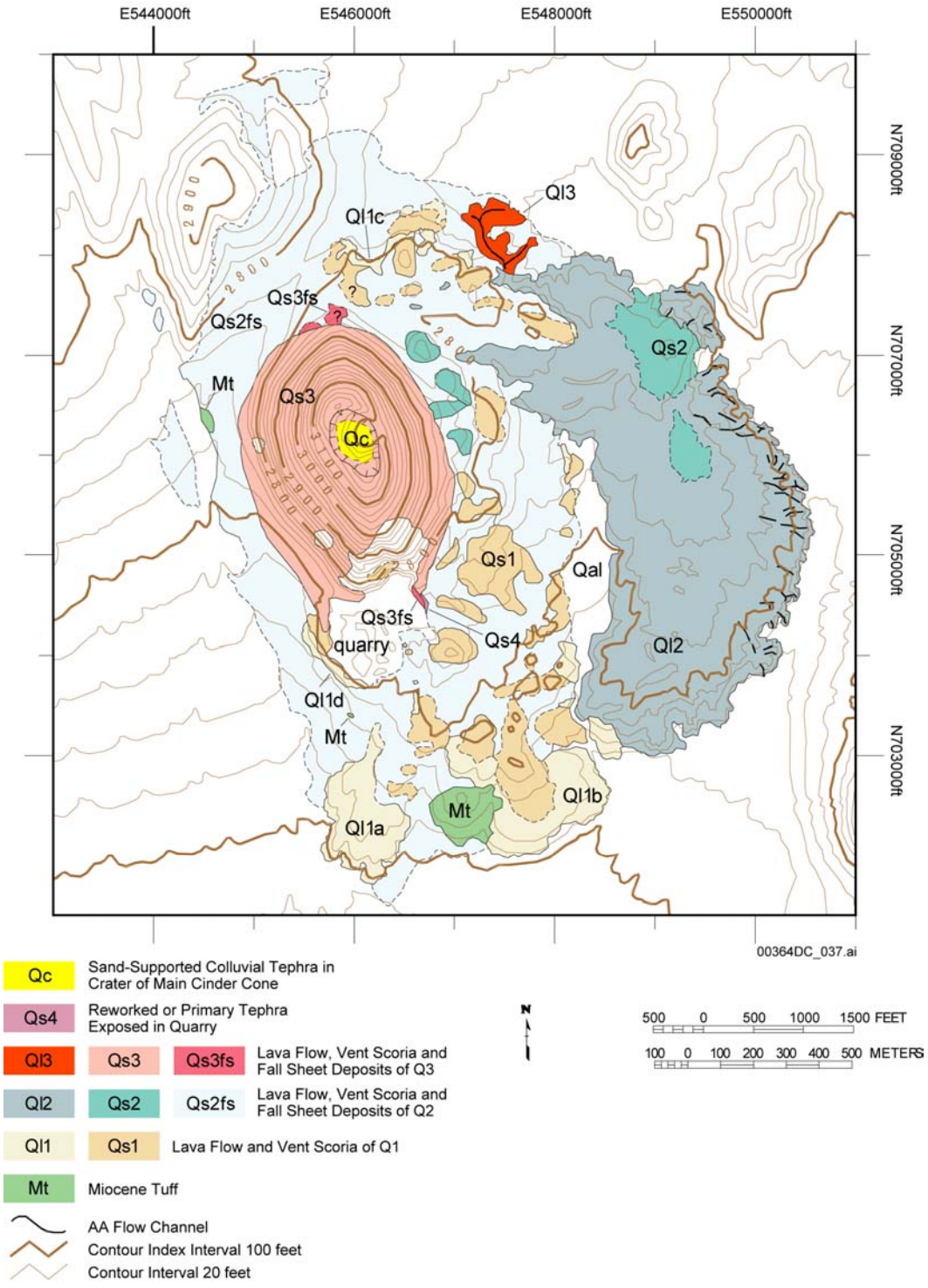

Source: Perry et al. 1998.

NOTE: The alphanumeric designations (e.g., Ql1a, b, and c) refer to subunits (lava flow and scoria) of chronostratigraphic units Q1, Q2, Q3, and Q4.

Figure 3-3. Geologic Map of the Lathrop Wells Volcanic Center

3.4.1 Scoria Cone

The Lathrop Wells scoria cone (Figure 3-4) is approximately 140 m high and oval, with its long axis oriented NNW-SSE. The cone measures 875 m by 525 m at its base and is capped by a similarly elongate, 190-m by 145-m crater that is about 20 m deep. The outer slopes of the cone range from 28° to 32° and consist of mostly loose scoria lapilli. The cone shape has been somewhat modified by erosion and is rapidly changing because of active quarrying along the south margins. Quarrying is revealing the three-dimensional structure of the cone, currently exposing approximately one-quarter of the cone's interior. Figure 3-5 is a digital elevation model portraying the relief of the cone and surrounding area as if illuminated from the northwest. It shows the locations of samples used to investigate the physical volcanology of the volcano, details of which are given in *Characterize Eruptive Processes at Yucca Mountain, Nevada* (BSC 2001; BSC 2003b).

Source: BSC 2003b, Figure 16.

Figure 3-4. Lathrop Wells Scoria Cone and Adjacent Lava Flows (Capped by Beige Eolian Sand) Viewed from the North

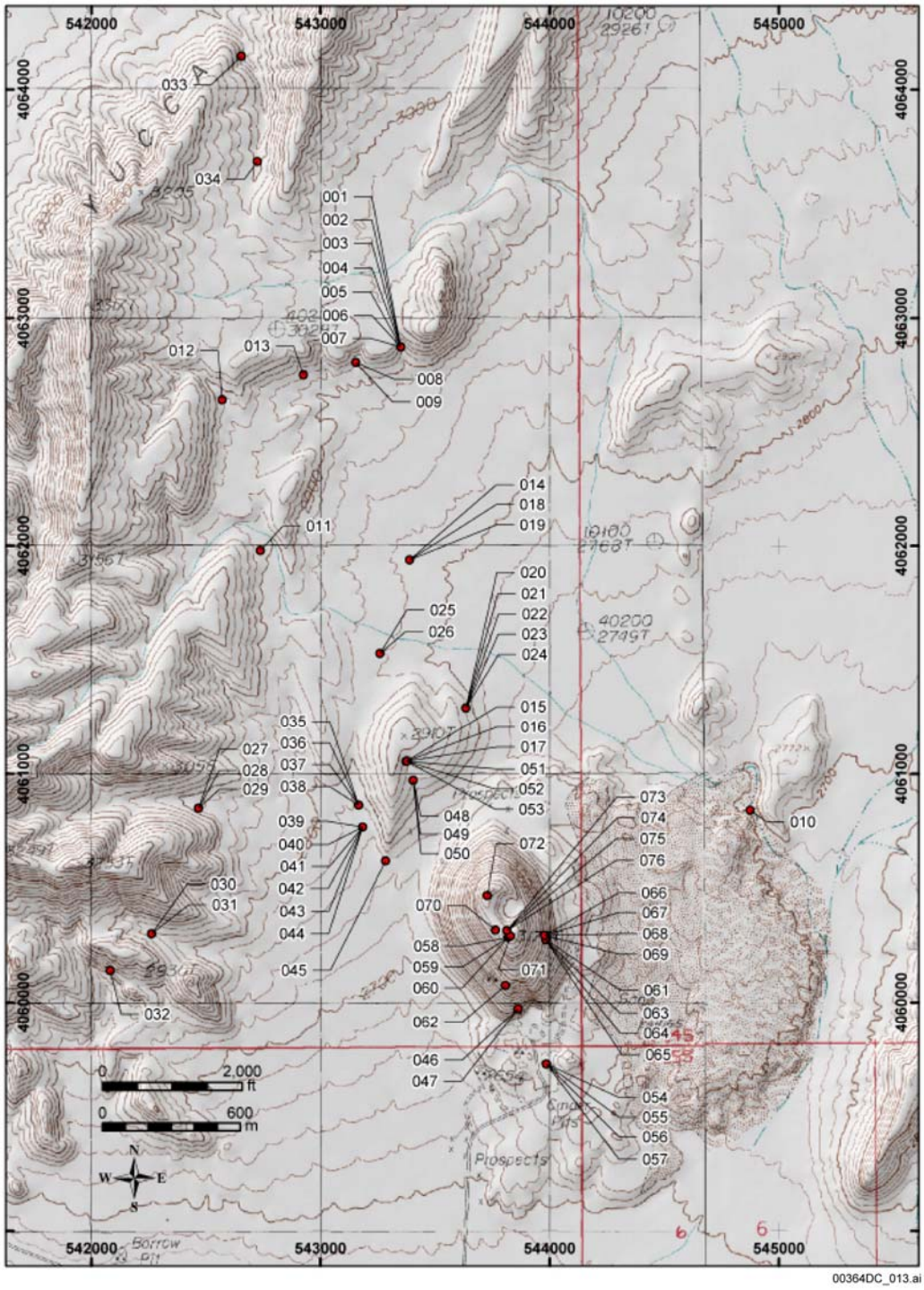

Source: BSC 2003b, Figure 17.

NOTE: The Lathrop Wells Cone occupies the lower center of the map. The dots show locations of samples; grid is NAD 1927 UTM, Zone 11 North, in meters. Contour interval is 20 feet.

Figure 3-5. Topographic Map and Tephra Sample Locations for Lathrop Wells Cone Area

Most cone deposits exposed in the quarry dip concentrically outward from the cone (Figure 3-6), and the lowest deposits exposed in the quarry are irregular masses of welded scoriaceous bombs and lapilli. Some of these agglutinate masses dip inward approximately 10° toward the presumed location of the vent.

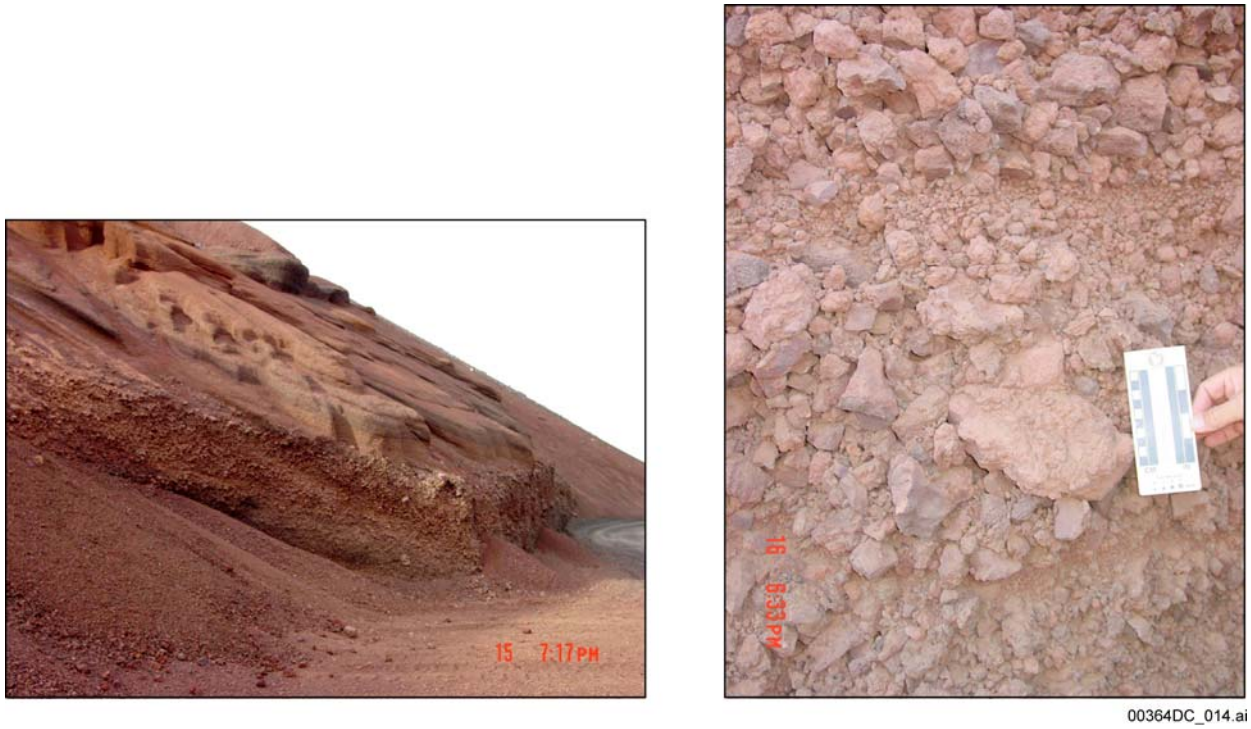

Source: BSC 2003b, Figure 18.

NOTE: Left photo: Exposures of cone interior showing sharp transition from nonwelded, massive or poorly bedded, lapilli- and bomb-size ballistic ejecta to overlying moderately bedded avalanche deposits of ash and lapilli (more than 50 percent ash); most clasts are deposited at angle of repose as ballistic ejecta. Height of the lower coarse beds is about 2.5 m. Right photo: Close-up of ejecta (at base of left image), mostly broken scoria bombs and lapilli. The scale is 10 cm.

Figure 3-6. Lathrop Wells Cone Interior Showing Scoria and Close-Up of Ejecta

3.4.2 Lithic Clasts in the Lathrop Wells Cone Deposits

Estimates of the volume and types of lithic clasts are important to repository risk assessment because the same processes that erode dike and conduit wall rock could influence the volume of waste reaching the surface (e.g., Crowe, Self et al. 1983, p. 270 to 271).

Larger and more interior quarried exposures provide a better opportunity to measure lithic clast abundances within the Lathrop Wells Cone now than in the past. Results from Crowe, Wohletz et al. (1986), based on only four nonhydrovolcanic samples of the cone, ranged from 0.3 to 2.4 vol% in the less than 0.707-mm size fraction. Table 3-2 lists results of counts of 18 1-m^2 areas located at several elevations in the cone. Access to outcrops in quarry walls and road cuts means that the elevations recorded with each measurement accurately reflect relative stratigraphic position. Measurements of lithic clasts greater than 1 mm were made in nonwelded deposits of coarse ash, lapilli, and larger material; they are not representative of the

stratigraphically lower, short pulse of hydrovolcanic activity recorded in deposits outside the cone (BSC 2003b, Section 6.4.2.3, Figure 26; Wohletz 1986, p. 258).

Table 3-2. Lithic Clast Measurements in the Lathrop Wells Scoria Cone

Patch	Elevation (ft)	Volume Fraction	
17	3146	0.000140	
15	3136	0.000200	
12	3119	0.000160	
14	3106	0.000029	
13	3079	0.000083	
18	3074	0.000940	
16	3056	0.000290	
11	2940	0.000039	
7	2926	0.006700	
8	2926	0.000940	0.004985
9	2926	0.008700	Mean (7–10)
10	2924	0.003600	
1	2886	0.009100	
2	2886	0.005800	
3	2886	0.000075	
4	2886	0.001300	0.002899
5	2886	0.001100	Mean (1–6)
6	2886	0.000018	

Source: BSC 2003b, Table 18, p. 94; DTN: LA0302GH831811.003.

NOTE: Lithic clast measurements were done in eighteen 1-m^2 areas in Lathrop Wells Cone outcrops. Elevations reflect relative stratigraphic position (early to late cone activity), as explained in the text. Multiply volume fraction by 100 to obtain percent.

Mean lithic-clast abundances range from 0.29 vol% to less than 0.002 vol% (maximum value noted here is the mean of patches 1 through 6 measured within the same unit; maximum single measured value is 0.9 vol%) (BSC 2003b, p. 18). The volume data indicate that lithic clasts abundance is greatest within the measured lower stratigraphic levels in the scoria cone and decreases one to two orders of magnitude upward in younger scoria intervals. Not surprisingly, the lithic clast production during eruption was not uniform throughout the cone construction period, and the variation suggests less vigorous conduit enlargement with time. This observation is tempered with the recognition that much of the scoria (and included lithic clasts) within volcanic cones is subject to avalanching, slumping, and redeposition during construction (McGetchin et al. 1974, p. 3268).

Lathrop Wells Cone lithic clast abundances are not unusually high. Within the studied exposures, which represent a substantial vertical section through the cone, no lithic clast abundances were encountered that are indicative of significant conduit-clearing activity at the cone (BSC 2003b, Section 6.4.2.1, p. 95).

There is a common occurrence of secondary mineralization by silica and/or carbonate that coats many lapilli and larger grain surfaces that may be the cause of the elevated volume of lithic

clasts obtained using computer-assisted image analysis (0.9 vol%; Doubik and Hill 1999, p. 60). Using this approach (digital images and image analysis) will result in a high estimate of lithic clasts.

3.4.3 Eruption Mechanisms and History for the Lathrop Wells Cone and Tephra Fall

The history of eruption phenomena that built the Lathrop Wells volcano is contained in the tephra cone and fall deposits, as described in *Characterize Eruptive Processes at Yucca Mountain, Nevada* (BSC 2003b) and by Crowe, Perry, Geissman et al. (1995) and Perry et al. (1998). Evolution of the Lathrop Wells volcano is tied to a general model of scoria cone formation proposed by McGetchin et al. (1974) and shown in Figure 3-7.

1. Within 1 km of the vent, the earliest eruption deposited moderately sorted coarse ash with up to 52 percent vesicular sideromelane droplets. These are similar in shape and composition to glassy droplets produced in fire (lava) fountains. The fire fountaining could have been from a north-south-trending fissure (parallel to the long axis of the oval-shaped Lathrop Wells Cone and equivalent to stages 1 and 2 in Figure 3-7). The predominantly glassy droplets imply a largely unimpeded spray of melt from a vent or fissure. Some conduit opening is implied from the 7.6 percent tuff lithic clasts in the ash. Closer to the vent, a greater proportion of tachylite and glassy tachylite than sideromelane is present, indicating that some quench-crystallization was occurring within the rising magma, possibly due to avalanching of scoria and ash back down the incipient crater slopes to intermittently block the vent. There are four or five repeating, upward-coarsening tephra sequences in the lowest 125 cm of the observed section, with no recognized unconformities. This can be interpreted either as a continuous "pulsing" eruption or the result of varying wind directions during this part of the eruption.

2. The tephra deposits immediately northwest of the Lathrop Wells Cone are representative of the hydrovolcanic phase of the eruption (Vaniman and Crowe 1981; Wohletz 1986). Hydrovolcanic activity can occur when rising magma comes into contact with water in an aquifer(s) or a shallow-water body at the ground surface (Fisher and Schmincke 1984; Wohletz and Heiken 1992). The resulting steam explosions fragment the magma into predominantly ash- and lapilli-sized particles and produce large amounts of kinetic energy. When these explosions occur below the ground surface, the host rocks are highly fractured and the eruption products contain abundant lithic clasts. Hydrovolcanic deposits consist mostly of ash deposited in density currents (surges), leaving distinctive thin planar beds and cross-beds, which are typical of the sequence immediately northwest of Lathrop Wells Cone. Most basaltic hydrovolcanic pyroclasts in hydrovolcanic deposits are glassy and have low vesicularity and blocky shapes (Heiken and Wohletz 1985). However, in many examples, there is some rounding, perhaps by grain-to-grain interactions in surges. Pyroclasts in hydrovolcanic surge deposits of the Lathrop Wells volcano are characterized by considerable edge modification (rounding). The fragmentation process produces consistently fine-grained tephra, at the Lathrop Wells Cone, median grain sizes for this tephra range from 0.15 mm to 0.5 mm. Volume fractions of lithic clasts in the fine-grained ash deposits range from 0.003 to 0.036 and consist mostly of white tuff and rounded quartz and feldspar sand grains. The presence of rounded

quartz and feldspar grains and tuff xenoliths in the hydrovolcanic deposits suggest the water-magma encounter may have occurred in the shallow surficial deposits upon which the cone was built. Crowe, Wohletz et al. (1986, p. 38) ascribe the dominant tuff xenoliths to the Tiva Canyon Tuff, which forms most of the surface outcrops in the area and is also a major constituent of the surficial colluvium. This hydrovolcanic event occurred during the early phases of the eruption.

3. Later cone-forming activity deposited moderately sorted lapilli with 81 percent to 92 percent tachylite and glassy tachylite pyroclasts. These are similar to ash and lapilli formed during later stages of scoria cone construction (Figure 3-7, stages 3 and 4; Heiken and Wohletz 1985). During later stages of cone formation, avalanching of scoria and ash down crater slopes blocked the vent, allowing degassing of magma and quench-crystal growth to occur (in contrast with the glass droplets formed during lava fountaining). Sporadic blasts carried out a mixture of scoria bombs, comminuted fragments of partly crystalline, quenched melt and recycled scoria bombs, lapilli, and ash that slumped into the crater. Lithic clast concentrations are low in these tephra-fall deposits.

   Exposed within the lower quarry wall is an abrupt transition from coarse Strombolian scoria lapilli to overlying fine lapilli and ash (Figure 3-6). This transition is inferred to mark an increase in eruption energy from Strombolian to violent Strombolian. Lapilli and ash fallout from a violent Strombolian eruption column were deposited on the upper slopes of the cone, became oversteepened, and avalanched downslope to be deposited as grain-flow material together with primary air-fall material raining down from the eruption column. These upper deposits are estimated to compose about two-thirds of the cone volume. The ash fall that is mapped beyond the scoria cone (Figure 3-8) is inferred to be related to this phase of the eruption.

4. Quarry exposures of the cone suggest cone building continued largely unabated. An event toward the end of the eruption deposited nearly 0.5 m of inward dipping, thin planar ash beds and cross beds, interpreted as hydrovolcanic in origin. Rounded quartz grains, although not numerous in the deposit, suggest this event may have occurred, once again, at shallow depth in or near the elevation of prevolcanic surficial deposits. Shallow groundwater in alluvium or sand-ramp deposits is inferred to have reached the near-surface conduit system, fueling a steam explosion. Above these fine-grained beds, coarse scoria deposits indicate a return to the less violent eruptions that preceded this brief hydrovolcanic event. These scoria deposits are some of the last observed units that were deposited on the cone.

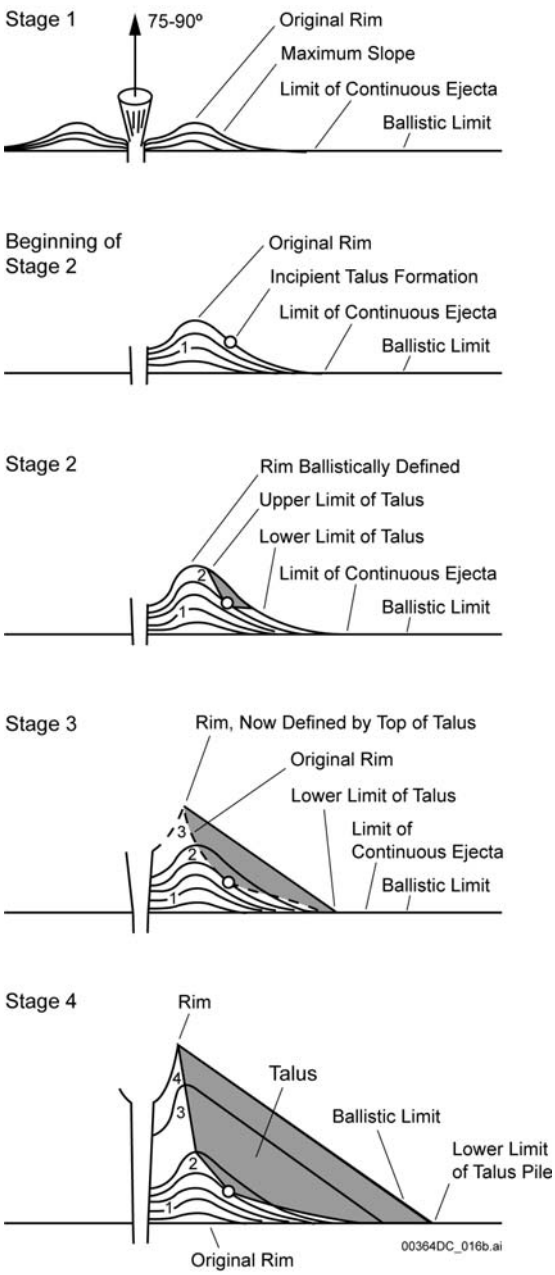

Source: McGetchin et al. 1974, p. 3,268.

NOTE: In stages 1 and 2, nearly all tephra are deposited ballistically (with the exception of finer material carried away by the wind). Much of this activity could be characterized as lava fountaining. At the Lathrop Wells Cone, this sequence would include hydrovolcanic activity that formed hydrovolcanic beds outside the low-rimmed scoria ring. Early activity could have consisted of fountaining along a fissure, accounting for the N-S elongation of the cone.

In stages 3 and 4, cone growth occurs during Strombolian and violent Strombolian activity. Early Strombolian activity consists of bursting gas bubbles in ponded lava; blockage of the vent by slumping of unconsolidated ejecta leads to intermittent Strombolian blasts. Later violent Strombolian activity involves fallout of lapilli and ash from sustained eruption column(s), adding to the cone volume and depositing a tephra blanket beyond the cone flanks. Occasional interbeds of hydrovolcanic tephra reflect intermittent interaction with groundwater.

Figure 3-7. Stages of Scoria Cone Formation

3.4.4 Tephra Distribution and Description

The tephra deposits beyond the Lathrop Wells Cone flanks provide important information about the character of eruptive processes that could result in the dispersal of waste-contaminated material in the event that a similar volcano erupted through the repository.

Figure 3-8 shows estimated isopachs for the thickness of tephra from violent Strombolian eruptions of the Lathrop Wells volcano. The isopachs are drawn based on a visual fit to the data collected from both hand-dug pits and natural exposures. The tephra thicknesses in most instances represent minima because of erosion of the tops of the sections of tephra. The maximum thickness of the tephra-fall deposits is 2.5 to 3 m in exposures near the base of the scoria cone, and the approximate area enclosed by the 1-cm isopach is 300 km^2. The northern 1-cm isopach is chosen to be near the location of Solitario Canyon fault trench T8, where U.S. Geological Survey workers exposed Lathrop Wells ash within deposits in the fault plane (Perry et al. 1998, p. 425). The amount and condition of ash particles suggest they represent ash runoff from the surrounding slopes and deposition in the fault plane when it was open during or soon after the earthquake that exposed the fault plane. Scattered basaltic ash on the west side of Busted Butte (Crowe 1996, p. 54) suggests that some Lathrop Wells ash was also deposited there. Although no primary ash deposits are preserved at these two distal exposures, the original thickness of ash deposited was probably about 1 cm.

The known tephra distribution around the Lathrop Wells Cone suggests that during eruption the lofted basaltic ash column was dispersed northward by prevailing winds, with minimal ash deposition south of the cone.

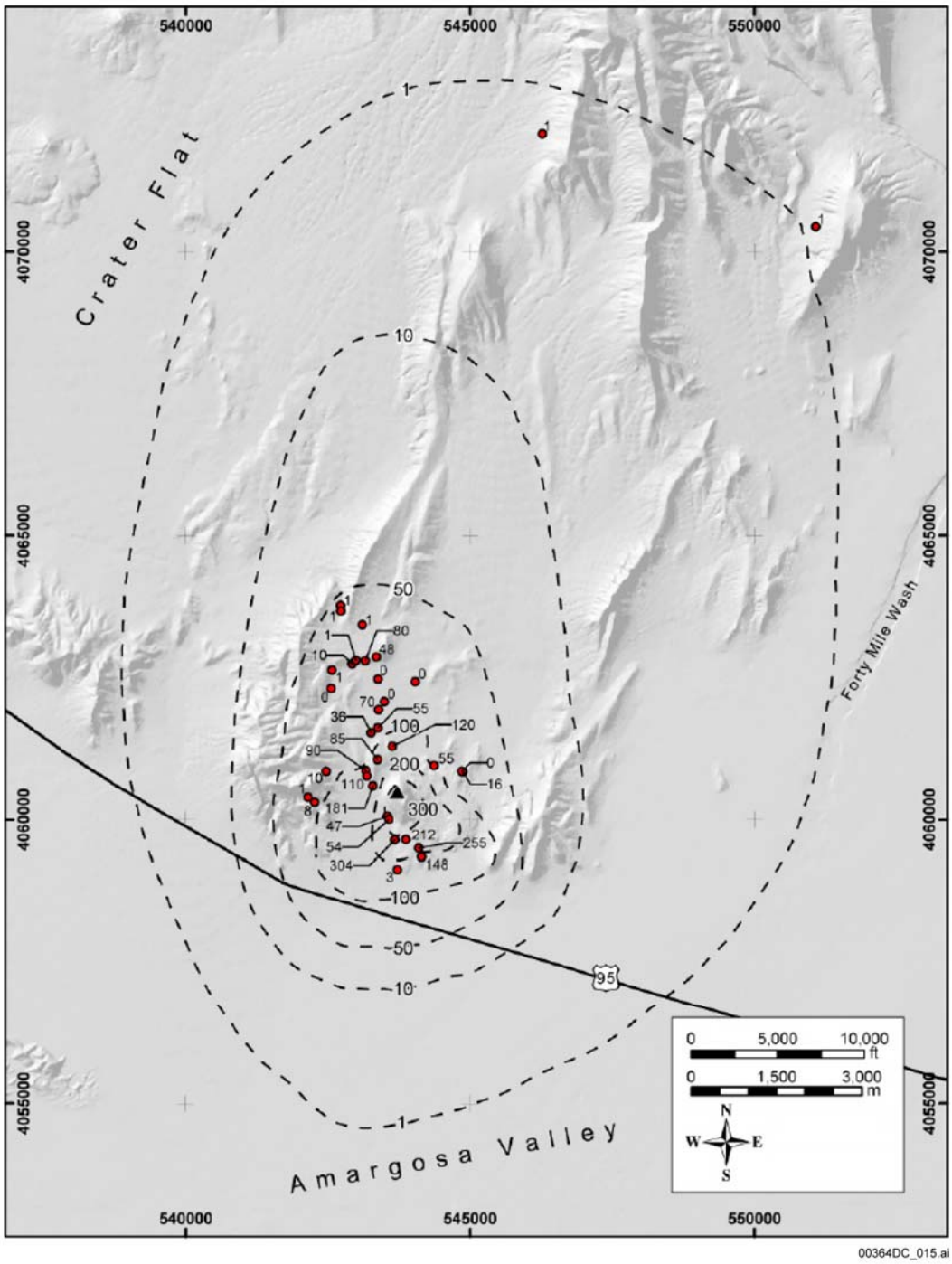

Source: Krier and Harrington 2003, p. 153.

NOTE: The triangle marks the volcano summit; the numbers are thicknesses, in centimeters, in dug pits or natural exposures. Approximate limit of the ash deposit is indicated by the 1 cm isopach.

Figure 3-8. Isopach Map (Estimated) of Tephra Fall from the Lathrop Wells Volcano

3.4.5 Magma Eruption Rates and Duration

The duration and magma-eruption rates of Yucca Mountain basaltic volcanism can be estimated by using information from the observed eruptions of analog volcanoes. No single analog volcanic system makes a perfect fit for the monogenetic, alkali-basalt scoria cone in a continental setting with eruptive volume in the range of 0.01 to 1 km^3, because volcanic eruptions are unique events. Detournay et al. (2003, p. 17-19, Appendix 2) surveyed and discussed eruption narratives from Strombolian and violent Strombolian eruptions to show the variability of such eruptions and their relevance to Pliocene-Quaternary and possible future volcanism at Yucca Mountain.

The duration of short-lived basaltic eruptions ranges from less than a day to tens of months. During violent Strombolian eruptions, peak mass eruption rates of approximately 10^6 kg/s are possible, and a sustained violent Strombolian eruption could produce 0.1 km^3 (the total Lathrop Wells volume) in about one day. This is extreme behavior, and for the more typical Strombolian eruption rates of approximately 10^4 to 10^5 kg/s, eruption durations are on the order of months to years. Eruptions that produce 0.1 to 1 km^3 typically last one to several years (Detournay et al. 2003, Appendix 2, Section A2.5.2 and Table 2D). The erupted volumes of Pliocene-Quaternary Crater Flat volcanic centers are between about 0.01 and 0.1 km^3 (Table 2-1). These volumes suggest eruptive durations in the range of weeks to months, assuming an average Strombolian rate of 10^4 kg/s over the course of the eruptions. At such a rate, the Lathrop Wells volcano would have formed in about 5 months. The rates cited above are peak rates. If periods of normal and violent Strombolian activity are interspersed with the effusion of lavas, then average mass-flow rates of approximately 10^3 kg/s are more representative, and the Lathrop Wells eruption may have continued for several years.

4. CHARACTERISTICS OF DIKE WIDTHS, DIKE SWARMS, AND ERUPTIVE CONDUITS

4.1 DIKE WIDTHS

Crowe, Self et al. (1983, p. 266) measured basaltic dikes intruded into tuff at eroded volcanic centers of the Yucca Mountain region, and observed dike widths ranging from 0.3 m to 4 m, with most dikes between 1 and 2 m wide. The typical dike-width dimension assigned by the PVHA experts was 1 m (CRWMS M&O 1996, Appendix E).

4.2 DIKE SWARMS

Most basaltic volcanoes in the Yucca Mountain region are small in volume and fed by one main dike, along which a central and subsidiary vents formed, but sets of dikes are also present. The Lathrop Wells volcano is probably underlain by three dikes (inferred from Perry et al. 1998, Figure 2.10): (1) the dike that fed the main cone and small spatter vents in a chain to the north and south of the cone, (2) a dike that fed spatter and scoria mounds in a parallel chain just to the east of the main dike, and (3) a possible dike that fed scoria vents near the northern edge of the volcano, although these could be an extension of (2) above. Although not exposed by erosion or quarrying, there are also likely to be small dikes that radiate outward from the conduit of the main cone. This is suggested by the short (within a few hundred meters of the central vent), crudely radiating dikes that are enclosed in near-vent scoria at the eroded Pliocene basalt centers of Crater Flat (Vaniman and Crowe 1981) (Figure 2-11). The Paiute Ridge intrusive complex, approximately 55 km NE of Yucca Mountain, which appears to have fed at least one volcanic vent (evidenced by the presence of lava-flow remnants and a plug-like body), may have as many as 10 dikes, in addition to sill-like bodies (as inferred from examination of Perry et al. 1998, Figures 5.15 and 5.16).

Analyses of a variety of basaltic volcanic fields indicates that the spacing between multiple dikes can vary from about 100 m to approximately 1 km. Based upon field observation and map measurement, the estimated dike spacing at Lathrop Wells volcano is approximately 320 m between the two inferred NW-trending dikes that fed the cone and the linear set of scoria mounds (vents) immediately east of the cone. Spacing is approximately 700 m between the mounds and an inferred third dike related to scoria mounds on the eastern lava flows. For the Paiute Ridge, intrusion, measurements from the geologic map of Byers and Barnes (1967) show that the mean dike spacing for dikes greater than 1 km long is approximately 995 m (maximum 1,440 m; minimum 250 m) (Perry et al. 1998, Figure 5-15). For the 3.7-Ma-old Crater Flat basalts, dike spacing is approximately 385 m (Perry et al. 1998, Appendix 2-M1). Map measurements from the Rim Rock, Texas dike swarm (18–23 Ma; Dasch et al. 1969), taken from a population of about 100 dikes, gives an average of 410 m (standard deviation equal to 430 m) for a N-trending dike set and 690 m (standard deviation equal to 482 m) for a NW-trending dike set. Dike spacing in the Yucca Mountain region generally ranges from about 100 m to 690 m (BSC 2003b, Table 37).

4.3 ERUPTIVE CONDUITS

Most observed basaltic eruptions begin as fissure eruptions, discharging magma where a dike intersects the Earth's surface, and soon focus into roughly cylindrical conduit eruptions. The best data to constrain conduit diameters and depths to which conduits extend would come from basaltic volcanic necks exposed by erosion, where direct measurements could be made of conduit diameter and variation with depth. Although many volcanic necks have been mapped as part of regional studies, few have been measured in detail, at least for the basaltic compositions of interest in the Yucca Mountain region. Without direct measurements of conduit diameter in the Yucca Mountain region, estimates are based on analog volcanoes.

The transition from magma flow in a subplanar dike to flow in a cylindrical plug has been inferred at many field locations (e.g., Delaney and Pollard 1978, p. 1212; Hallett 1992a, p. 140). From a continuum-mechanics view, a planar dike is the preferred form for propagation of magma through brittle and elastic host rock, whereas a cylindrical conduit is the preferred form for magma flow and delivery to the surface (Delaney and Pollard 1981, p. 1). Several processes have been put forward to explain this transition, including (1) magma viscosity variations induced by the solidification of magma at dike margins (Wylie et al. 1999); (2) brecciation and erosion of the dike wall rocks, as in the Shiprock NE dike (Delaney and Pollard 1978; Delaney and Pollard 1981) and the San Rafael dikes (Delaney and Gartner 1997); and (3) progressive melting of the host rocks, enhancing localized flow (Quareni et al. 2001).

Once a zone of widening and flow focusing has initiated, the evolving conduit may continue to widen. Several hypothetical processes, similar to those for the initial dike enlargement, have been described to explain this: (1) erosion from shear stress of flowing magma below the fragmentation level (Dobran 2001, p. 481), (2) thermoelastic stressing of wall rock (McBirney 1959, p. 443; Valentine and Groves 1996, p. 85), (3) erosion from particle collision above the fragmentation level (Valentine and Groves 1996, p. 85; Dobran 2001, p. 481), (4) conduit-wall collapse due to variations in magma pressure or shock/rarefaction waves) (Dobran 2001, pp. 480 to 484), (5) hydromagmatic processes involving the interaction of magma with groundwater or saturated sediment (McBirney 1959, pp. 443 to 445; Valentine and Groves 1996, p. 85), (6) conduit-wall collapse due to offshoot dikes (Valentine and Groves 1996), and (7) pore-pressure buildup (Delaney 1982, Valentine and Groves 1996, p. 85; McBirney 1959, p. 443).

Volcanic conduits are features that integrate magma paths over the duration of a volcanic eruption. Although a conduit may be large, only a fraction of it might be active at any given time during an eruption: the entire cross-sectional area of a conduit may transfer magma to the vent (e.g., Keating and Valentine 1998; WoldeGabriel et al. 1999), or to only a fraction of its cross-sectional area within a localized flow annulus, due to variations in flow velocity or viscosity (Hallett 1992b; Detournay et al. 2003).

Basaltic conduits vary greatly in diameter, depth and geometry. Valentine and Groves (1996) used the well-established sedimentary stratigraphy beneath the tephra deposits of Alkali Buttes, Lucero Volcanic field, New Mexico, to evaluate the variations in conduit size beneath a monogenetic alkali-basalt center. Based on xenolith data and assuming a 1.5-m-thick feeder dike, the conduit that formed in the sedimentary country rock is calculated to range in diameter

from 3.5 to 10 m. The upper 500 m of country rock at Alkali Buttes consists of mudstones and shales that provided a wet host rock, as indicated by lithic-rich hydromagmatic deposits. Conduit-size calculations, based on the proportion of lithics in these hydromagmatic deposits, indicate that a cylindrical conduit up to 40 m wide may have formed in the uppermost strata. A flared conduit could also have developed, varying in size from 6 m at depth to 300 m at the surface, which is a diameter equivalent to the mapped extent of the hydromagmatic deposits (Valentine and Groves 1996, p. 75).

In a similar investigation, Mastin (1991) calculated the size of a rhyolite conduit, using both the proportion of lithics in the eruption deposits and the results from a drillcore through the conduit (Eichelberger et al. 1988, p. 13,208). About 1 km^3 of tephra was erupted, and the dominant eruption mechanism was hydromagmatic, with less than 10 percent juvenile material. At 300 to 600 m beneath the vent, the conduit was estimated to be on the order of 20 to 30 m in diameter (Mastin 1991, p. 590).

An upper bound for basaltic conduit diameter in the Yucca Mountain region is 150 m, which is the diameter of the Grants Ridge conduit in New Mexico (Keating and Valentine 1998, p. 41; WoldeGabriel et al. 1999, p. 392). A conduit diameter of this size is expected to be a conservative upper bound for Yucca Mountain, because the Grants Ridge plug formed during an eruption of several cubic kilometers of alkali basalt (compared, for example, to the much smaller Lathrop Wells volcano with its approximate total volume of 0.086 km^3). Based on data from the Yucca Mountain region and selected analog regions, the conduit diameter for a future basalt volcano is, therefore, constrained at its lower bound by 1- to 2-m-wide dikes, and at its upper bound by the 150-m Grants Ridge plug.

Doubik and Hill (1999, p. 59) used a process that may overestimate the volume fraction of tuff xenoliths (see Section 3.4.2) to estimate a 50-m conduit diameter for the Lathrop Wells scoria cone. Thick Miocene volcanic units beneath the Lathrop Wells volcano are lithologically similar, making it difficult to assign relative proportions of those units represented by lithics. Given the limitations on specific data to test the assumptions made by Doubik and Hill (1999, p. 59), their estimate of a 50-m conduit diameter for the Lathrop Wells Cone is used as a mode or most likely value for conduit diameter at depth for potential eruptions at Yucca Mountain.

INTENTIONALLY LEFT BLANK

5. SUMMARY OF THE VOLCANIC CONSEQUENCES ANALYSIS

Because the probability that volcanic events could intersect a repository at Yucca Mountain has been estimated to be slightly greater than one chance in 10,000 over 10,000 years (a mean value of 1.7×10^{-8} per year), DOE has evaluated the potential consequences of such activity. Based on the geologic and volcanic history of the Yucca Mountain region, it is expected that any future igneous or volcanic activity would be similar to the basaltic activity that formed the small scoria cones in southern Crater Flat. The Lathrop Wells Cone is the largest of these. These small volcanic systems are fed by narrow basaltic dikes that ascend from depths of 40 km or more, and are typically a few kilometers in length and 1 to 2 m in width (BSC 2003b, Section 7). The intersection of such a dike with the repository could impact repository performance by thermally or mechanically damaging waste packages inside emplacement drifts, or by affecting the geochemical environment and hydrologic conditions within the repository (BSC 2002, Section 4.2, paragraph 3). Damaged or breached waste packages would be susceptible to percolating water that could contact, dissolve and transport radionuclides away from the repository. This is known as the "igneous intrusion groundwater transport" scenario.

If the dike continued ascending to the surface and fed a volcanic eruption, it could damage or destroy packages within the eruptive conduit and entrain package materials and spent nuclear fuel or high-level radioactive waste within the volcanic ejecta (BSC 2002, Section 4.2, paragraph 2). This "volcanic eruption" scenario is important because it could lead to the airborne transport of radionuclides and direct exposure to the environment.

Figure 5-1 is a schematic depiction of a dike intersecting a repository: the first panel (upper left) shows the dike approaching an emplacement drift; the second panel (upper right) shows the dike intruding magma into the repository and continuing to ascend toward the surface; the third panel (lower left) shows the dike erupting at the surface, and the fourth panel (lower right) shows the dike cooling and degassing in place. The extent of consequences of a dike intersection and/or volcanic eruption would depend on the characteristics of the basaltic magma, the geologic and hydrologic conditions in the repository, and the configuration and design of the repository and its engineered barrier systems.

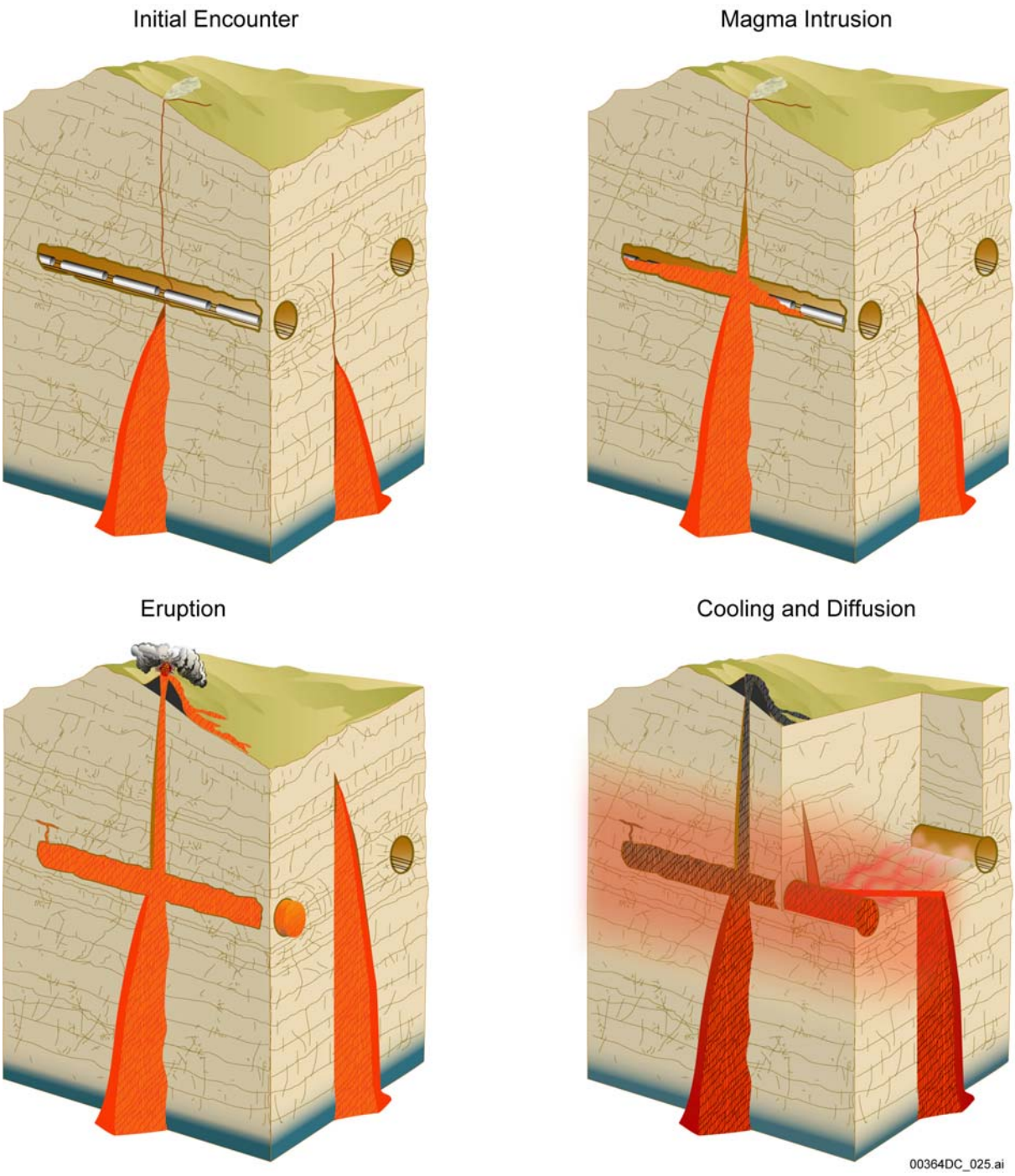

Source: BSC 2003a, Figure 1.

Figure 5-1. Schematic Drawing of the Processes Associated with a Dike Intrusion into or Eruption through a Repository

The analyses presented in the following sections describe the processes that could lead to radionuclide releases from a repository. The consequences associated with igneous intrusion are summarized separately from those associated with a volcanic eruption through a repository. Both of the analyses depend on the probability estimates summarized in Section 2.

Section 5 is organized as follows:

- Section 5.1 describes a model developed to analyze the interaction of ascending basaltic dikes with the drifts containing waste in the repository. These processes determine the number of waste packages that could be affected, as well as the extent of potential damage to the packages.

- Section 5.2 describes analyses of how many drifts and waste packages would be affected by a dike intrusion into the repository. It discusses the length, width and orientation of dikes that could intersect the repository, the geometry of the repository emplacement drifts, and the number of packages that could be exposed to magma intrusion.

- Section 5.3 describes the effects that an intruding magma could have on the integrity of drip shields and waste packages, from the thermal and mechanical effects associated with an intrusion, and from geochemical changes to the underground environment caused by the exsolution of magmatic gas.

- Section 5.4 evaluates the consequences associated with a volcanic eruption through the repository. It describes the size, number and characteristics of eruptive conduits that could intersect the repository, and the number of waste packages that would be involved. It summarizes an analysis of the effect of erupting magma on waste packages and the waste form, including and the potential for packages to be destroyed and waste entrained in volcanic ash.

- Section 5.5 describes the areal distribution of volcanic ash and entrained waste that could be ejected in plumes during volcanic eruptions.

- Section 5.6 describes the redistribution of ash and radionuclides by surficial processes.

The models describing analyses of igneous and volcanic consequences are summarized in a series of analysis and model reports shown on Figure 5-2. The key references are *Characterize Eruptive Processes at Yucca Mountain, Nevada* (BSC 2003b); *Dike/Drift Interactions* (BSC 2003a); *Characterize Framework for Igneous Activity at Yucca Mountain, Nevada* (BSC 2003e); *Number of Waste Packages Hit by Igneous Intrusion* (BSC 2003c); and *Atmospheric Dispersal and Deposition of Tephra from a Potential Volcanic Eruption at Yucca Mountain, Nevada* (BSC 2003f). In addition, potential damage to waste packages during an intrusion is evaluated in *Igneous Intrusion Impacts on Waste Packages and Waste Forms* (BSC 2003d).

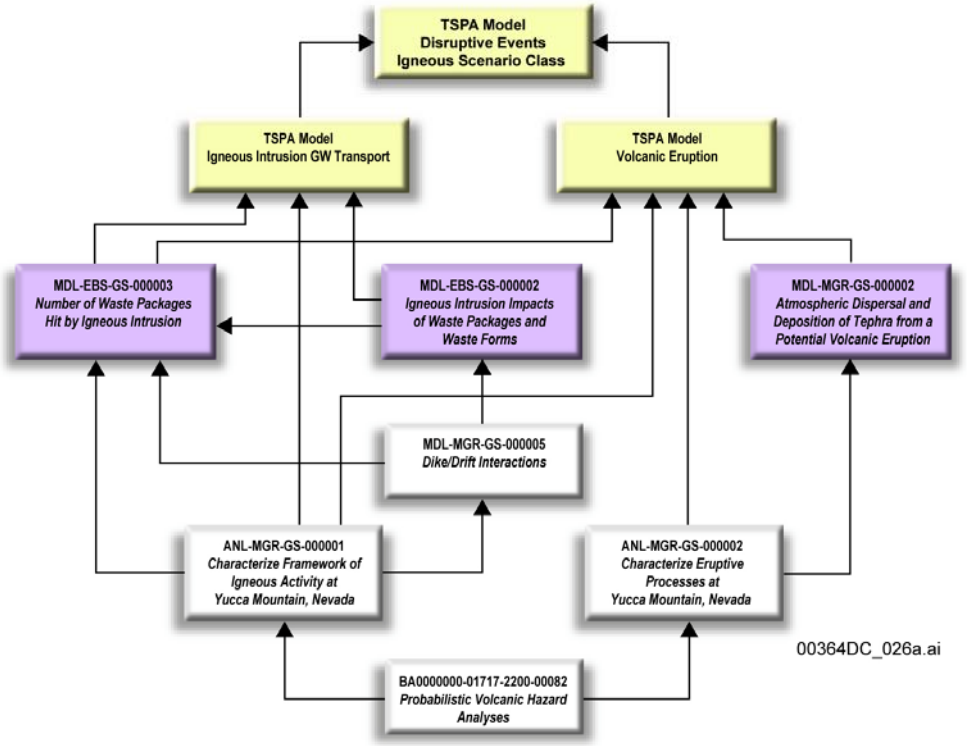

Figure 5-2. Model/Document Hierarchy Depicting the Relationship of Analyses and Models Supporting the Evaluation of Igneous and Volcanic Consequences

5.1 DIKE DRIFT INTERACTION MODEL SUMMARY

5.1.1 Model Description

The dike/drift interaction model was developed to analyze the behavior of magma and gases in ascending dikes that could intersect a repository. The model consists of two main components, a dike propagation model and a model of magma flow to the surface (BSC 2003a). Post emplacement effects (gas flow from the cooling magma and magma cooling) are also analyzed and discussed. These models describe processes ranging from initial propagation of the dike from depth, how the repository structure itself modifies that propagation, magma breakout to the surface, and effects such as cooling and gas transport. The key parts of the models, and the software codes used for the simulations, are shown on Table 5-1. Several alternative models of dike/drift interaction are also described and evaluated. One of these models (Woods et al. 2002) proposed that dikes intruding a repository could result in highly energetic pyroclastic eruptions accompanied by shock waves that travel the length of repository drifts. In this scenario, waste packages and other materials could be damaged and ejected from the repository through other repository openings such as ventilation shafts or through a new dike initiating at another point down the drift resulting in a "dog-leg."

Table 5-1. Table Outlining the Components of the Dike/Drift Interactions Model and the Software Codes Used for the Analysis

Dike/Drift Interactions Model Components	Software Code
Dike Propagation Model	
Propagation From Depth	NPHF2D
Effect of Natural Stresses on Dike Propagation	FLAC3D
Effect of Repository Structure on Dike Propagation	FLAC3D, spreadsheet
Diversion of Magma Into a Drift	NPHF2D, FLAC3D, spreadsheet
Model For Magma Flow	
Flow Through Mined Openings	FLAC3D
Crack Opening Rates	UDEC, FLAC3D
Stress-Related Effects	spreadsheet
Fracture Criteria	N/A
Magma Cooling Rates	spreadsheet
Synthesis for Dog-Leg	N/A
Postemplacement Effects	
Gas Flow Between Drifts	TOUGHREACT
Magma Cooling and Solidification	spreadsheet

The conceptual model for dike propagation considers a dike to be a pressurized fracture, much like a hydraulic fracture created in an oil or gas well, which is fed by a high-pressure source of magma deep in the earth. Figure 5-3 schematically depicts the key features, processes, and properties that control the ascent of magma in dikes through the shallow crust. The hydraulic-fracture model includes a sink point or drain to model loss of magma flowing into a repository.

The pressure of the magma in the dike pushes aside the surrounding rock, creating dike widths up to several meters. The restricted width of the dike induces frictional losses in the magma that result in a pressure drop along the length of the dike. Thus, the overall dike-propagation model is constrained by a balance between the pressure necessary to keep the dike open at a given width and the appropriate restriction (width) necessary to keep the pressure at the required level through viscous losses (energy dissipation).

Although liquid or vapor such as water can move from the magma into the wall rock surrounding the ascending dike, the magma viscosity is too high for it to leak into the host rock. The model simulates the propagation of the crack tip ahead of the ascending magma and includes a free surface, so that effects near the earth's surface, such as unstable growth and an altered width distribution, can be evaluated.

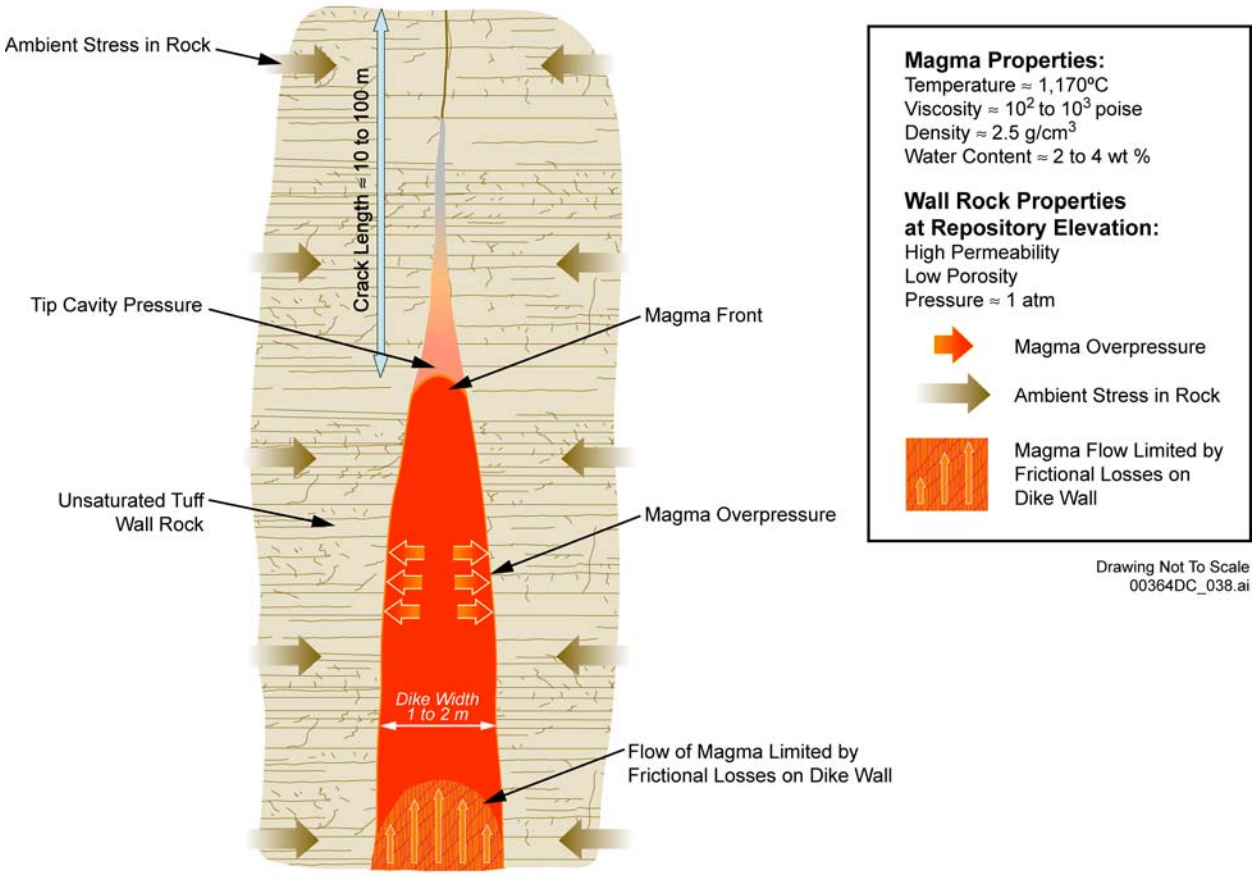

Source: Modified from Detournay et al. 2003, Figure 3-1.

Figure 5-3. Schematic Depicting a Magma-Filled Dike Ascending through the Crust, Showing Magma, Rock Properties, and Physical Conditions that Affect the Rate of Ascent

Most dikes have a limited strike length (approximately 1 to 5 km) compared to their depth of origin. Thus, although they are clearly three-dimensional features, it is reasonable in near-surface environments such as the repository to use a two-dimensional approximation of dike propagation for calculating dike parameters. The basic components of the dike model include (1) the elastic deformation of a crack due to the internal pressure of the fluid, (2) the viscous losses of the moving magma within the fracture, (3) fluid losses into the surrounding medium, and (4) a crack propagation criterion that accounts for the resistance of the rock to fracture. These components must be calculated interactively to assure proper coupling of the various mechanisms. A detailed description of the mathematical formulation of the dike-propagation model, including the simplifying assumptions and limitations, is presented in *Dike/Drift Interactions* (BSC 2003a).

The input data for the dike propagation model consist of formation (rock) properties, magma properties, boundary stresses, and dike parameters. The inputs are summarized in *Dike/Drift Interactions* (BSC 2003a, Section 6.3.4.2). There are uncertainties in these parameters because

of the scale of the calculations (dike length of several kilometers) and the possible changes in properties over such distances. The formation properties (those of the repository country rock) include Young's modulus, Poisson's ratio, and density and fracture toughness. Fracture toughness has not been specifically measured for the repository, but the results of the analysis are not sensitive at this scale.

Rock properties representative of units that host the repository were used for the model (BSC 2003g, Attachment V, Table V-5). Magma properties were derived from a survey of relevant literature, as described in *Characterize Eruptive Processes at Yucca Mountain, Nevada* (BSC 2001). Various dike velocity and width distributions were used to obtain the flow rate for the dike propagation. A range of magma densities between 751 and 2282 kg/m^3 was considered to allow for volatile exsolution. Viscosities between 10 and 40 Pa·s were used in the analysis. Most results are for a viscosity of 10 Pa·s, which is conservative because lower viscosities enhance dike/drift interaction by maximizing magma flow in drifts. The boundary stresses include the overburden stress and the distribution of the minimum principal horizontal in situ stress (against which the crack must open). The distribution of the minimum principal horizontal in situ stress is taken from either (1) stress measurements at Yucca Mountain for in situ conditions or (2) thermal-mechanical modeling of the repository due to heating. Both cases are considered in the calculations and serve as the two logical end points of possible stress distributions. The density of the rock mass was used to establish a value for magma buoyancy and to fix the magnitude of overburden stresses in the dike propagation model.

The rock mass, which in reality is a heterogeneous, layered medium, is modeled as homogeneous and isotropic, and ground surface is assumed to be planar. A uniform depth of the repository (300 m) was used as an input for the analysis.

Dike widths and dike propagation rates depend on rock mass density, the coefficient of horizontal stress, and magma density. In the model, these three parameters are combined in a dimensionless group called relative density. Conditions of dike ascent are controlled by value of relative density. A wide range of relative density between 2.67 and 20.28 has been investigated. Boundary conditions for the model can be specified to be either the magma injection rate at the source depth or the far-field magma velocity and dike width. Because conditions of dike propagation are usually specified in terms of far-field velocity and width, these parameters were used as boundary conditions. Magma velocities between 1 and 15 m/s, and dike openings between 0.12 and 3.49 m were analyzed.

The inputs for the magma flow into drifts analysis are the diameter (5.5 m) and spacing of drifts (assumed to be 80 m), the diameter of waste packages (assumed to be 1 m), the density (2000 kg/m^3) and viscosity of the magma (1 to 10 Pa·s), the velocity of the magma front approaching the drift level (1 to 10 m/s), and the width of a dike at drift level (1 m). The waste package diameter was varied to illustrate how its presence would affect the flow of magma. The effect of reduced flow due to obstructions such as waste packages is greater than just that of a reduced open cross-section of a drift, because of increased viscous drag. This combined effect is included in the equations to be solved as the "hydraulic radius" (R_h) defined as the open cross-sectional area divided by the wetted perimeter of the flow.

The magma density is a nominal value that is more than the fully expanded density that would be found in a pyroclastic flow but less than the fully condensed value provided in *Characterize Eruptive Processes at Yucca Mountain, Nevada* (BSC 2001). It is intended to represent a magma which is partially degassed enough to flow into the drift effusively. The results of the analysis are affected only for the case of flow from a dike into a pipe, which is the controlling mode of flow when the magma supply rate and magma viscosity are high, and then only late in the short history of filling a drift. The magma viscosity and magma supply velocity are chosen to represent the lower and upper ends of the ranges described in *Characterize Eruptive Processes at Yucca Mountain, Nevada* (BSC 2001). Use of bounding values allows illustration of the effects of these variables on the solution.

5.1.2 Summary of Model Results

Although an ascending dike could theoretically be deflected around a repository by topographic and/or thermal-mechanical stress, the modeling described here makes the assumption that the dike will propagate through the repository. As the dike approaches the level of the drifts, the crack tip advances ahead of the magma front. This separation results in a vapor-filled cavity, which is the first part of the propagating dike that encounters the drift. A significant difference between the present model and previous analyses (see CRWMS M&O 2000c), is that the cavity pressure is taken to be negligible in the present model because of the very high gas permeability of the tuff (Detournay et al. 2003, p. 50). As the magma rises in the dike, the flow will be concentrated toward the center of the dike. There are two possibilities for the state of the magma as it moves upward into the cavity. One is that it steadily releases gas as it approaches the cavity. The other involves catastrophic gas release. Analysis using Stokes law indicates that gas bubbles formed as the magma ascends will rise faster than the liquid magma, so that the liquid at the magma front will have lost much of its volatile content. If this occurs, the magma will not be likely to produce violent explosive behavior when it encounters the repository, and it will flow effusively into the drifts. The results of a model of effusive flow into drifts are presented below. Alternative scenarios (in which gas explosively exsolves, and the magma flows into drifts as a fully or partially coupled two-phase gas-magma flow) are discussed in Section 5.1.3.

When the dike reaches the level of the repository, magma will be available to flow into drifts, like a fluid flowing into a pipe or over a weir in a channel. Figure 5-4 is a schematic drawing that depicts the hydraulic features of the flow model. The rate at which drifts are filled with magma will depend on the magma flow rate, as determined by the hydraulic properties (particularly viscosity) of the magma. The model used to calculate flow into the drifts is simplified, ignoring frictional losses at the dike/drift interface, and ignoring the hydraulic impedance of waste packages and drip shields within the drifts. Limited sensitivity studies have been performed to assess how restricted openings caused by obstructions could affect flow (BSC 2003a, Section 6.3.9.2.3.1.2). These analyses indicate that, for the range of magma supply rates and viscosities considered in the model, the rate at which magma would flow into drifts would not be significantly affected. Given the assumptions summarized above, magma

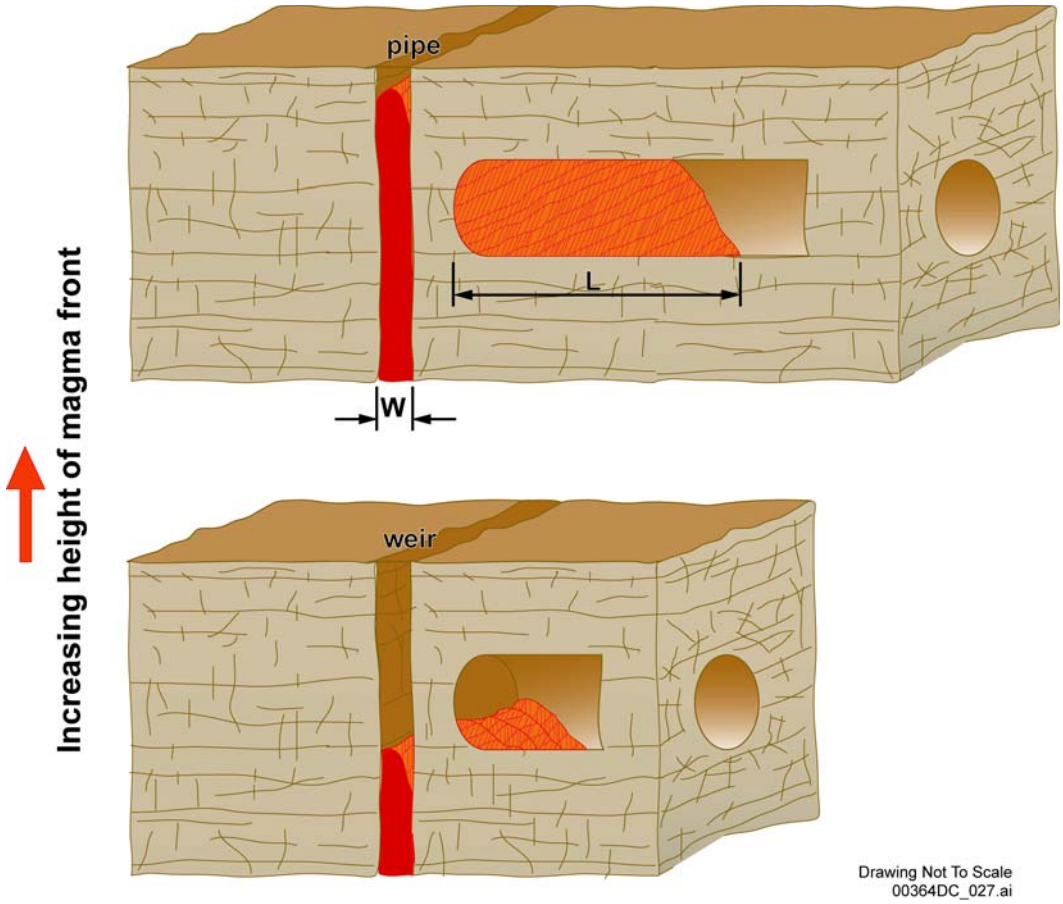

NOTE: The figure represents flow of magma for two distinct situations. In the lower drawing, the magma has not risen to the top of the drift, and a weir equation is used. In the upper drawing, viscous drag in either the dike or the drift limits flow and is appropriate.

Figure 5-4. Schematic Depicting Magma Flow from a Dike into a Repository Emplacement Drift

ascending at 1 m/s and with viscosity between 10 Pa·s and 100 Pa·s would flood the drifts in about 5 minutes. The magma front would not rise much above the drift level until the drifts were essentially filled. Magma rising at 10 m/s would fill the drifts in less than 1 minute. In this case, magma would continue rising in the dike, but its rate of advance would be slower as the magma drained into drifts. Drainage of magma into drifts would reduce magma front velocities from 5 m/s to 0.1 to 0.3 m/s for lower-viscosity (10 Pa·s) magma and to about 2 m/s for the higher-viscosity (100 Pa·s) magma (BSC 2003a, Sections 8.1 and 6.3.9.2.3.2). As the dike approaches the free surface, the crack tip accelerates, although the speed of the magma front is little changed. As a result, the vapor-filled cavity between the tip and the magma will lengthen. For a dike with the properties postulated, this process will already be underway when the tip reaches repository level. In the absence of any drifts, the crack would take about 100 s to grow from repository depth to breakout at the surface. This conclusion is based on treating the magma as an incompressible fluid.

Although loss of magma into drifts may slow the progress of the magma front to the surface, it will have little effect on the tip of the dike cavity, which will already have begun accelerating in response to the presence of the free surface and will reach it only seconds after passing the drift

horizon. Three-dimensional simulation of the diversion of magma from a dike to a drift (BSC 2003a, Section 6.3.9.2.3.3 and 6.3.9.2.3.4) has demonstrated that the diversion will cause both the height of magma in the dike and the pressure in the magma to be depressed directly above the drift, compared to portions of the dike that are between drifts. However, the delay in magma ascent will be short-lived, as the drifts would be filled with magma within a few minutes.

5.1.3 Alternative Conceptual Models

A variety of alternative conceptual models have also been considered in connection with the analysis of dike propagation and magma flow. Examples include analytic solutions of the fracture propagation problem, as well as a number of commercially available hydraulic-fracture models that are used in geothermal and waste injection applications.

Analytic conceptual models are useful for parameter estimation and have been used as a check on the models that predict the length, width, and pressure conditions in fractures of a given height. However, these models have limited applicability to the dike propagation and magma flow problem because they do not permit analysis of the effects of a free surface, and they do not include a sink point at a specific location that would enable the modeling of magma flow out of the dike and into a repository (BSC 2003a, Section 6.3.3).

Industrial hydraulic-fracture models are based on the same concepts as the analytic solutions, but numerical solutions allow additional flexibility in defining the problems modeled, especially with respect to the evolution of the height and length of fractures. As proprietary models, however, no detailed accounting of the equations, algorithms, or applications is available. Review papers indicate that various models yield widely different fracture geometries and pressures for the same input parameters. In addition, these models are primarily appropriate for fracturing at distances far from the free surface in layered media, not in near-surface situations. Due to these limitations, industrial models have not been used for simulating dike/drift interactions in a repository.

Several models of dike propagation using hydraulic-fracture principles with the addition of buoyancy effects were also evaluated. Although buoyancy may be important to the upward growth of a dike, and to magma density, none of the available models can accommodate a free surface or a leak-off point that would allow simulation of magma flow out of the dike. Thus, models considering buoyancy effects have not been used in the dike/drift interaction analysis (BSC 2003a, Section 6.3.3).

The Alternative Models of Woods et al. (2002)–The models described in Section 5.1.2 consider the effusive flow of low viscosity magma upward in dikes and laterally into repository drifts. An alternative model of dike/drift interaction at a repository was proposed by Woods et al. (2002). In this conceptual model, a dike intersecting a drift was hypothesized to cause the drift to fill with magma, after which the pressure would rebuild to generate a new crack opening some distance downdrift. This new opening would propagate to the surface (a “dog-leg” scenario) and become the main surface opening of the system. This model has been analyzed in detail in *Dike/Drift Interactions* (BSC 2003a, Section 6.4.11). The analysis considered the propagation of pressure and stress through the dike system, and the effect of cooling on magma

properties, and concluded that a secondary "dog-leg" dike could not propagate more than a few meters from the drift (BSC 2003a, Section 6.4.11.5).

Woods et al. (2002) presented another alternative model for flow of magma from a dike to a drift. Unlike the analysis described in Section 5.1.2, which simulates effusive flow into the drift, this model proposed rapid, explosive decompression, such that the bubbles formed would not be able to coalesce. In this case, the magma would rapidly expand as a two-phase mixture (a pyroclastic mixture of magma and gas), would accelerate upward (the only direction in which it is unconstrained) until reaching the drifts, and would then expand both into the drift and upward into the crack tip.

This explosive model assumes that the magma consists of liquid and vapor fractions that are fully coupled, meaning that they are constrained to move at exactly the same velocities and that they are at the same pressures and temperature. Vapor is also always assumed to be at equilibrium with the liquid—that is, that vapor exsolves (or dissolves) from the liquid instantaneously in response to pressure changes. Given these limiting assumptions, Woods et al. (2002) solved the hydrodynamic equations in a quasi-one-dimensional form in which the flow in both the dike and the drift is treated as being in the same direction. The equations used do not solve for any motions transverse to the direction of flow, and as such, the model is not two-dimensional. The boundaries of the drift and dike are treated as impermeable and rigid, much like a shock tube. The initial condition is that magma at high pressure fills the dike portion of the model and air at atmospheric pressure fills the remainder of the computational volume. The Woods et al. (2002, pp. 19-2 to 19-3) model predicts a wall of magma accelerating into the drift at speeds reaching:

> …tens to hundreds of meters per second, with the density decreasing as the pressure falls. Air is displaced and compressed ahead of the magma-volatile mixture and, as a result, a shock forms in the air and moves down the drift at speeds of several hundred meters per second. …on reaching the end of the drift, the shock is reflected and its amplitude increases by an order of magnitude. The shock then propagates back upstream, moving into the magma-volatile mixture and back towards the dike at speeds of 20–30 m/s. As the shock moves through the magma-volatile mixture, the mixture is recompressed. A region of higher pressure, of order several MPa, and hence higher density, develops between the end of the drift and the shock… The calculations suggest that, if the dike intersects the drift 200–300 m from the end of a closed drift, then the pressure within this drift will build up to about the initial level in the dike in a time of order 10 s.

The Woods et al. (2002) model represents a valuable first step toward developing a valid model of the flow of magma from a dike into a drift. However, the initial and boundary conditions in the Woods et al. (2002) model are unrealistic (Detournay et al. 2003, p. 51). In particular, the initial condition is not physically realizable and leads to results that are not achievable in nature. As described in *Dike/Drift Interactions* (BSC 2003a, Section 6.3.8.2), magma does not fill the propagating crack completely, nor does the crack reach its full width immediately after opening. Rather, there will be a vapor-filled tip, which is expected to be on the order of tens to hundreds of meters long. Near the tip, this crack will be only millimeters wide. Even if the magma were

to fill the crack nearly to the tip, the cross-sectional area of the intersection would be only a fraction of a square meter in this early phase, rather than the approximately 5.5 m^2 assumed by the Woods et al. (2002) model. This cross section would gradually increase as the crack propagated beyond the repository, a process that could take seconds to minutes (BSC 2003a, Section 6.3.9.2.3.1). At the rates of flow associated with effusive magmas (e.g., 5 m/s), shock waves would be unlikely to form in the drift. Specific analysis of the potential effects of a pyroclastic flow rising at a rate on the order of 100 m/s have not been performed, but may require further investigation.

The assumption of rigid, impermeable boundaries in the Woods et al. (2002) model adds to the severity of the consequences of magma interaction with drifts. Air, pressurized by the shock they describe, would seep into the walls of the drift, reducing the pressure behind the shock and decreasing its amplitude as it propagated. An even larger effect is to be expected at the blocked end of the drift, where the shock will encounter backfill. The backfill is quite compressible and will not reflect an incident shock wave nearly as efficiently as the rigid wall assumed in the calculation. In addition, the edge of the backfill will not be a vertical wall, as required by the one-dimensional numerical model of Woods et al. (2002), but will lie at the angle of repose. The net result of these real-world situations will be to greatly reduce the amplitude of reflection of any shock that might develop.

In addition, the Woods et al. (2002) model ignores phase separation between the silicate liquid and the volatiles. Although this assumption may provide an adequate estimate of steady flow in such a mixture, it is precisely the response to dynamic events such as shocks and rapid decompression that is not well treated with this assumption. In situations with such high accelerations, the differences in density between the vapor and the silicate magma become important, and the magma and vapor will move at different speeds. Only later, as viscous forces have had a chance to act, will the velocities approach each other. If these effects were included in the model, the result would be to reduce the sharpness of both compression and decompression waves and to increase dissipation of kinetic energy. Shock waves would be considerably dampened when propagating through such mixtures. Woods et al. (2002, p. 19-2) state that "the drift is assumed to be empty, and since the drift cross-sectional area is much larger than that of a 1.8-m-diameter canister, $A(x)$ is taken to be the total drift cross-sectional area." Although it is true that the ratio of area of the drift (approximately 23.8 m^2) to that of a canister (approximately 2.5 m^2) is large, a more important comparison would be that of hydraulic radii, R_h, equal to A/P, where A is the cross-sectional area and P is the perimeter (both exterior and interior) of the flow. The ratio of hydraulic radii is about 0.67, whereas the ratio of open areas is about 0.89. The smaller value will result in more drag and loss of energy in the flows than in the Woods et al. (2002) model. By not considering waste canisters, the Woods et al. (2002) model eliminates another mechanism for energy dissipation in the shock wave that their model produces.

In summary, the Woods et al. (2002) model of magma expansion into a drift overestimates the violence of the encounter. Realistic boundary conditions including compressible walls and backfill, permeable country rock and backfill, phase separation in the magma-volatile mixture, partial blockage of the drift by waste canisters and other engineering features, and the axial spacing of the canisters would combine to greatly reduce the amplitude of any shock wave that might form in the initial encounter. More importantly, use of realistic initial conditions such as a

dike tip would preclude the formation of a shock wave for all but the most rapid magma ascent rates.

Partially Coupled Liquid and Vapor Phase (Pyroclastic) Alternative Model–A third model for magma and gas flow in drifts is a partially coupled model in which the vapor phase and the condensed-liquid phase are free to move at different velocities subject to viscous drag of the continuous phase on the discontinuous one. Detournay et al. (2003, Section 3.3.3.2) postulated that magmatic material would be likely to first enter drifts as a pyroclastic flow resulting from gas exsolution and expansion of the magma–gas mixture. Although the fully coupled highly explosive scenarios considered by Woods et al. (2002) have been discounted, a model incorporating partially coupled magma and gas flow is probably the most realistic of the models considered. This model could also be used to simulate the potential for a pyroclastic "dog-leg" scenario, in which the magma–gas mixture would open and sustain a crack downdrift from the intruding dike and then flow upward to the surface. It is also the most complicated and difficult to simulate numerically.

If the discontinuous phase is vapor, then the fluid is magma with bubbles which may rise faster than the silicate liquid. Two-phase flow in which the continuous phase is the silicate liquid is not expected to be much different from the effusive case of the magma flow model (Section 5.1.2) because the liquid properties will dominate the flow. If the continuous phase is the vapor, then the rising magma will consist of droplets of magma suspended in vapor streaming past them. This latter case can be termed pyroclastic and, because of the large velocities that may result, is of concern. Such vapor-dominated flow can arise by decompression of a magma with dissolved gases, or by mixing of magma with water as the magma penetrates the environment. This latter mechanism would be termed "hydrovolcanic."

Four preliminary single-phase simulations have been conducted of the flow of a pyroclastic magma into a preexisting crack (initially 1 mm thick) using material properties representative of those derived by Heiken et al. (1988) in order to determine the feasibility of a similar phenomenon occurring at Yucca Mountain (BSC 2003h, Section 6.3.3.5). Details of the method are described in *Dike/Drift Interactions* (BSC 2003h, Section 6.4.10.2.1), where the model is applied to effusive flow. The calculation used the following properties:

- Overburden–300 m at density 2,400 kg/m^3
- Overburden Stress (Horizontal)–3.6 MPa (lateral stress coefficient of 0.5)
- Crack Orientation–Vertical along axis of drift
- Country Rock Young's Modulus–15 GPa
- Magma Pressure–12.6 MPa (9 MPa above overburden)
- Magma Viscosity–0.5 Pa·s.

In addition to these values, the bulk modulus of the pyroclastic magma was set at 50 MPa according to the following rationale. The bulk modulus of an ideal gas is equal to its pressure; however, with density near 1.0 due to mass loading by magmatic liquid and (perhaps) comminuted country rock, much of the volume will not be available to the gas component, so the mixture will be stiffer than an ideal gas, just as in a van der Waals gas. Thus, a value about four times the ideal gas value was selected for the simulation.

Four calculations of crack growth and magma flow were carried out at various scales: one with a zone size of 1 m extending to a height of 100 m above the drift, one with 2.7-m zones extending to 150 m above the drift, and two with 10-m and 20-m zones extending 300 m to the surface. Boundary conditions were varied to simulate an infinitely long dike in the strike direction and a dike of smaller strike length. The drift was explicitly represented in the small- and intermediate-scale calculations. In the large-scale calculations, a point source with prescribed magma pressure was assigned to the location of the drift. The small and intermediate calculations provide detail on the crack growth near the drift but do not extend to late enough times or large enough ranges to illuminate crack propagation to the surface. On the other hand, the large-scale calculations can follow the crack to the surface but will miss fine details.

The results of these calculations include the crack-width history at selected locations, the location of the magma front in the opening crack, and the velocity of the magma front. In the fine-scale calculation, the maximum crack width is about 27 mm. By 1.65 s, the magma has almost reached 32 m above the drift, where the crack width has opened to about 8 mm. The maximum crack opening for the large-scale simulations is about 170 mm at about 110 m from the dike; the opening at the surface is about 100 mm.

The two large-scale calculations indicate that the pyroclastic dike will reach the surface in 6 to 10 s. Linear extrapolation of the intermediate-scale calculations supports the conclusion, although the calculated time to breakout would be about twice as long (18 s).

The velocities of the propagating-magma front range from about 5 m/s to more than 75 m/s. Because the calculation models the magma as a single phase and the bulk modulus is at least four times the pressure, the velocity of the front will be close to the magma flow velocity. These results are consistent with the findings of Heiken et al. (1988), which were obtained with analytical forms, thus increasing confidence in the results.

Based on the results of these preliminary calculations, it appears that a pyroclastic dike as a "dog-leg" could reach the surface, if certain conditions were met. First, as noted above, the eruptive energy associated with a dike intrusion depends in part on the availability of water. Given a width of 0.2 m, an average velocity of 50 m/s, and a strike length of 10 m, the total volume flow rate would be 100 m^3/s, corresponding to a total mass (given the assumed density of the pyroclastic flow) of about 1,000 MT over 10 s. For a hydrovolcanic source, such flow rates may be reasonable, as sufficient water volumes could be present at the water table or in a perched water body. However, because of the very dry nature of the Yucca Mountain site, hydrovolcanic activity is thought to be unlikely (Crowe, Self et al. 1983).

A second assumption not addressed by these preliminary calculations is whether pressure in the propagating crack and dike of 9 MPa above overburden can be maintained for the 6 to 10 s needed for a pyroclastic dike to reach the surface. Detournay et al. (2003, Section 3.2.2.3) suggested that the large intrinsic permeability of the fractured tuffs that would host the repository was too high to maintain pressures approaching 10 MPa. For a nonhydrovolcanic source, where the pressure would derive from the kinetic energy of a pyroclastic flow down a drift, velocities in excess of 300 m/s would be needed with a flow density of 100 kg/m^3; this is not a likely flow environment (see BSC 2003h, Section 6.3.3.4) and would be unlikely to generate sustained pressures. This approximation also indicates that insufficient pressure to sustain a pyroclastic

dog-leg would accompany dike intrusion unless the magma came in contact with a substantial source of groundwater.

In summary, for a variety of reasons, Detournay et al. (2003, Section 3.4.8) considered the propagation of either a magmatic or pyroclastic "dog-leg" scenario to be quite improbable. The calculations summarized in Section 5.1.2 have confirmed this assessment for the magmatic (effusive) scenario. Analyses presented in this section indicate that the fully coupled and highly explosive pyroclastic flow scenario postulated by Woods et al. (2002) is inconsistent with the volcanic processes that would operate and conditions that would exist if a dike intersected the repository. However, Detournay et al. (2003, Section 3.5) also recommended further analyses to assess the impacts of a partially coupled pyroclastic flow scenario on repository performance. Preliminary analyses have been performed to identify under what conditions pyroclastic flows could occur and to assess their behavior during dike/drift interactions.

Further analyses to refine the partially coupled pyroclastic flow model are underway. These analyses will address several of the key assumptions and uncertainties that have not been addressed to date. A partial list of additional features that may be incorporated in the model includes accounting for cavity pressures in the propagating crack that are less than the magma vapor pressure, as well as other aspects of the coupling between vapor and condensed phases, variable material properties (e.g., temperature, composition, viscosity), and the dimensionality of the analysis (three-dimensional versus two-dimensional).

5.1.4 Uncertainties, Assumptions, and Limitations

The dike propagation and magma flow problem is relatively complex, and numerical modeling entails uncertainties, including the complexities introduced by the three-dimensional nature of the problem uncertainties with regard to fluid and rock properties, and the model assumption that the fluid is incompressible and has constant properties. The large range of possible magma properties (e.g., viscosity, density, temperature) has been dealt with through the evaluation of a range of conditions in an attempt to bound the problem. The boundary-element approach also requires homogeneous material properties for the host rock, and stratigraphic variability is therefore not accounted for.

Some of the key assumptions and limitations of the numerical models are summarized below (BSC 2003a, Section 6.3.5 and 6.4.6). Additional analysis of the effects of these uncertainties is planned to assess their effects on conclusions about the behavior of basaltic magma interacting with drifts. However, the bounding analyses and sensitivity studies completed to date indicate that the basic conclusions about magma flow are unlikely to change.

- Magma compressibility: The analysis of dike propagation assumes that the magma is incompressible, whereas basaltic magma within several hundred meters of the surface is a mixture of liquid and exsolved gas (with or without crystalline solids) that can be highly compressible (BSC 2001).

- Two-dimensional calculation: Although the problem of a dike propagating away from a deep magma source clearly is a three-dimensional problem, the behavior as the dike approaches the surface is considerably more constrained. First, the extent of the dike

along strike is generally much less than the length of the dike from source to tip. Second, the effect of the free surface will attract the dike as it approaches, thus limiting further breadth. As a result, the dike propagating upward near the surface takes on two-dimensional characteristics that are much more amenable to modeling.

- Elastic behavior: Elastic behavior is a reasonable assumption for small-scale pressurized fractures in the Earth but may be questionable for a dike-scale event within 1 km of the earth's surface where rocks are fractured. A dike would cross many discontinuities in the rock and would generate small earthquakes as slippage occurs in response to the changes in stress generated by the propagating dike. However, inelastic effects will serve to increase the width of the dike and decrease the pressure. These are competing effects. Because the pressure is the main factor for the subsequent calculation, using elastic behavior is a conservative assumption because it serves to generate the highest pressures.

- Linear-elastic properties: Most rocks have nonlinear behavior with lower moduli (a) at low stress and (b) at shallow depths in the presence of joints and bedding planes. Linear-elastic behavior produces the greatest possible pressure and is, thus, a conservative assumption.

- Homogeneous, isotropic material: Rocks are typically jointed, faulted and stratigraphically heterogeneous. Also, characteristics of the strata, joints and faults deep in the Earth are not known. Dike behavior near the repository has been modeled by using the rock properties measured at the repository. This assumption results in tractable models and a complete set of input parameters but is not necessarily conservative.

- Single fracture: Although many hydraulic fractures and dikes are known to exhibit multiple fracture strands and *en échelon* behavior, the overall impact of dike intersections with drifts is reasonably modeled with a single fracture. The high viscosity of the magma does not allow easy penetration of the fluid into joints or faults, and thus, secondary fracture strands are not easily initiated. Most volcanic systems are fed by one, or a small number of dikes.

- Laminar flow: Laminar flow of the magma in the dike is essential for pressure drop calculations under the Poiseuille formulation. Laminar flow is expected to occur for Reynolds numbers less than 2,000. Although Reynolds numbers do approach and may exceed 2,000 for some combinations of conditions, fully turbulent flow is unlikely for any possible set of conditions. Thus, it seems reasonable to assume laminar-flow behavior under all circumstances.

- Lubrication approximation: The lubrication approximation is appropriate (and exact) for slow motion of viscous fluids so that the viscous forces are considerably greater than the inertial forces, thus allowing the inertial forces to be neglected. The approximation appears to be appropriate for flow in a long two-dimensional fracture ("parallel flow") and has been used for 40 years in hydraulic fracturing with good success and no apparent discrepancies. Thus, this approximation appears reasonable and appropriate here.

- Newtonian fluid: A Newtonian fluid is one for which the relationship between stress and rate of strain is linear. This formulation simplifies calculations of fluid resistance and is known to apply to many common fluid systems. Although a more complex fluid rheology could be used (e.g., with yield stress and power-law behavior), little is known about magmas, and the additional parameters in such models would be highly uncertain. It seems more appropriate to assume Newtonian rheology and to vary the viscosity in accord with temperature and pressure changes.

- Stress-intensity factor governs tip behavior: The applicability of linear-elastic fracture mechanics has been questioned for large-scale fractures propagating under internal pressure. The dike-propagation problem is concerned with an even larger-scale feature and undoubtedly involves anelastic behavior in the surrounding rock. Thus, linear-elastic fracture mechanics may not be strictly appropriate for this application. However, the linear-elastic fracture mechanics formulation allows the fracture toughness to be used as a parameter that is indicative of the resistance of the rock to fracture, whatever the actual mechanism. Treated as a parameter, fracture toughness can be used to investigate the effect of any mechanism that resists fracture growth and thus increases the pressure.

- Horizontal free surface: The surface relief at Yucca Mountain is relatively severe, but the dike propagation model treats it as a horizontal surface. This approach is a conservative assumption because the additional load of the mountain would serve to deflect any dike away from the mountain (e.g., into the basins). However, analysis indicates that topography probably has a negligible effect on the dike path.

5.2 NUMBER OF REPOSITORY DRIFTS AND WASTE PACKAGES INTERSECTED BY IGNEOUS INTRUSION

The number of emplacement drifts that would be directly affected by igneous activity depends on the number, length, and orientation of the basaltic dike(s) intruding the repository, as well as the configuration of the drifts containing waste packages. Figure 5-5 depicts a dike approximately 4 km in length that would intersect 46 emplacement drifts along the north-south extent of the repository. This is the maximum number of drifts (spaced 81 m apart) that could be encountered by a single planar dike.

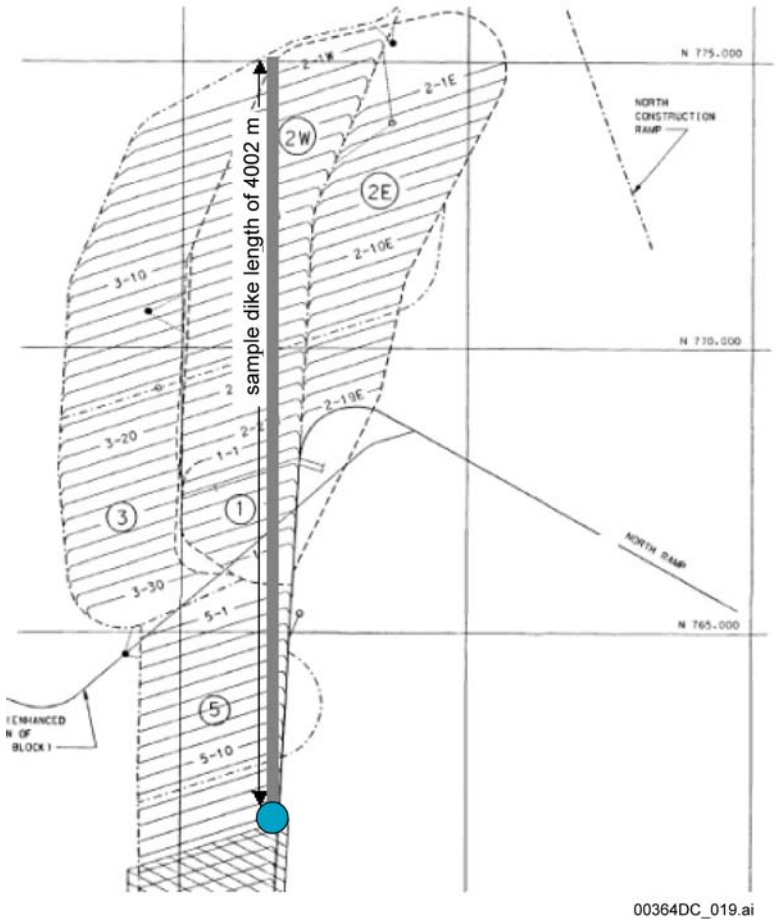

Source: BSC 2003c, Figure 2.

NOTE: For illustration purposes only. Dike width is exaggerated for clarity. The dike length in this example is approximately 4 km, which would encompass the entire length of the repository. The anchor point (shown as a blue dot) marks the point where the dike enters the repository.

Figure 5-5. Example of a Single Dike Intruding the Repository at Zero-Degree Azimuth

As described previously, typical lengths for individual dikes in the Yucca Mountain region range from about 1 to 5 km, and the range of maximum dike lengths has been estimated at 17 to 22 km (see Figure 2-10). Volcanic centers may be fed by a single dike, but systems with multiple dikes (known as dike swarms) also occur. For example, at the Lathrop Wells Cone, three dikes have been inferred. In determining the number of drifts intersected by a volcanic event, the number of dikes per event has been represented as a lognormal distribution with 3 as the mode, 1 as the minimum, and 6 as the 95th percentile. The distance between dikes (dike spacing) associated with single basaltic systems in the Yucca Mountain region is typically on the order of hundreds of meters (see Section 4.2). For the calculations described below, the distance between dikes is based on observations in the Yucca Mountain region and is specified as a uniform distribution ranging from 100 to 690 m.

The expected orientation of dikes that could intrude the repository has also been analyzed, and the effect of orientation on the probability of drift intersection has been characterized. Dikes tend to orient perpendicular to the least compressive horizontal stress (i.e., the direction of

extension), which in the Yucca Mountain region is oriented about N60W. Therefore, vertical dikes are expected to propagate within a range of azimuths but will favor an orientation of about N30E (see Section 2.1.2). Figure 5-6 shows the expected orientation of potential dikes. Because the emplacement drifts at Yucca Mountain trend at about N70E, dikes would most likely intersect the drifts at an angle of approximately 40°. The number of intersections would decline as the angle between dikes and drifts decreased. Dikes striking approximately N70E would intersect the fewest drifts, since dikes with that orientation would be parallel to the drifts.

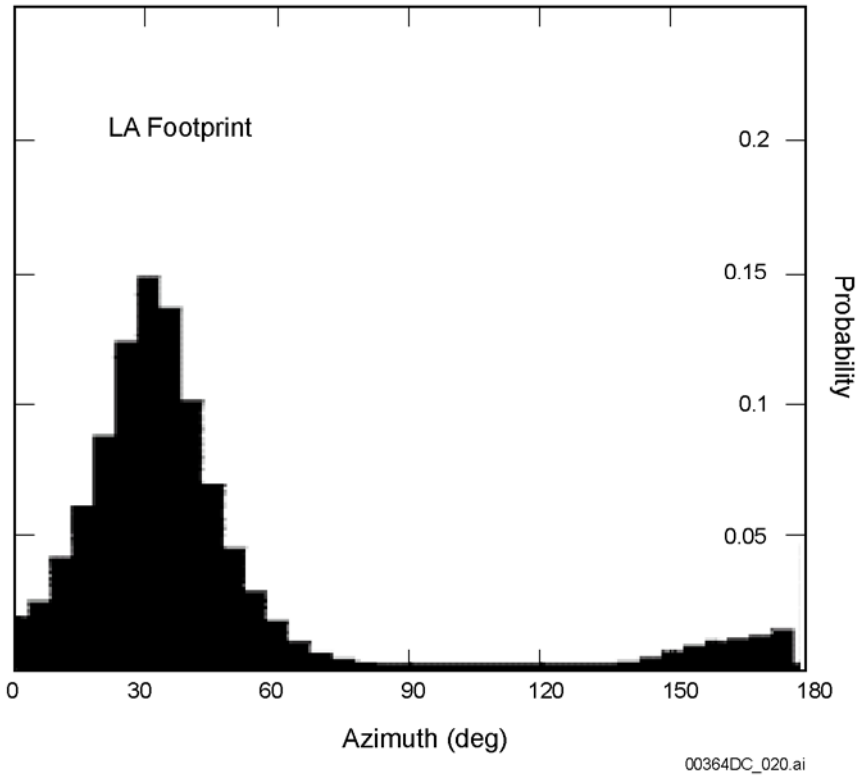

Source: BSC 2003e, Figure 22.

NOTE: The mean dike azimuth is about 30º (N30E), perpendicular to the least principal stress in the Yucca Mountain region.

Figure 5-6. Likely Orientation of Dikes Intruding the Repository

To calculate the potential number of dike–drift intersections associated with igneous or volcanic activity within the repository footprint, the ranges and distributions of the length, number, spacing (in the case of dike swarms), entry points (also called anchor points), and orientations of possible dikes have been probabilistically combined. The results of this analysis are documented

in *Number of Waste Packages Hit by Igneous Intrusion* (BSC 2003c; DTN: SN0311T0503303.003).

Figure 5-7 depicts several of the key parameters used to estimate the number of potential dike intersections with the repository if an igneous event occurred. A dike swarm is associated with a specific geographic location referred to as an "anchor point" and shown in blue in Figure 5-7. This point represents the entry point for the central dike of a swarm into the repository. The spacing between dikes can vary from 100 to 690 m. The dike lengths are constrained by the variability of the dike-length parameter. All dikes in a swarm are assumed to be parallel, but the azimuth angle is constrained by the sampled azimuth angle parameter.

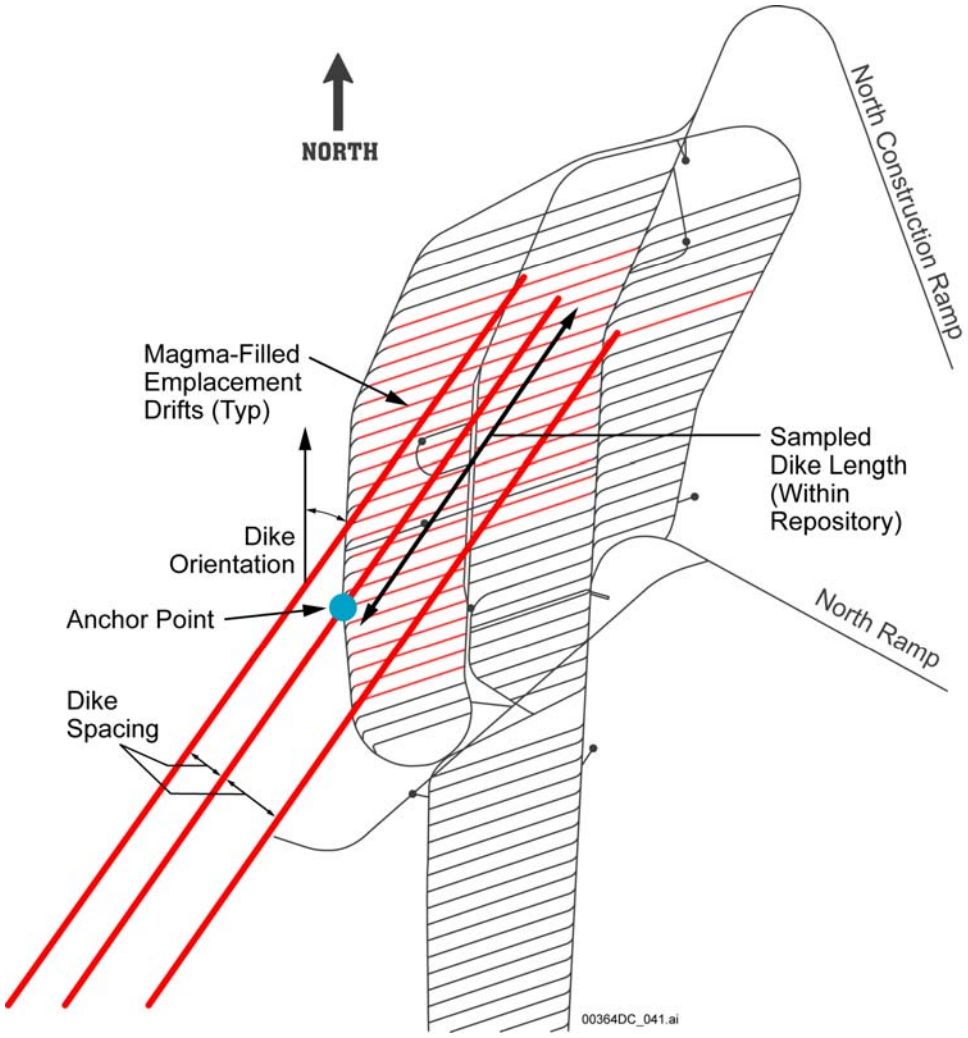

Source: DTN: SN0311T0503303.003.

NOTE: For illustration purposes only. Dikes shown in red are not to scale; dike widths are exaggerated for clarity. Drifts highlighted in red are those intersected by dikes. The anchor point is shown as a blue dot. The figure shows the parameters sampled by the model, including the number of dikes and dike orientation, spacing, and dike length within the repository.

Figure 5-7. Illustration of Dike-Swarm Implementation

The number of waste packages that would be contacted by magma intruding a repository depends on the number of drifts encountered and on the extent of downdrift flow of magma. As described in the previous section, the results of the dike–drift interactions model (BSC 2003a, Section 6.3.9.2.3.1.6) indicate that magmas may behave as low-viscosity fluids or as pyroclastic mixtures of magma and gas that could completely fill emplacement drifts, covering or engulfing all of the drip shields and waste packages contained in each intersected drift. Thus, the number of waste packages hit can be directly estimated from geometric analysis. The combined length of an average waste package plus the spacing between packages is 5.2 m (BSC 2003c, Section 4.1). For each drift that is intersected by a dike, the emplacement drift length is simply divided by 5.2 m. The average length of an emplacement drift is approximately 600 m, and, therefore, the average estimated number of waste packages per drift is approximately 115.

Each of the stochastic parameters is sampled to calculate the range and probability of the number of dike–drift intersections. In conjunction with that sampling, each intersection between the resulting configuration of dikes and drifts is calculated. The drifts that are intersected are used to calculate the number of waste packages hit, and the number of waste package hit is tallied for each case. The results are then averaged to generate a single composite cumulative distribution function, which is shown as Figure 5-8.

Figure 5-8 is a graph of the composite cumulative distribution function for the number of waste packages hit by a swarm of dikes intruding the repository. A wide range of possibilities is displayed, from virtually no waste packages hit to the entire inventory of more than 11,000 waste packages hit. The 50th percentile (median) shows approximately 1,610 waste packages hit.

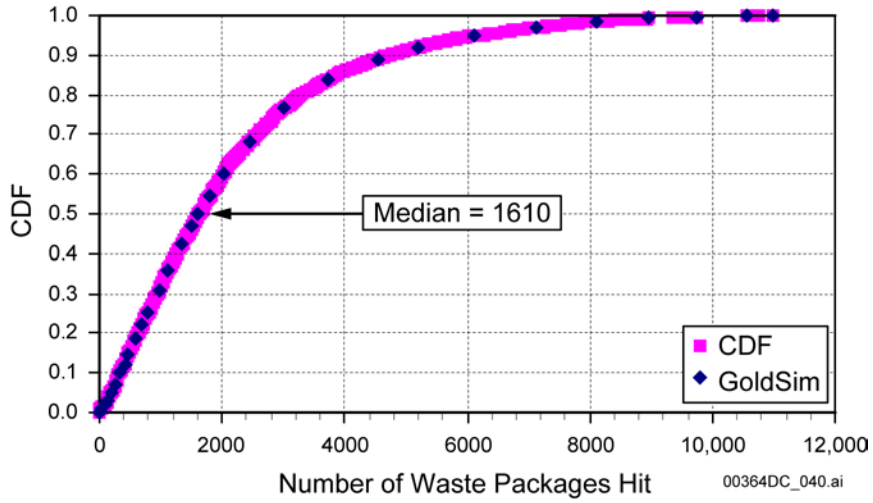

Source: DTN: SN0311T0503303.003.

NOTE: CDF = cumulative distribution function.

Figure 5-8. Cumulative Distribution Function of Number of Waste Packages Hit: Igneous Intrusion Scenario

As described in *Number of Waste Packages Hit by Igneous Intrusion* (BSC 2003c, Sections 5 and 6.3; DTN: SN0311T0503303.003), the assumptions used in this analysis are based on geologic observations (e.g., dike length, orientation, and number) of the characteristics of

volcanic events in the Yucca Mountain region. The parameter distributions used are considered to be representative of the potential future events. The analysis does, however, include some conservative elements. For example, it was assumed that all waste packages in each intersected drift would be damaged (BSC 2003c. Section 5.2).

5.3 DAMAGE TO ENGINEERED BARRIERS ASSOCIATED WITH IGNEOUS INTRUSION

The analysis of consequences to engineered barriers associated with igneous intrusion processes is built on the conceptual model of dike-drift interaction, which indicates that intruding magmas could, under certain conditions, flow down the length of repository emplacement drifts. In this case, all of the drip shields and waste packages in the affected drifts would be directly contacted and affected by the magma (this area within the repository is referred to as Zone 1). In adjacent drifts (referred to as Zone 2), the potential for damage to drip shields and waste packages due to deleterious geochemical conditions caused by heat and volatiles from the intruding magmas has also been evaluated.

During an igneous intrusion, drip shields, waste packages, and the other engineered features within the drift would be engulfed by magma. Depending on the magma characteristics and the energy associated with the intrusion, this would result in varying degrees of mechanical damage to the drip shields and waste packages and would expose them to thermal and geochemical conditions that would likely affect their integrity.

Although no direct testing or evidence has been identified to constrain the extent of damage that could occur in an intrusive event, several observations and related analogs have been considered in developing the consequence models. These are summarized below.

The temperature of intruding magma is estimated to range from 1,046° to 1,169°C (BSC 2003b, Table 37). The melting temperatures of the drip shield (Titanium Grade 7: 1,660°C), and the waste package materials (Alloy 22: 1,357°C; structural Stainless Steel Type 316NG: 1,375°C) (CRWMS M&O 1999, Section 5.1) are well above the magma temperature, but the strength of the metals would certainly decrease at magmatic temperatures.

Waste Package Behavior in Magma (CRWMS M&O 1999) provides calculations of the pressure that would develop within waste packages as the result of gas expansion at high temperatures. It concludes that as temperatures approach 1,200°C the resulting stresses on the packages would reach the tensile strength of the package materials. If a package was weakened by corrosion or other factors, its tensile strength could be exceeded by the internal pressure at temperatures lower than 1,200°C. Thus, thermal stresses provide a possible mechanism for package breaching.

A literature review on the performance of waste package and drip shield materials, documented by Structural Integrity Associates (Gordon 2003), suggested that the structural integrity of these materials would be compromised by exposure to magmatic environments. For example, Types 310 and 446 stainless steels, exposed to Hawaiian basaltic lava at 1,300°C for 100 hours, were extensively reacted and damaged, while alloy 718 suffered a loss of structural integrity (Gordon 2003).

Testing of transportation containers also provides anecdotal evidence that high energy impacts and high temperatures can damage metal containers. These tests considered 120 miles per hour truck impact accidents (with linear forces of up to 100,000 pounds/ft), variable energy shocks and vibrations, engulfing fire at 800°C temperature, and high energy explosions (Sanders et al. 1992, Appendix III; Fischer et al. 1987, Section 6.0; Sandoval et al. 1983). The containers were damaged to varying degrees during these tests, although the direct relevance to the igneous intrusion scenario is uncertain because the energy associated with the impacts and explosions probably greatly exceeds what would be expected during an igneous intrusion into a drift.

If magma intrudes the repository, waste packages and other engineered materials may be subject to enhanced corrosion, the degree of which will depend on material and magma composition, the temperature on contact and during cooling, and the in situ geochemical environment. The geochemical environment in the drift will be affected by the composition and volume of exsolving volatile gases, such as H_2O, H_2, CO_2, CO, SO_2, S_2, HCl, HF, and H_2S.

A variety of literature studies regarding the potential for enhanced corrosion in magmatic environments are summarized in *Igneous Intrusion Impacts on Waste Packages and Waste Forms* (BSC 2003d). These studies, which include tests and observations conducted over periods of time ranging from minutes to weeks, indicate that high temperatures and corrosive geochemical environments can measurably increase the corrosion rates of steel and other metal alloys.

Although none of the analyses described above indicate that the metallic engineered barriers would be destroyed or fail instantaneously, it appears that the effects would be rapid compared to the 10,000-year regulatory period for the repository. Therefore, because of the uncertainty associated with analyzing the effects of enhanced corrosion rates, performance assessment analyses for Yucca Mountain conservatively assume that any engineered materials contacted by magmas (e.g., drip shields, waste packages, cladding) during an intrusion will no longer provide any waste isolation function. Specifically, this assumption means that none of the engineered barriers in Zone 1 (within the drifts intersected by magma) would impede the movement of water to and through the waste package or the contact of water with the waste forms. The magmas that encase the waste packages are further assumed to have hydrologic properties similar to the fractured tuff in the drift wall, so that the magma filling the drifts also provides no barrier to the movement of water or to the contact of water and the waste form. The analyses do assume that the geochemistry of the water inside the drifts would be controlled by the contact of water with basaltic igneous rock.

An analysis of the effects on engineered barrier integrity was also performed for the drip shields and waste packages in emplacement drifts that were not intersected by magmatic intrusions (Zone 2 of the repository). This analysis included evaluation of the thermal impacts of dike intrusion in adjacent drifts and a gas-flow analysis, which describes the movement of potentially corrosive magmatic vapors through the rock and backfilled drifts separating the Zone 2 drifts from the magma filled drifts (BSC 2003a, Section 6.5.1 and 6.5.2; BSC 2003d, Section 6.5.1).

Predicting the possible impacts of an igneous dike-intrusion event on the waste packages and waste forms in potentially affected Zone 2 emplacement drifts requires several simplifying assumptions to determine the amount and composition of volcanic gases that could be released

from the cooling magma. The volume of the magma is assumed to be equal to the total volume of the emplacement drift minus the volume of waste packages. This assumption yields a conservatively large estimate of the volume (and mass) of magma in Zone 1 drifts, and it is, therefore, conservative for calculating the molar volumes of emanating gases and modeling the gas diffusion and heat conduction between Zones 1 and 2 emplacement drifts.

After intrusion, it is assumed that an average 3.5 weight percent out of 4.0 weight percent dissolved water will be released as volatile water containing corrosive gases and will diffuse away from the intrusive body. The data on water contents of post–Miocene basaltic magma in the Yucca Mountain region is sparse, but based on the considerations summarized in Section 3.3, the selected values are considered to be conservative.

The advective flow of water vapor and other volatiles from the magma in the emplacement drifts is two dimensional from the magma filled drift to the adjacent emplacement drifts on both sides. The analyses were performed assuming linear flow with the initial moles and volume halved. This linear flow assumption is conservative because it ignores radial movement that would not reach the Zone 2 drifts and allows volatile components to move down a pressure gradient from the higher temperature, higher-pressure magma filled drifts to a lower-pressure-and-temperature state. The model of gas migration assumes that the ideal gas law is applicable over Van der Waals Equation. Analysis of this assumption indicates that the ideal gas law can be used for pressures less than 7.5 atm (110 psi). The gas in the magma is assumed to be in pressure communication throughout. This assumption is conservative and will ensure the full volume of gas will be available for flow into the backfill and rock matrix. The initial pressure is represented by the pressure resulting from the elevated gas temperature associated with the magma intrusion, not by pressure conditions within the magma. The initial gas pressure was calculated as 2.35 atm. The full volume of volatile gases will not be immediately available for movement after the intrusion but will evolve slower than the magma movement.

The migration of volcanic gas associated with a magma-filled drift into a neighboring drift was analyzed using reaction-transport modeling that couples thermal, hydrological, and chemical processes for a multiphase, multicomponent, multimineralic system. Simulation results were obtained for the migration of volcanic gas out of a waste-emplacement drift through the fractured tuff repository rock and, alternatively, through a backfilled access drift (BSC 2003a, Section 6.5.1). Figure 5-9 is a schematic drawing showing the configuration of Zone 1 and Zone 2 drifts simulated by the model.

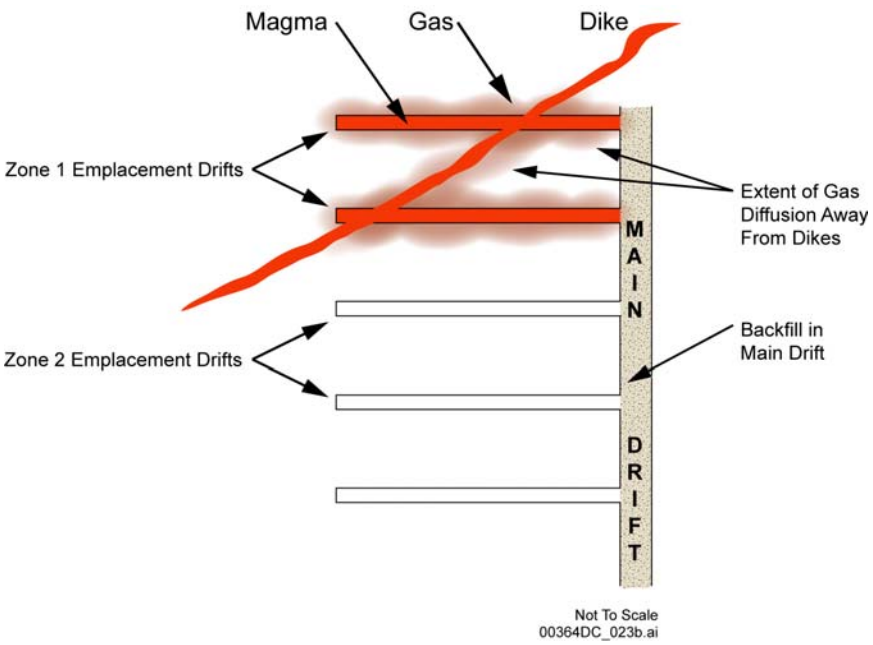

Source: BSC 2003a, Figure 144.

NOTE: The drawing is not to scale. Dikes would typically be 1 to 2 m in width. Drifts are 5.5 m in diameter and are spaced 81 m apart.

Figure 5-9. Schematic View of the Configuration of Zone 1 and Zone 2 Drifts Simulated in the Reactive Gas Transport Model

Several simulations were performed to bound the potential rate of advance of the gas and to examine the controls on the migration of soluble gas species. Diffusive and advective gas phase transport of air, H_2O, CO_2, and SO_2 were modeled along with the appropriate equilibrium gas-water solubility relations. Calculations of gas density and pressure considered only water vapor and air. The model of the geochemical system includes the major aqueous species, minerals, and gaseous components in the unsaturated zone. Additionally, minor species such as F^-, are included for their relevance to waste package corrosion. The geochemical model consists of the following primary aqueous species: H^+, Na^+, K^+, Ca^{2+}, Mg^{2+}, AlO_2^-, NO_3^{2-}, SO_4^{2-}, SO_2(aq), F^-, Cl^-, HCO_3^-, SiO_2(aq), and $HFeO_2$(aq). Gaseous components include air, H_2O, CO_2, and SO_2. Oxidation-reduction reactions were not treated; however, reactions involving sulfur oxidation would result in stronger retardation of SO_2 (BSC 2003a, Section 6.5.1.1).

The initial mineralogy of the tuff matrix and fracture coatings is represented by the following assemblage (some as end members of an ideal solid-solution phase): α-cristobalite, opal, tridymite, quartz, K-feldspar, albite, anorthite, Ca-smectite, Na-smectite, Mg-smectite, illite, calcite, fluorite, rhyolitic glass, hematite, stellerite, clinoptilolite, mordenite, and heulandite. Several other potential secondary phases are considered (e.g., amorphous silica, kaolinite, sepiolite, gypsum) as well as various salt phases, such as halite and sylvite, which precipitate only under conditions of complete evaporation (BSC 2003a, Section 6.5.1.1).

The high solubility in water of SO_2 and to a lesser extent CO_2, along with the development of a boiling zone around a drift where magma has been emplaced, would limit the migration of these gases through the repository host rock. Preliminary model results, under ambient pressure

conditions, indicate that these gases would not migrate to adjacent drifts through the rock in less than 10 years. This period of time is significantly longer than the period over which volcanic gas from a single intrusion would be present in significant volume (BSC 2003a, Section 6.5.1.6.6).

Under prolonged elevated pressure conditions (2 bars for 1 day or more), gas transport through the relatively dry high-permeability fractured tuff is rapid. However, the volume of the gas would be relatively small because it is moving through fractures that make up less than 1 percent of the total rock volume. After the pressure subsides back to ambient values, the CO_2 and SO_2 in the fractures diffuse into the rock matrix where they dissolve readily and are immobilized (BSC 2003a, Section 6.5.1.6.6).

Gas migration may also be relatively rapid through a tunnel filled with coarse crushed tuff, such as the repository main drifts that connect emplacement drifts. In this case, an adjacent drift could be affected by migrating volcanic gas within a year or less without any strong advective flow due to large pressure differences. Depending on the volume of gas emplaced, though, the gas could be strongly diluted by air as it migrates through the connecting drifts (BSC 2003a, Section 6.5.1.6.6). Therefore, the impact of volcanic gases on geochemical conditions would be limited.

Additional thermal and geochemical simulations of the effects on Zone 2 drifts are reported in *Igneous Intrusion Impacts on Waste Packages and Waste Forms* (BSC 2003d, Sections 6.5.2.1.1 and 6.5.2.2.3). Maximum temperature increases in drifts adjacent to magma filled drifts are small (less than 10°C), as the rock provides effective thermal insulation. Therefore, waste packages in Zone 2 emplacement drifts would not be affected by the heat from magma intruded into adjacent drifts. See additional discussion in Appendix C.

Geochemical analyses, using the EQ3/6 geochemical code, similarly showed that gas movement associated with magmatic intrusions would be very short lived and minimal in volume. The model predicts that the gas front would extend only about 3.6 m into the host rock adjacent to intruded drifts, and about 1.4 m into backfilled drifts adjacent to the emplacement drifts. In summary, multiple analyses indicate that the thermal and geochemical effects of magma intrusion on Zone 2 drifts would be negligible.

5.4 NUMBER OF WASTE PACKAGES HIT BY ERUPTIVE CONDUITS INTERSECTING THE REPOSITORY

If a volcano erupted through the repository, the consequences (in terms of radionuclide releases) would depend on the style and energy associated with the eruption. Section 3 described the eruptive styles typical of the small basaltic scoria cones that occur in the Crater Flat Volcanic Zone. As the basaltic dikes that feed eruptive centers ascend to the surface, the flow of magma becomes concentrated in conduits in which the magma fragments as volatiles exsolve.

The size (width and depth) of the conduits feeding eruptions is important to repository performance analyses because it directly influences the potential for waste materials to be incorporated in the eruption. In general, considerations described in *Characterize Eruptive Processes at Yucca Mountain, Nevada* (BSC 2003b), indicate that conduits feeding small volcanoes like the Lathrop Wells Cone will likely range from 0 to about 900 m in depth. If the

conduit formed at a depth of less than 300 m, then its only expression at the depth of the repository would be the dike(s) feeding it, which are typically 1 to 2 m wide. If the conduit extends to depths greater than 300 m, then its dimensions at the level of the repository would depend on its shape and volume.

Evidence summarized in *Characterize Eruptive Processes at Yucca Mountain, Nevada* (BSC 2003b, Section 6.3.1) from several volcanoes that are analogous (to varying degrees) to the basaltic systems in Crater Flat indicates that the width of potential conduits could range from a few meters to as much as 150 m (Section 4.3).

Total system performance analyses have conservatively adopted 50 m as the median conduit size for an eruption through a repository. The minimum conduit diameter used for the calculation is 5 m. The minimum conduit diameter is constrained by the dike width parameter, and the 95th percentile of dike width cumulative distribution function is 4.5 m. The slightly more conservative value of 5 m has been selected as minimum conduit diameter (BSC 2003c, Section 5.4). Based on observations at another potential analog volcano (Grants Ridge in New Mexico), the maximum size of the potential conduit has been chosen as 150 m. This value is believed to bound the range of conduit sizes for a potential Yucca Mountain volcanic event, given that the Lathrop Wells Cone (which is the largest of the Crater Flat volcanic centers) has a basal diameter of about 700 m and a height of 140 m.

The entire width of a conduit is not necessarily actively transferring magma to the vent at all times during an eruption. Due to variations in local flow geometry, magma velocity and viscosity and other factors, the eruption may use only a small fraction of the conduit at any one time. Using conduit width estimates based on analog observations provides a conservative estimate of the total volume of rock (and the total area of a repository) that could be affected during a single event.

The number of waste packages destroyed by a system of eruptive conduits is treated as a joint probability, dependent on both the number of conduits and the diameter of the conduits. The distributions for the number of conduits associated with a dike intersecting the repository has 14 bins, ranging from 0 conduits to 13, with a maximum probability of 1 conduit.

For any particular realization in the performance assessment analysis, it is assumed that all conduits have the same diameter. This is a simplifying assumption, but the analysis does sample a distribution of conduit diameters (BSC 2003c, Section 5.5) when all realizations are considered.

The analysis of the number of waste packages intersected by conduits is facilitated by an abstraction in which the number of waste packages within a conduit is simply a function of conduit area and the average waste package density within the repository. This geometric simplification does not affect the mean number of packages hit by any individual conduit, but it does affect the range of packages incorporated in each conduit. Ignoring the actual location of waste packages in linear emplacement drifts will decrease the number of conduits that see no waste packages (i.e., that erupt entirely through the pillars in the repository), but may also decrease the maximum number of packages in a conduit that erupts through a drift. No attempt is made to specifically determine or assign where in the repository a conduit occurs. Although

magma associated with an eruption may contact other packages along the drift, the magma moving with sufficient velocity to entrain waste in an eruption is assumed to be located only within the conduit (BSC 2003c, Section 5.6).

The result of the calculation of the number of waste packages hit by volcanic conduits is shown on Figure 5-10. The number of packages intersected by conduits during an eruption varies from zero to about 40 (at the 95th percentile of the cumulative distribution function). The mean number of packages hit by conduits is about six.

The Effect of Volcanic Eruptions on Waste Packages and the Waste Form–As noted in Section 5.3, no known analog observations, tests, or experiments provide evidence that would enable analysts to constrain how completely waste packages would be damaged or destroyed and the waste forms inside the packages fragmented in the event of a volcanic eruption. For this reason, performance assessment analyses of the effects of volcanic eruptions have conservatively assumed that the waste packages would be completely destroyed, and the waste form pulverized such that particle sizes range from 0.0001 to 0.05 cm, with a mode of 0.002 cm (CRWMS M&O 2001). This size distribution makes virtually the entire waste inventory of the intersected waste packages available for airborne transport along with the volcanic ash associated with the eruption. It is also conservatively assumed that the waste is entirely composed of spent nuclear fuel which has higher concentrations of radionuclides than the high-level radioactive waste glass also disposed in the repository.

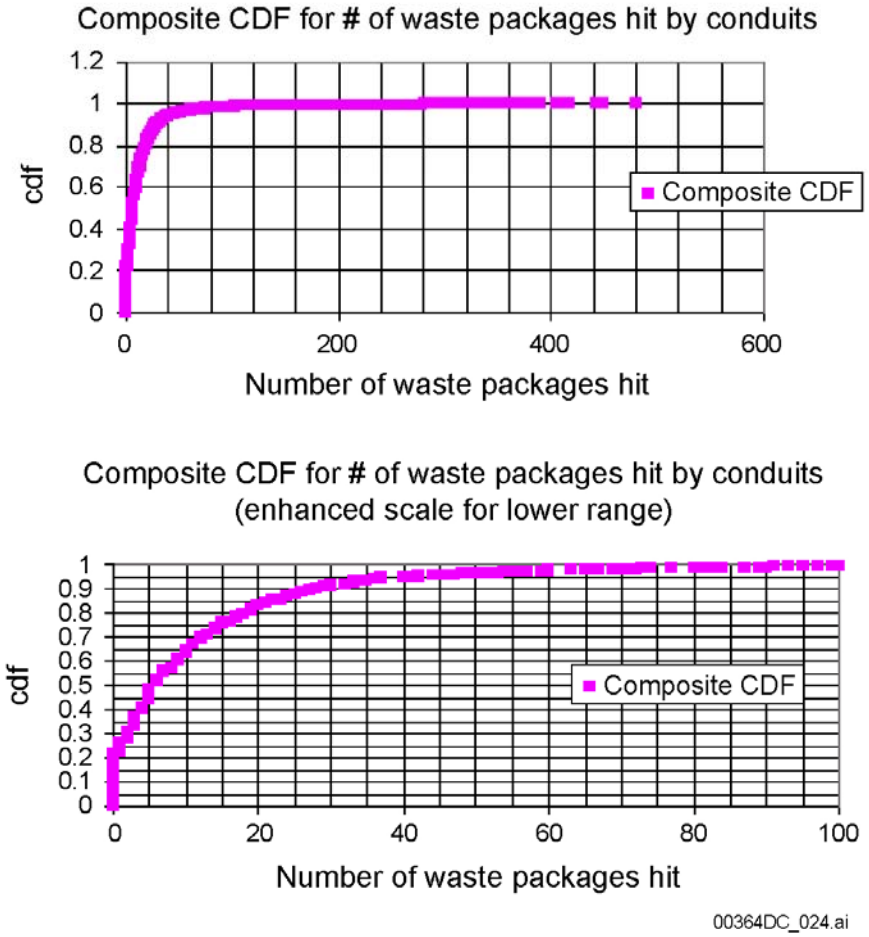

Source: BSC 2003c, Figure 12.

Figure 5-10. Composite Cumulative Distribution Function for Number of Waste Packages Hit by Conduits

5.5 THE AREAL DISTRIBUTION OF ENTRAINED WASTE IN PLUMES OF VOLCANIC ASH

The potential distribution of volcanic ash and radioactive waste during and after a volcanic eruption is described in *Atmospheric Dispersal and Deposition of Tephra from a Potential Volcanic Eruption at Yucca Mountain, Nevada* (BSC 2003f). A conceptual and mathematical model has been developed for atmospheric dispersion and subsequent deposition on the land surface of tephra from a potential eruption at Yucca Mountain, Nevada. The model is implemented in a computer code known as ASHPLUME. Figure 5-11 is a schematic representation of an eruption, showing the transport of volcanic ash and waste in an ash plume. The conceptual model accounts for the entrainment of spent nuclear fuel particles within the gas and ash ejected during a hypothetical eruption through the repository and describes the factors controlling downwind transport of contaminated tephra. The mathematical model describes the conceptual model in mathematical terms to allow for prediction of radioactive waste/ash deposition on the ground surface given that the hypothetical eruptive event occurs. The distribution and amounts of ash and waste predicted by ASHPLUME are used to calculate the

dose resulting from exposure to waste-contaminated ash and redistributed contaminated soils at the location of the receptor (known as the reasonably maximally exposed individual, or RMEI). The ASHPLUME numerical model and computer code are a component of the total system performance assessment (TSPA) model of Yucca Mountain.

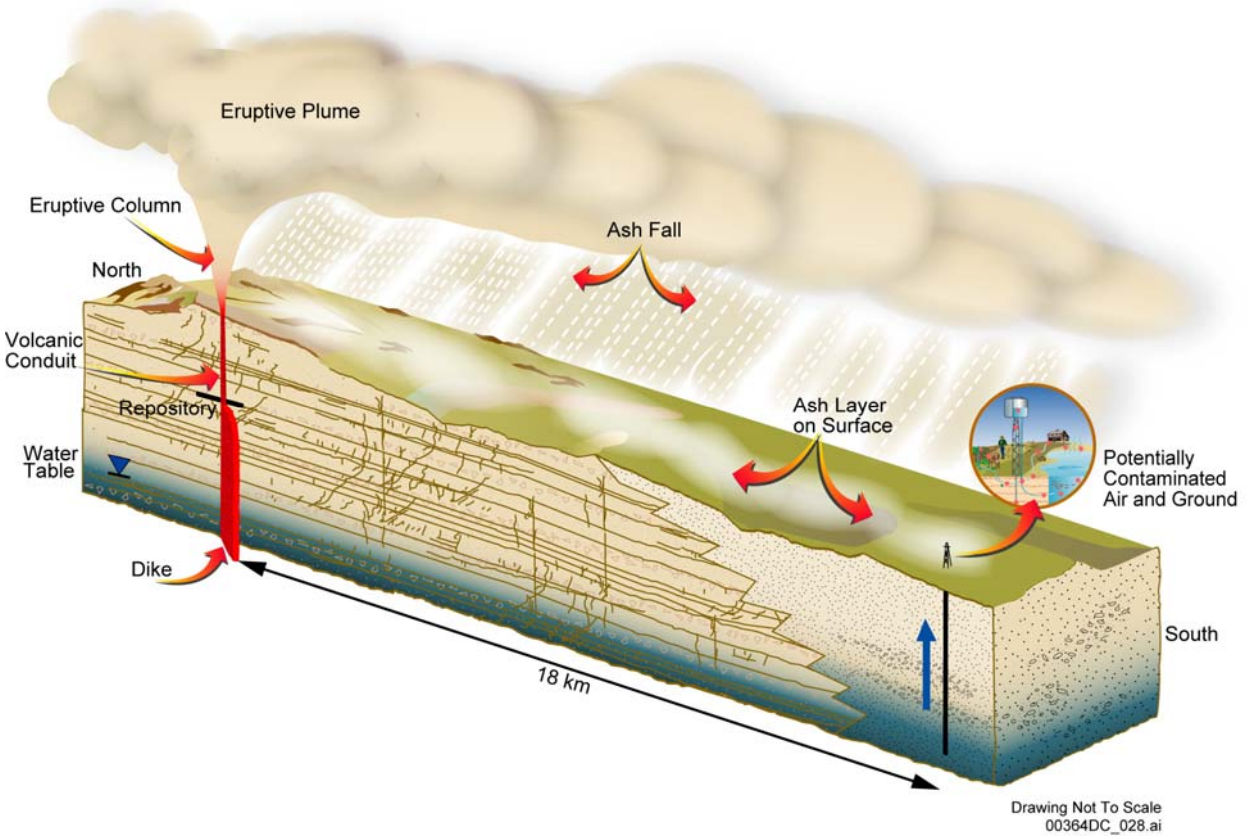

Figure 5-11. Schematic Representation of a Volcanic Eruption at Yucca Mountain, Showing Transport of Radioactive Waste in an Ash Plume

Section 5.4 described the number of packages encountered within eruptive conduits, and explained the conservative assumption that all waste contained in waste packages within the conduit would be pulverized to a fine grain size that could be entrained in the erupting magma. This section discusses the postentrainment and atmospheric transport portions of the eruptive conceptual model, specifically the following topics:

- Eruptive styles associated with atmospheric transport of ash
- Entrainment of waste in an ash plume in the atmosphere
- Atmospheric transport of waste in the ash plume
- Deposition of waste and ash.

Conceptual and Mathematical Model–The ASHPLUME mathematical model is based on a two-dimensional diffusion model in which only horizontal turbulent diffusion is considered. The movement of air in the atmosphere is random due to the many eddy currents that exist (Suzuki 1983). The movement of particles within the air mass is also random for the same

reason. Particles diffuse in the atmosphere in both vertical and horizontal directions, but because the scale of horizontal turbulence is much greater than the scale of the vertical turbulence (Suzuki 1983), horizontal diffusion is the dominant factor in determining the width of a plume as it moves downwind. Therefore, the ASHPLUME model is based on a two-dimensional diffusion equation in which only horizontal turbulent diffusivity is considered.

The ASHPLUME conceptual model for the atmospheric dispersal and deposition of contaminated tephra begins with a magmatic dike rising through the Earth's crust and intersecting the repository at Yucca Mountain (Figure 5-1). An eruptive conduit, or conduits, can form when a portion of the dike begins to widen and forms a preferential pathway to focus an eruption that penetrates the Earth's surface. If the conduit intersects the repository, the assumption is made that all canisters located partially or entirely within the conduit provide no further protection to the waste, which will become entrained within the rising magma.

Typical eruptions from the types of scoria cones characteristic of the Yucca Mountain region are known as Strombolian eruptions. Strombolian eruptions are characterized by the explosive ejection of a high-speed column of a gas–pyroclast mixture. The column consists of two regions. The lower region directly above the vent is called the gas-thrust region, and it behaves as a ballistic fountain of tephra moving under the influence of its eruption momentum. The upper region of the column is called the convective-thrust region, in which tephra rise by buoyant convective currents. Strombolian eruptions typically vary in eruptive intensity as measured by the degree of magma fragmentation and eruptive velocity. A violent Strombolian eruption is one that is dominated by an energetic upper column, with atmospheric transport of the fragmented magma and gas mixture that approximates a thermally buoyant plume. Eruptive sequences at a representative volcano, such as the Lathrop Wells scoria cone, might include intermittent and sporadic periods of lava fountaining, Strombolian blasts, and periods of violent Strombolian eruptions that may last for a few days (BSC 2003b, Section 6.3.5.1). The ASHPLUME model specifically simulates the atmospheric transport of ash (and waste particles) associated with violent Strombolian eruptions.

As the eruptive mixture rises in the plume of a violent Strombolian eruption, it entrains and heats air, which, in turn, reduces the bulk density of the mixture, and the plume becomes buoyant and continues to rise (BSC 2003f, Section 6.3). The plume rises to an altitude of neutral buoyancy compared to the surrounding atmosphere, in which it then spreads laterally as an anvil cloud and is transported down wind. Tephra particles fall out from both the vertical eruption column and from the anvil cloud according to their settling velocities. Such eruptions produce a fallout sheet of varying thickness extending from the volcanic vent. The thickness of the deposit depends on factors such as particle density, eruptive parameters, wind speed and direction, and distance from the vent.

Wind speed and direction vary with altitude, so the model incorporates wind data that are consistent with observations for the Yucca Mountain region. Meteorological data characterizing the variability in wind speed and wind direction in the Yucca Mountain region under present climatic conditions are described by Quiring (1968, pp. VI-1–VI-21) and have been augmented by more recent data from the Desert Rock airport near Mercury, Nevada (NOAA n.d.). The Desert Rock data have been used to calculate variability in both wind speed and direction as a function of altitude up to 13 km (BSC 2003f, Appendix 3).

Modeling studies of past climatic conditions provide insight into projections of future climatic conditions at Yucca Mountain. Kutzbach et al. (1993, p. 60) have modeled global climates at 3,000-year intervals during the last 18,000 years using general circulation models with available paleoclimatic information used to define boundary conditions. Resolution of the model is very coarse (grid blocks are 4.4º latitude by 7.5º longitude (Kutzbach et al. 1993, p. 60), and results are, therefore, not intended to be interpreted at local scales. However, at a regional scale, the model provides qualitative information about modeled wind speeds and directions throughout the southwestern United States. Model results are provided for 18,000 years ago, at the end of the last major glaciation of northern North America; at 12,000, 9,000, and 6,000 years ago; and also for present conditions. Climatic conditions over this time interval span the range of conditions that might reasonably occur during a glacial transition in the next 10,000 years.

The wind speeds and directions modeled by Kutzbach et al. (1993) for the transition from glacial to interglacial climates in the southwestern United States are not significantly different from modern conditions. The largest changes, occurring during full glacial conditions 18,000 years ago, appear qualitatively to correspond to a decrease in the relative frequency of winds blowing toward the RMEI location south of Yucca Mountain. Therefore, these changes are reasonably and conservatively neglected, and the significant variability in present wind conditions is assumed to adequately represent variability in future conditions.

ASHPLUME models eruption behavior as a thermally buoyant plume, calculating the atmospheric dispersion of tephra and its deposition on the ground. The total mass of waste materials that can potentially be entrained in an eruption is determined by the number of packages hit by the volcanic conduits. The waste is assumed to have been finely fragmented by the force of the eruption, and waste particles are assumed to combine with larger ash particles for airborne transport. ASHPLUME defines an "incorporation ratio," which relates the minimum ash particle size needed to carry a given waste particle size in the plume, to calculate the fraction of waste entrained in the erupted plume (Jarzemba et al. 1997; BSC 2003f, Section 6.5.1). By doing so, the fallout of tephra carries contamination to where it is deposited on the ground, forming a contaminated fallout deposit. The contaminated fallout has the potential to affect the food and water supplies of the RMEI by direct contamination or by later surface redistribution of fallout deposits, which could be caused by a number of mechanisms (BSC 2003i, Sections 5.6 and 6.6.1). The outputs of the ASHPLUME model include the distribution and surface area density (g/cm^2) of volcanic ash and associated concentrations of waste, which is specified to be spent nuclear fuel. These outputs are then input into biosphere models that predict dose.

The ASHPLUME model has been tested by comparison to several analog sites, including the Lathrop Wells Cone, Cerro Negro volcano in Nicaragua, and a Holocene cinder cone in Lassen Volcanic National Park in California. In each case, the ash distribution patterns, and depths predicted by ASHPLUME were consistent with observations from known eruptions.

5.6 ASH REDISTRIBUTION MODEL

If an eruption were to occur through the repository at Yucca Mountain, radioactive waste particulates could be ejected along with the volcanic ash as attached and individual particles. The result would be a tephra sheet containing radioactive waste. Shortly after deposition of the tephra sheet, normal sedimentary processes (Folk 1980) would begin redistributing the ash.

Wind and water would begin eroding, transporting, sorting, and depositing the unconsolidated ash in greater or lesser concentrations of waste, depending on the mixing processes. The RMEI could then be exposed to the radionuclides contained within the redistributed deposits. For this reason, surface redistribution of contaminated tephra deposits has been evaluated for inclusion in TSPA (BSC 2003f, Sections 6.6 and 6.7).

The transport of tephra occurs by both wind and water action; however, while water can transport large amounts and much larger sizes of material in a short period of time (flooding event), wind is a continuous source of transport. Transport of tephra by water begins with hillslope erosion processes, continues as sediment moves into drainages and is transported in the beds of drainages that coalesce into larger and larger channels. At all scales within drainage systems, water and sediment from different channels begin a process of mixing that ultimately leads to a homogeneous sediment containing elements derived from all drainages in the basin (Folk 1980, pp. 14 to 15). This mixing of sediments occurs in all environments where sediment is transported by water, including intermittent and perennial stream systems, and occurs at higher rates and is able to carry larger clast sizes in larger drainages than smaller ones and on steeper hillslopes than on low-gradient landscape surfaces. Sediment mixing also occurs from wind action by transporting sediment across the landscape. Drainage channels that form and flow across newly deposited tephra sheets exhibit the same processes as observed in streams, and, after small transport distances, have well-mixed sediment loads.

Sedimentary depositional systems at the Lathrop Wells volcanic cone near Yucca Mountain and at Sunset Crater in the San Francisco volcanic field near Flagstaff, Arizona (Harrington 2003, pp. 14 to 16) have been studied to evaluate the potential redistribution of tephra and radioactive waste after a possible volcanic eruption through Yucca Mountain. Both areas have tephra-draped slopes of 5º to 10º. Drainage systems that have formed on the slopes at both locations show a similar pattern of development from normal sedimentary processes (BSC 2003f, Section 6.6).

In small channels, material is moved downslope by incorporating ash and sand in mixtures with water until the channel is choked, thereby causing the material to overflow out of the channel sides and move downslope as small debris flows. Depending on the slope angle, the transport of the tephra could begin with small debris flows. Thus, tephra moves downslope progressively, until it reaches the base of the tephra sheet or, more commonly, until it reaches a channel at the base of the slope. In these channels, which are part of a larger drainage system, the tephra is mixed with the sediment load from upstream. Depending on the size of the drainage system and the area of the tephra deposit, the majority of sediment in the larger channels is likely to be composed of materials other than fresh tephra (Harrington 2003, pp. 14 to 16).

In the Yucca Mountain area, sediments in drainage channels are commonly clasts of siliceous welded tuff and eolian quartz sand, which are more durable than the basaltic tephra. Mixing of the sediments occurs very rapidly, and welded tuff clasts and quartz sand/silt deposits are more abundant in the larger channels, so that the Lathrop Wells ash component has been progressively diluted during transport relative to the total sediment volume. Eolian processes also contribute to the mixing of sand and silt with the fluvially transported ash and other channel material. On the tephra sheet, sand and silt is trapped in the ash interstices. As this ash-dominant material moves downslope, more and more nonash and noneolian material is incorporated at channel

confluences. Thus, the quantity of basaltic ash (ratio of ash to nonash) continues to decrease (BSC 2003f, Section 6.6).

Studies of ash redistribution near Lathrop Wells have been performed to evaluate the fraction of basaltic ash components as a function of transport distance from the tephra sheet. These data indicate that the concentration of basaltic ash in sediments decreases to about 50 percent within 1 km of the head of the tephra sheet drainage on the eastern side, whereas the channel on the west side has less than 40 percent basaltic ash after 1 km of transport. These results indicate a dilution factor of 50 to 60 percent per kilometer.

Fortymile Wash is a major 800-km^2 drainage basin that includes the entire eastern slope of Yucca Mountain and the Fortymile Wash alluvial fan; therefore, understanding the redistribution processes along Fortymile Wash is important to volcanic-eruption consequence scenarios. The fan spreads out into the Amargosa Valley from the mouth of Fortymile Wash. In the upper or northern half of the fan, the channels are well defined and widely spaced, with sizable interstream area between all pairs of channels. These interstream divide tracts are more prominent on the upper fan. On the lower fan they are neither as topographically prominent nor as wide because the distributary channels become progressively closer on the lower fan.

From the mid-1950s through the mid-1960s, worldwide aboveground nuclear tests introduced radioactive ^{137}Cs into the atmosphere (Ely et al. 1992, p. 196). ^{137}Cs forms a time-stratigraphic marker in alluvial or eolian deposits and can be used to assess the extent of local erosion and deposition. Also, the depth to which ^{137}Cs infiltrates into the soil can be used as a general proxy for the depth to which sorbing radionuclides may infiltrate after deposition with volcanic ash (BSC 2003f, Section 6.7.2.1).

To evaluate erosion rates on the upper Fortymile Wash fan, soil samples were taken for analysis of ^{137}Cs concentrations (BSC 2003b). The analyses indicate that the upper-fan interstream-divide areas have been eroding over the last 50+ years and have lost 1 to 2 cm of the upper soil horizon. This stripping of the upper centimeter has most likely occurred as a result of wind erosion, rather than from removal by fluvial processes (BSC 2003b).

Although wind erosion can be inferred from the ^{137}Cs data, there is also evidence of some eolian deposition on these same surfaces. The evidence includes stratified eolian horizons of fine sand and silt, marked by the presence of gas bubble vesicles (Av horizons). Such soil horizons are found on most geomorphic surfaces that have been stable for several hundred years (YMP 1993, pp. 24 to 25). The presence of Big Dune in proximity to the Fortymile Wash fan, from which material is being removed and deposited almost continuously, clearly demonstrates that eolian processes play an important role in landscape modification.

Ash Redistribution Model Results–The upper half of the Fortymile Wash alluvial fan consists primarily of an interstream divide area (82 percent); secondarily of distributary channels (17 percent); and the balance (1 percent) of minor areas of overbank deposits, sand dunes (coppice), and sand areas. Thus, the majority of the fan surface is interstream divide area, from which 1 to 2 cm of material, on average, has been removed during the last 50 years.

When large flood events occur, the flood waters can carry large quantities of sediment rapidly southward across the fan to the Amargosa River and may overflow channel banks to form small patches of overbank deposits. As flood levels subside, the suspended and bedload materials in the channel flow are deposited within the channel. The resulting deposits are stored in the channel until the next flood occurs. This may be a considerable time (more than 50 years) (BSC 2003b). Although water erosion can be significant, wind erosion appears to be continuous. The 50-year ^{137}Cs record suggests that eolian removal of material has been the major process causing erosion (BSC 2003f, Section 6.7).

Different processes of erosion and sedimentation will result in differing concentrations of contaminated ash and radionuclides on each of the major landforms. Therefore, the TSPA model calculates dose estimates separately for each region (interstream divide areas and distributary channels) and combines them, weighted by their areal frequency (0.82 and 0.18, respectively). The overbank deposits, dunes, and sand areas are combined with the distributary channel areas because their fractional area is small and their sediment composition is largely derived directly from the channel deposits (BSC 2003f, Section 6.7).

Several important factors control the contribution to dose to the RMEI, including the amount of soil removal, the extent and amount of tephra deposits at the location of the RMEI, and the contamination of residual ash after erosion of the tephra sheet.

In the interstream divide areas, erosion removes sediment at a relatively rapid rate (1 to 2 cm per 50 years, as noted above). Therefore, the TSPA model will calculate doses using the initial ash-layer thicknesses and radionuclide concentrations from ASHPLUME, modified by a time dependent soil removal factor, estimated to range from 0.02 to 0.04 cm/yr. Given these erosion rates, the ash layers will be removed within a few centuries, depending on initial thickness. Based on field observations, it is likely some fine-grained ash and radionuclides will persist in the soil below the initial ash layer, and some additional radionuclides may be brought into the interstream divide areas by infrequent flooding events that cover the entire fan. Based on ^{137}Cs data, it is estimated that residual contamination after erosion removal of the tephra deposits will be on the order of 0.01 of the initial ASHPLUME radionuclide concentration (BSC 2003f, Section 6.7).

In contrast to the interstream divide areas, the amount of sediment deposited in channels varies greatly from location to location, and it is not feasible to provide a single realistic estimate for the thickness of a potentially contaminated layer of redistributed tephra. For the purposes of TSPA, distributary channel areas will be modeled as having a layer of contaminated ash of uncertain thickness that appears immediately following the eruption. This layer will be of variable thickness, ranging from zero to perhaps several tens of centimeters (represented by a uniform distribution from 0 to 15 cm). Although sediment thickness may exceed 15 cm, it is likely that contributions to dose from radionuclides at greater depths will be negligible. Observations of ^{137}Cs content also indicate that radionuclides are unlikely to migrate more than 9 cm into sediment below the ash layer due to the widespread presence of carbonate layers in soil (Harrington 2003, pp. 28 to 53).

Conceptually, the contaminated layer in the channel areas represents a reasonable approximation of the amount of contaminated ash that might be present in transient storage in a channel at any

time following a volcanic eruption. Within any portion of the fan, such as the location of the RMEI, contaminated ash will be both removed and deposited continuously, and the appropriate layer thickness to consider in the TSPA model is an average value for the amount present at any one time. Incorporating uncertainty in the layer thickness into a single sampled parameter that characterizes the entire region, rather than attempting to capture local variability explicitly, is reasonable because exposures to the RMEI will be derived from a spatially heterogeneous area. Although dilution of radionuclides in tephra is certain to occur during transport in distributary channels, as discussed earlier in this section, field data are insufficient to quantify this reduction in concentrations for the Fortymile Wash drainage and fan. Therefore, the TSPA will conservatively assume that the concentration of radionuclides in the contaminated sediment in the channel areas is the same as that derived from ASHPLUME for the mid-line of a plume about 18 km from the vent. The extent to which this assumption overestimates concentrations is not well known but may be large, especially for eruptive events in which the wind is blowing from the west or southwest and the ash deposition occurs upstream from the location of the RMEI. The use of a single concentration to represent a spatially variable parameter is believed to be reasonable because exposures would be integrated over a region that is relatively large compared to the scale of local variability (BSC 2003f, Section 6.7).

Observations from the Lathrop Wells Cone indicate that ash will not remain indefinitely in the channel area. The time scale over which most tephra is removed from the drainage is unknown but is substantially less than the age of the Lathrop Wells Cone. Given the limited presence of ash observed at all locations, except those immediately adjacent to intact tephra deposits, the time required to remove most ash from the distributary channels may be very short, perhaps on the scale of centuries. Therefore, the TSPA model applies a uniform removal rate to channel deposits such that the initial layer is removed fully within an uncertain period of time that is sampled uniformly between 100 and 1,000 years. Consistent with the approach taken above for the interstream-divide areas, some residual contamination will likely remain after the tephra deposits are eroded. This contamination is presumed to persist indefinitely (BSC 2003f, Section 6.7).

6. REFERENCES

6.1 DOCUMENTS CITED

Baker, D.R. and Eggler, D.H. 1983. "Fractionation Paths of Atka (Aleutians) High-Alumina Basalts: Constraints from Phase Relations." *Journal of Volcanology and Geothermal Research, 18,* 387-404. Amsterdam, The Netherlands: Elsevier. TIC: 246252.

Blakely, R.J.; Langenheim, V.E.; Ponce, D.A.; and Dixon, G.L. 2000. *Aeromagnetic Survey of the Amargosa Desert, Nevada and California: A Tool for Understanding Near-Surface Geology and Hydrology.* Open-File Report 00-188. [Denver, Colorado]: U.S. Geological Survey. TIC: 248767.

Brocher, T.M.; Hunter, W.C.; and Langenheim, V.E. 1998. "Implications of Seismic Reflection and Potential Field Geophysical Data on the Structural Framework of the Yucca Mountain-Crater Flat Region, Nevada." *Geological Society of America Bulletin, 110,* (8), 947-971. Boulder, Colorado: Geological Society of America. TIC: 238643.

Brocoum, S.J. 1997. "Evaluation of Data Provided at U.S. Department of Energy (DOE) and U.S. Nuclear Regulatory Commission (NRC) Igneous Activity Technical Exchange, February 25-26, 1997." Letter from S.J. Brocoum (DOE/YMSCO) to J.T. Greeves (NRC), June 4, 1997, with enclosure. ACC: MOL.19970722.0276; MOL.19970722.0277.

BSC (Bechtel SAIC Company) 2001. *Characterize Eruptive Processes at Yucca Mountain, Nevada.* ANL-MGR-GS-000002 REV 00 ICN 01. Las Vegas, Nevada: Bechtel SAIC Company. ACC: MOL.20020327.0498.

BSC 2002. *Total System Performance Assessment-License Application Methods and Approach.* TDR-WIS-PA-000006 REV 00. Las Vegas, Nevada: Bechtel SAIC Company. ACC: MOL.20020923.0175.

BSC 2003a. *Dike/Drift Interactions.* MDL-MGR-GS-000005 REV 00E. Las Vegas, Nevada: Bechtel SAIC Company. ACC: MOL.20030916.0259.

BSC 2003b. *Characterize Eruptive Processes at Yucca Mountain, Nevada.* ANL-MGR-GS-000002 REV 01C. Las Vegas, Nevada: Bechtel SAIC Company. ACC: MOL.20030711.0107.

BSC 2003c. *Number of Waste Packages Hit by Igneous Intrusion.* ANL-MGR-GS-000003 REV 00C. Las Vegas, Nevada: Bechtel SAIC Company. ACC: MOL.20030711.0099.

BSC 2003d. *Igneous Intrusion Impacts on Waste Packages and Waste Forms.* MDL-EBS-GS-000002 REV 00. Las Vegas, Nevada: Bechtel SAIC Company. ACC: DOC.20030819.0003.

BSC 2003e. *Characterize Framework for Igneous Activity at Yucca Mountain, Nevada.* ANL-MGR-GS-000001 REV 01C. Las Vegas, Nevada: Bechtel SAIC Company. ACC: MOL.20030711.0103.

BSC 2003f. *Atmospheric Dispersal and Deposition of Tephra from a Potential Volcanic Eruption at Yucca Mountain, Nevada.* MDL-MGR-GS-000002 REV 00D. Las Vegas, Nevada: Bechtel SAIC Company. ACC: MOL.20030922.0197.

BSC 2003g. *Drift Degradation Analysis*. ANL-EBS-MD-000027 REV 02. Las Vegas, Nevada: Bechtel SAIC Company. ACC: DOC.20030709.0003.

BSC 2003h. *Dike/Drift Interactions.* MDL-MGR-GS-000005 REV 00 Draft ICN 01A. Las Vegas, Nevada: Bechtel SAIC Company. ACC: MOL.20031029.0035.

BSC 2003i. *Biosphere Model Report*. MDL-MGR-MD-000001 REV 00A. Las Vegas, Nevada: Bechtel SAIC Company. MOL.20030124.0246.

Byers, F.M., Jr. and Barnes, H. 1967. *Geologic Map of the Paiute Ridge Quadrangle, Nye and Lincoln Counties, Nevada.* Map GQ-577. Washington, D.C.: U.S. Geological Survey. ACC: HQS.19880517.1104.

Connor, C.B. and Hill, B.E. 1995. "Three Nonhomogeneous Poisson Models for the Probability of Basaltic Volcanism: Application to the Yucca Mountain Region, Nevada." *Journal of Geophysical Research, 100*, (B6), 10,107-10,125. Washington, D.C.: American Geophysical Union. TIC: 237682.

Connor, C.B.; Stamatakos, J.; Ferrill, D.; Hill, B.E.; Magsino, S.B.L.; La Femina, P.; and Martin, R.H. 1996. "Integrating Structural Models into Probabilistic Volcanic Hazard Analyses: An Example from Yucca Mountain, NV." *Abstracts with Programs - Geological Society of America, 28,* (7), A-192. Boulder, Colorado: Geological Society of America. TIC: 247409.

Connor, C.B.; Stamatakos, J.A.; Ferrill, D.A.; Hill, B.E.; Ofoegbu, G.I.; Conway, F.M.; Sagar, B.; and Trapp, J. 2000. "Geologic Factors Controlling Patterns of Small-Volume Basaltic Volcanism: Application to a Volcanic Hazards Assessment at Yucca Mountain, Nevada." *Journal of Geophysical Research, 105,* (B1), 417-432. Washington, D.C.: American Geophysical Union. TIC: 247906.

Crowe, B. 1996. Volcanism Field Notebook EES-13-LV-01-93-05. Scientific Notebook EES-13-LV-01-93-05. ACC: MOL.20030721.0266.

Crowe, B.M.; Johnson, M.E.; and Beckman, R.J. 1982. "Calculation of the Probability of Volcanic Disruption of a High-Level Radioactive Waste Repository Within Southern Nevada, USA." *Radioactive Waste Management and the Nuclear Fuel Cycle, 3,* (2), 167-190. New York, New York: Harwood Academic Publishers. TIC: 222179.

Crowe, B.M. and Perry, F.V. 1990. "Volcanic Probability Calculations for the Yucca Mountain Site: Estimation of Volcanic Rates." *Proceedings of the Topical Meeting on Nuclear Waste Isolation in the Unsaturated Zone, FOCUS '89, September 17-21, 1989, Las Vegas, Nevada.* Pages 326-334. La Grange Park, Illinois: American Nuclear Society. TIC: 212738.

Crowe, B.M; Perry, F.V.; Geissman, J.; McFadden, L.; Wells, S.; Murrell, M.; Poths, J.; Valentine, G.A.; Bowker, L.; and Finnegan, K. 1995. *Status of Volcanism Studies for the Yucca Mountain Site Characterization Project.* LA-12908-MS. Los Alamos, New Mexico: Los Alamos National Laboratory. ACC: HQO.19951115.0017.

Crowe, B.M.; Perry, F.V.; Valentine, G.A.; Wallmann, P.C.; and Kossik, R. 1993. "Simulation Modeling of the Probability of Magmatic Disruption of the Potential Yucca Mountain Site." *Proceedings of the Topical Meeting on Site Characterization and Model Validation, FOCUS '93, September 26-29, 1993, Las Vegas, Nevada.* Pages 182-191. La Grange Park, Illinois: American Nuclear Society. TIC: 102245.

Crowe, B.M; Self, S.; Vaniman, D.; Amos, R.; and Perry, F. 1983. "Aspects of Potential Magmatic Disruption of a High-Level Radioactive Waste Repository in Southern Nevada." *Journal of Geology, 91*, (3), 259-276. Chicago, Illinois: University of Chicago Press. TIC: 216959.

Crowe, B.M.; Wohletz, K.H.; Vaniman, D.T.; Gladney, E.; and Bower, N. 1986. *Status of Volcanic Hazard Studies for the Nevada Nuclear Waste Storage Investigations.* LA-9325-MS. Volume II. Los Alamos, New Mexico: Los Alamos National Laboratory. ACC: NNA.19890501.0157.

CRWMS M&O (Civilian Radioactive Waste Management System Management and Operating Contractor) 1996. *Probabilistic Volcanic Hazard Analysis for Yucca Mountain, Nevada.* BA0000000-01717-2200-00082 REV 0. Las Vegas, Nevada: CRWMS M&O. ACC: MOL.19971201.0221.

CRWMS M&O 1998a. *Synthesis of Volcanism Studies for the Yucca Mountain Site Characterization Project.* Deliverable 3781MR1. Las Vegas, Nevada: CRWMS M&O. ACC: MOL.19990511.0400.

CRWMS M&O 1998b. "Geology." Book 1 - Section 3 of *Yucca Mountain Site Description*. B00000000-01717-5700-00019 REV 00. Las Vegas, Nevada: CRWMS M&O. ACC: MOL.19980729.0049.

CRWMS M&O 1999. *Waste Package Behavior in Magma*. CAL-EBS-ME-000002 REV 00. Las Vegas, Nevada: CRWMS M&O. ACC: MOL.19991022.0201.

CRWMS M&O 2000a. *Yucca Mountain Site Description.* TDR-CRW-GS-000001 REV 01 ICN 01. Las Vegas, Nevada: CRWMS M&O. ACC: MOL.20001003.0111.

CRWMS M&O 2000b. *Characterize Framework for Igneous Activity at Yucca Mountain, Nevada.* ANL-MGR-GS-000001 REV 00 ICN 01. Las Vegas, Nevada: CRWMS M&O. ACC: MOL.20001221.0001.

CRWMS M&O 2000c. *Dike Propagation Near Drifts.* ANL-WIS-MD-000015 REV 00 ICN 1. Las Vegas, Nevada: CRWMS M&O. ACC: MOL.20001213.0061.

CRWMS M&O 2001. *Miscellaneous Waste-Form FEPs.* ANL-WIS-MD-000009 REV 00 ICN 01. Las Vegas, Nevada: CRWMS M&O. ACC: MOL.20010216.0006.

Dasch, E.J.; Armstrong, R.L.; and Clabaugh, S.E. 1969. "Age of Rim Rock Dike Swarm, Trans-Pecos, Texas." *Geological Society of America Bulletin, 80,* (9), 1819–1824. Boulder, Colorado: Geological Society of America. TIC: 254238.

Delaney, P.T. 1982. "Rapid Intrusion of Magma into Wet Rock: Groundwater Flow due to Pore Pressure Increases." *Journal of Geophysical Research, 87*, (B9), 7739–7756. Washington, D.C.: American Geophysical Union. TIC: 254049.

Delaney, P.T. and Gartner, A.E. 1997. "Physical Processes of Shallow Mafic Dike Emplacement Near the San Rafael Swell, Utah." *Geological Society of America Bulletin, 109,* (9), 1177-1192. Boulder, Colorado: Geological Society of America. TIC: 247421.

Delaney, P.T. and Pollard, D. 1978. "Basaltic Subvolcanic Conduits Near Shiprock, New Mexico: Magma Flow, Heat Transport, and Brecciation of Host Rocks." *Eos Transactions, 59,* (12), 1212. Washington, D.C.: American Geophysical Union. TIC: 254390.

Delaney, P.T. and Pollard, D.D. 1981. *Deformation of Host Rocks and Flow of Magma During Growth of Minette Dikes and Breccia-Bearing Intrusions Near Ship Rock, New Mexico.* Geological Survey Professional Paper 1202. Washington, D.C.: U.S. Geological Survey. TIC: 254050.

Detournay, E.; Mastin, L.G.; Pearson, J.R.A.; Rubin, A.M.; and Spera, F.J. 2003. *Final Report of the Igneous Consequences Peer Review Panel.* Las Vegas, Nevada: Bechtel SAIC Company. ACC: MOL.20030325.0227.

Dobran, F. 2001. "Conduit Erosion." *Volcanic Processes, Mechanisms in Material Transport.* Pages 480-484. New York, New York: Kluwer Academic/Plenum Publishers. TIC: 254051.

Doubik, P. and Hill, B.E. 1999. "Magmatic and Hydromagmatic Conduit Development During the 1975 Tolbachik Eruption, Kamchatka, with Implications for Hazards Assessment at Yucca Mountain, NV." *Journal of Volcanology and Geothermal Research, 91,* 43-64. Amsterdam, The Netherlands: Elsevier. TIC: 246029.

Eichelberger, J.C.; Vogel, T.A.; Younker, L.W.; Miller, C.D.; Heiken, G.H.; and Wolhletz, K.H. 1988. "Structure and Stratigraphy Beneath a Young Phreatic Vent: South Inyo Crater, Long Valley Caldera, California." *Journal of Geophysical Research, 93,* (B11), 13208–13220. Washington, D.C.: American Geophysical Union. TIC: 254490.

Ely, L.L.; Webb, R.H.; and Enzel, Y. 1992. "Accuracy of Post-Bomb ^{137}Cs and ^{14}C in Dating Fluvial Deposits." *Quaternary Research, 38,* 196-204. [New York, New York]: Academic Press]. TIC: 254471.

Farmer, G.L.; Perry, F.V.; Semken, S.; Crowe, B.; Curtis, D.; and DePaolo, D.J. 1989. "Isotopic Evidence on the Structure and Origin of Subcontinental Lithospheric Mantle in Southern Nevada." *Journal of Geophysical Research, 94,* (B6), 7885-7898. Washington, D.C.: American Geophysical Union. TIC: 201800.

Ferrill, D.A.; Stamatakos, J.A.; Jones, S.M.; Rahe, B.; McKague, H.L.; Martin, R.H.; and Morris, A.P. 1996. "Quaternary Slip History of the Bare Mountain Fault (Nevada) from the Morphology and Distribution of Alluvial Fan Deposits." *Geology, 24*, (6), 559-562. Boulder, Colorado: Geological Society of America. TIC: 234557.

Fischer, L.E.; Chou, C.K.; Gerhard, M.A.; Kimura, C.Y.; Martin, R.W.; Mensing, R.W.; Mount, M.E.; and Witte, M.C. 1987. *Shipping Container Response to Severe Highway and Railway Accident Conditions.* NUREG/CR-4829. Volume 1. Washington, D.C.: U.S. Nuclear Regulatory Commission. ACC: NNA.19900827.0230.

Fisher, R.V. and Schmincke, H-U. 1984. *Pyroclastic Rocks*. New York, New York: Springer-Verlag. TIC: 223562.

Folk, R.L. 1980. *Petrology of Sedimentary Rocks.* Austin, Texas: Hemphill Publishing Company. TIC: 254754.

Fridrich, C.J. 1999. "Tectonic Evolution of the Crater Flat Basin, Yucca Mountain Region, Nevada." Chapter 7 of *Cenozoic Basins of the Death Valley Region.* Wright, L.A. and Troxel, B.W., eds. Special Paper 333. Boulder, Colorado: Geological Society of America. TIC: 248054.

Fridrich, C.J.; Whitney, J.W.; Hudson, M.R.; and Crowe, B.M. 1999. "Space-Time Patterns of Late Cenozoic Extension, Vertical Axis Rotation, and Volcanism in the Crater Flat Basin, Southwest Nevada." Chapter 8 of *Cenozoic Basins of the Death Valley Region.* Wright, L.A. and Troxel, B.W., eds. Special Paper 333. Boulder, Colorado: Geological Society of America. TIC: 248054.

Gordon, B.M. 2003. *Literature Review of Waste Package and Drip Shield Materials' Corrosion Performance in Magmatic-Type Environments.* SIR-02-168, Rev. 0. San Jose, California: Structural Integrity Associates. ACC: MOL.20030414.0260.

Hallett, R.B. 1992a. "Volcanic Geology of the Rio Puerco Necks." *San Juan Basin IV: New Mexico Geological Society, 43rd Annual Field Conference, September 30-October 3, 1992.* Lucas, S.G.; Kues, B.S.; Williamson, T.E.; and Hunt, A.P.; eds. 135-144. [Socorro, New Mexico]: New Mexico Geological Society. TIC: 239345.

Hallett, R.B. 1992b. "Volcanic Geology of Cerro Chafo." *San Juan Basin IV, New Mexico Geological Society Forty-Third Annual Field Conference, September 30–October 3, 1992.* Lucas, S.G.; Kues, B.S.; Williamson, T.E.; and Hunt, A.P.; eds. Pages 19-24. [Socorro, New Mexico: New Mexico Geological Society]. TIC: 254052.

Harrington, C. 2003. Ash and Soil Redistribution Studies. Scientific Notebook SN-LANL-SCI-285-V1. ACC: MOL.20030411.0312.

Heiken, G.H. and Wohletz, K. 1985. *Volcanic Ash.* Berkeley, California: University of California Press. TIC: 242991.

Heiken, G.; Wohletz, K.; and Eichelberger, J. 1988. "Fracture Fillings and Intrusive Pyroclasts, Inyo Domes, California." *Journal of Geophysical Research, 93,* (B5), 4335-4350. Washington, D.C.: American Geophysical Union. TIC: 252109.

Heizler, M.T.; Perry, F.V.; Crowe, B.M.; Peters, L.; and Appelt, R. 1999. "The Age of Lathrop Wells Volcanic Center: An $^{40}Ar/^{39}Ar$ Dating Investigation." *Journal of Geophysical Research, 104,* (B1), 767-804. Washington, D.C.: American Geophysical Union. TIC: 243399.

Hill, B.E. and Stamatakos, J.A. 2002. *Evaluation Of Geophysical Information Used to Detect and Characterize Buried Volcanic Features in the Yucca Mountain Region.* San Antonio, Texas: Center for Nuclear Waste Regulatory Analyses. TIC: 252846.

Ho, C-H. and Smith, E.I. 1998. "A Spatial-Temporal/3-D Model for Volcanic Hazard Assessment: Application to the Yucca Mountain Region, Nevada." *Mathematical Geology, 30*, (5), 497-510. New York, New York: Plenum Publishing Corporation. TIC: 245110.

Jarzemba, M.S.; LaPlante, P.A.; and Poor, K.J. 1997. *ASHPLUME Version 1.0—A Code for Contaminated Ash Dispersal and Deposition, Technical Description and User's Guide.* CNWRA 97-004, Rev. 1. San Antonio, Texas: Center for Nuclear Waste Regulatory Analyses. ACC: MOL.20010727.0162.

Keating, G.N. and Valentine, G.A. 1998. "Proximal Stratigraphy and Syn-Eruptive Faulting in Rhyolitic Grants Ridge Tuff, New Mexico, USA." *Journal of Volcanology and Geothermal Research, 81*, 37-49. Amsterdam, The Netherlands: Elsevier. TIC: 246096.

Knutson, J. and Green, T.H. 1975. "Experimental Duplication of a High-Pressure Megacryst/Cumulate Assemblage in a Near-Saturated Hawaiite." *Contributions to Mineralogy and Petrology, 52,* 121-132. Berlin, Germany: Springer-Verlag. TIC: 225057.

Kotra, J.P.; Lee, M.P.; Eisenberg, N.A.; and DeWispelare, A.R. 1996. *Branch Technical Position on the Use of Expert Elicitation in the High-Level Radioactive Waste Program.* NUREG-1563. Washington, D.C.: U.S. Nuclear Regulatory Commission. TIC: 226832.

Krier, D. and Harrington, C.D. 2003. *Ash Redistribution, Lava Morphology, and Igneous Processes Studies.* Scientific Notebook SN-LANL-SCI-286-V1. ACC: MOL.20030701.0109.

Kutzbach, J.E.; Guetter, P.J.; Behling, P.J.; and Selin, R. 1993. "Simulated Climatic Changes: Results of the COHMAP Climate-Model Experiments." Chapter 4 of *Global Climates Since the Last Glacial Maximum.* Wright, H., Jr.; Kutzbach, J.; Webb, T., III; Ruddiman, W.; Street-Perrott, F., Bartlein, P., eds. Minneapolis, Minnesota: University of Minnesota Press. TIC: 234248.

Langenheim, V.E.; Kirchoff-Stein, K.S.; and Oliver, H.W. 1993. "Geophysical Investigations of Buried Volcanic Centers Near Yucca Mountain, Southwest Nevada." *High Level Radioactive Waste Management, Proceedings of the Fourth Annual International Conference, Las Vegas, Nevada, April 26-30, 1993. 2,* 1840-1846. La Grange Park, Illinois: American Nuclear Society. TIC: 208542.

Magsino, S.L.; Connor, C.B.; Hill, B.E.; Stamatakos, J.A.; La Femina, P.C.; Sims, D.A.; and Martin, R.H. 1998. *CNWRA Ground Magnetic Surveys in the Yucca Mountain Region, Nevada (1996-1997).* CNWRA 98-001. San Antonio, Texas: Center for Nuclear Waste Regulatory Analyses. TIC: 247807.

Mahood, G.A. and Baker, D.R. 1986. "Experimental Constraints on Depths of Fractionation of Mildly Alkalic Basalts and Associated Felsic Rocks: Pantelleria, Strait of Sicily." *Contributions to Mineralogy and Petrology, 93,* 251-264. New York, New York: Springer-Verlag. TIC: 225072.

Mastin, L.G. 1991. "The Roles of Magma and Groundwater in the Phreatic Eruptions at Inyo Craters, Long Valley Caldera, California." *Bulletin of Volcanology, 53,* 579-596. [Heidelberg, Germany]: Springer-Verlag. TIC: 239071.

McBirney, A.R. 1959. "Factors Governing Emplacement of Volcanic Necks." *American Journal of Science, 257,* (1), 431–448. New Haven, Connecticut: Yale University, Sterling Tower. TIC: 254240.

McGetchin, T.R.; Settle, M.; and Chouet, B.A. 1974. "Cinder Cone Growth Modeled after Northeast Crater, Mount Etna, Sicily." *Journal of Geophysical Research, 79,* (23), 3257-3272. Washington, D.C.: American Geophysical Union. TIC: 246027.

NOAA (National Oceanic and Atmospheric Administration) n.d. *Upper Air Data: Desert Rock, Nevada, 1978-1995.* Reno, Nevada: National Oceanic and Atmospheric Administration, Western Regional Climate Center. TIC: 249335.

O'Leary, D.W.; Mankinen, E.A.; Blakely, R.J.; Langenheim, V.E.; and Ponce, D.A. 2002. *Aeromagnetic Expression of Buried Basaltic Volcanoes Near Yucca Mountain, Nevada.* Open-File Report 02-020. Denver, Colorado: U.S. Geological Survey. ACC: MOL.20020627.0225.

Parsons, T. and Thompson, G.A. 1991. "The Role of Magma Overpressure in Suppressing Earthquakes and Topography: Worldwide Examples." *Science, 253,* (5026), 1399-1402. Washington, D.C.: American Association for the Advancement of Science. TIC: 239733.

Perry, F.V.; Crowe, B.M.; Valentine, G.A.; and Bowker, L.M., eds. 1998. *Volcanism Studies: Final Report for the Yucca Mountain Project.* LA-13478. Los Alamos, New Mexico: Los Alamos National Laboratory. TIC: 247225.

Perry, F.V. and Straub. K.T. 1996. *Geochemistry of the Lathrop Wells Volcanic Center.* LA-13113-MS. Los Alamos, New Mexico: Los Alamos National Laboratory. ACC: MOL.19961015.0079.

Pollard, D.D. 1987. "Elementary Fracture Mechanics Applied to the Structural Interpretation of Dykes." *Mafic Dyke Swarms, A Collection of Papers Based on the Proceedings of an International Conference held at Erindale College, University of Toronto, Ontario, Canada,* June 4 to 7, 1985. Halls, H.C. and Fahrig, W.F., eds. Special Paper 34, 5-24. St. John's, Newfoundland, Canada: Geological Association of Canada. TIC: 247071.

Quareni, F.; Ventura, G.; and Mulargia, F. 2001. "Numerical Modelling of the Transition from Fissure- to Central-Type Activity on Volcanoes: A Case Study from Salina Island, Italy." *Physics of the Earth and Planetary Interiors, 124,* ([3-4]), 213-221. New York, New York: Elsevier. TIC: 254053.

Quiring, R.F. 1968. *Climatological Data Nevada Test Site and Nuclear Rocket Development Station.* ESSA Research Laboratories Technical Memorandum - ARL 7. Las Vegas, Nevada: U.S. Department of Commerce, Environmental Science Services Administration Research Laboratories. ACC: NNA.19870406.0047.

Ratcliff, C.D.; Geissman, J.W.; Perry, F.V.; Crowe, B.M.; and Zeitler, P.K. 1994. "Paleomagnetic Record of a Geomagnetic Field Reversal from Late Miocene Mafic Intrusions, Southern Nevada." *Science, 266,* 412-416. Washington, D.C.: American Association for the Advancement of Science. TIC: 234818.

Reamer, C.W. 1999. "Issue Resolution Status Report (Key Technical Issue: Igneous Activity, Revision 2)." Letter from C.W. Reamer (NRC) to Dr. S. Brocoum (DOE/YMSCO), July 16, 1999, with enclosure. ACC: MOL.19990810.0639.

Sanders, T.L.; Seager, K.D.; Rashid, Y.R.; Barrett, P.R.; Malinauskas, A.P.; Einziger, R.E.; Jordan, H.; Duffey, T.A.; Sutherland, S.H.; and Reardon, P.C. 1992. *A Method for Determining the Spent-Fuel Contribution to Transport Cask Containment Requirements.* SAND90-2406. Albuquerque, New Mexico: Sandia National Laboratories. ACC: MOV.19960802.0116.

Sandoval, R.P.; Weber, J.P.; Levine, H.S.; Romig, A.D.; Johnson, J.D.; Luna, R.E.; Newton, G.J.; Wong, B.A.; Marshall, R.W., Jr.; Alvarez, J.L.; and Gelbard, F. 1983. *An Assessment of the Safety of Spent Fuel Transportation in Urban Environs.* SAND82-2365. Albuquerque, New Mexico: Sandia National Laboratories. ACC: NNA.19870406.0489.

Savage, J.C.; Svarc, J.L.; and Prescott, W.H. 1999. "Strain Accumulation at Yucca Mountain, Nevada, 1983-1998." *Journal of Geophysical Research, 104,* (B8), 17627-17631. Washington, D.C.: American Geophysical Union. TIC: 245645.

Sawyer, D.A.; Fleck, R.J.; Lanphere, M.A.; Warren, R.G.; Broxton, D.E.; and Hudson, M.R. 1994. "Episodic Caldera Volcanism in the Miocene Southwestern Nevada Volcanic Field: Revised Stratigraphic Framework, $^{40}Ar/^{39}Ar$ Geochronology, and Implications for Magmatism and Extension." *Geological Society of America Bulletin, 106,* (10), 1304-1318. Boulder, Colorado: Geological Society of America. TIC: 222523.

Sisson, T.W. and Grove, T.L. 1993. "Temperatures and H2O Contents of Low-MgO High-Alumina Basalts." *Contributions to Mineralogy and Petrology, 113,* 167-184. New York, New York: Springer-Verlag. TIC: 246251.

Smith, E.I.; Feuerbach, D.L.; Naumann, T.R.; and Faulds, J.E. 1990. "The Area of Most Recent Volcanism Near Yucca Mountain, Nevada: Implications for Volcanic Risk Assessment." *High Level Radioactive Waste Management, Proceedings of the International Topical Meeting, Las Vegas, Nevada, April 8-12, 1990. 1,* 81-90. La Grange Park, Illinois: American Nuclear Society. TIC: 202058.

Smith, E.I.; Keenan, D.L.; and Plank, T. 2002. "Episodic Volcanism and Hot Mantle: Implications for Volcanic Hazard Studies at the Proposed Nuclear Waste Repository at Yucca Mountain, Nevada." *GSA Today, 12,* (4), 4-10. Boulder, Colorado: Geological Society of America. TIC: 253146.

Stamatakos, J.A.; Connor, C.B.; and Martin, R.H. 1997. "Quaternary Basin Evolution and Basaltic Volcanism of Crater Flat, Nevada, from Detailed Ground Magnetic Surveys of the Little Cones." *Journal of Geology, 105,* 319-330. Chicago, Illinois: University of Chicago. TIC: 245108.

Stock, J.M. and Healy, J.H. 1988. "Stress Field at Yucca Mountain, Nevada." Chapter 6 of *Geologic and Hydrologic Investigations of a Potential Nuclear Waste Disposal Site at Yucca Mountain, Southern Nevada.* Carr, M.D. and Yount, J.C., eds. Bulletin 1790. Denver, Colorado: U.S. Geological Survey. TIC: 203085.

Stock, J.M.; Healy, J.H.; Hickman, S.H.; and Zoback, M.D. 1985. "Hydraulic Fracturing Stress Measurements at Yucca Mountain, Nevada, and Relationship to the Regional Stress Field." *Journal of Geophysical Research, 90,* (B10), 8691-8706. Washington, D.C.: American Geophysical Union. TIC: 219009.

Suzuki, T. 1983. "A Theoretical Model for Dispersion of Tephra." *Arc Volcanism: Physics and Tectonics, Proceedings of a 1981 IAVCEI Symposium, August-September, 1981,* Tokyo and Hakone. Shimozuru, D. and Yokoyama, I., eds. Pages 95-113. Tokyo, Japan: Terra Scientific Publishing Company. TIC: 238307.

Valentine, G.A. and Groves, K.R. 1996. "Entrainment of Country Rock During Basaltic Eruptions of the Lucero Volcanic Field, New Mexico." *Journal of Geology, 104,* 71-90. Chicago, Illinois: University of Chicago Press. TIC: 246146.

Vaniman, D. and Crowe, B. 1981. *Geology and Petrology of the Basalts of Crater Flat: Applications to Volcanic Risk Assessment for the Nevada Nuclear Waste Storage Investigations*. LA-8845-MS. Los Alamos, New Mexico: Los Alamos Scientific Laboratory. ACC: HQS.19880517.1541.

Vergniolle, S. and Mangan, M. 2000. "Hawaiian and Strombolian Eruptions." *Encyclopedia of Volcanoes.* Sigurdsson, H., ed. Pages 447–462. San Diego, California: Academic Press. TIC: 254454.

Wernicke, B.; Davis, J.L.; Bennett, R.A.; Elosegui, P.; Abolins, M.J.; Brady, R.J.; House, M.A.; Niemi, N.A.; and Snow, J.K. 1998. "Anomalous Strain Accumulation in the Yucca Mountain Area, Nevada." *Science, 279,* 2096-2100. New York, New York: American Association for the Advancement of Science. TIC: 235956.

Wohletz, K.H. 1986. "Explosive Magma-Water Interactions: Thermodynamics, Explosion Mechanisms, and Field Studies." *Bulletin of Volcanology, 48,* 245-264. Berlin, Germany: Springer-Verlag. TIC: 225183.

Wohletz, K.H. and Heiken, G. 1992. *Volcanology and Geothermal Energy.* Berkeley, California: University of California Press. TIC: 241603.

WoldeGabriel, G.; Keating, G.N.; and Valentine, G.A. 1999. "Effects of Shallow Basaltic Intrusion into Pyroclastic Deposits, Grants Ridge, New Mexico, USA." *Journal of Volcanology and Geothermal Research, 92,* ([3]), 389-411. [New York, New York]: Elsevier. TIC: 246037.

Woods, A.W.; Sparks, S.; Bokhove, O.; LeJeune, A-M.; Conner, C.B.; and Hill, B.E. 2002. "Modeling Magma-Drift Interaction at the Proposed High-Level Radioactive Waste Repository at Yucca Mountain, Nevada, USA." *Geophysical Research Letters, 29,* (13), 19-1 through 19-4. [Washington, D.C.]: American Geophysical Union. TIC: 254467.

Wylie, J.J.; Helfrich, K.R.; Dade, B.; Lister, J.R.; and Salzig, J.F. 1999. "Flow Localization in Fissure Eruptions." *Bulletin of Volcanology, 60,* (8), 432–440. New York, New York: Springer-Verlag. TIC: 254054.

YMP (Yucca Mountain Site Characterization Project) 1993. *Evaluation of the Potentially Adverse Condition "Evidence of Extreme Erosion During the Quaternary Period" at Yucca Mountain, Nevada.* Topical Report YMP/92-41-TPR. Las Vegas, Nevada: Yucca Mountain Site Characterization Office. ACC: NNA.19930316.0208.

Yoder, H.S., Jr. and Tilley, C.E. 1962. "Origin of Basalt Magmas: An Experimental Study of Natural and Synthetic Rock Systems." *Journal of Petrology, 3,* (3), 342-532. London, England: Oxford University Press. TIC: 247024.

Yogodzinski, G.M. and Smith, E.I. 1995. "Isotopic Domains and the Area of Interest for Volcanic Hazard Assessment in the Yucca Mountain Area." *Transactions of the American Geophysical Union, 76,* (46), F669. Washington, D.C.: American Geophysical Union. TIC: 237939.

Zoback, M.L. and Zoback, M.D. 1989. "Tectonic Stress Field of the Continental United States." Chapter 24 of *Geophysical Framework of the Continental United States.* Pakiser, L.C. and Mooney, W.D., eds. Memoir 172. Pages 523-539. Boulder, Colorado: Geological Society of America. TIC: 247937.

6.2 DATA, LISTED BY DATA TRACKING NUMBER

LA000000000099.002. Major Element, Trace Element, Isotopic, and Mineral Chemistry Data from Lathrop Wells. Submittal date: 08/02/1995.

LA0004FP831811.002. Volume of Volcanic Centers in the Yucca Mountain Region. Submittal date: 04/14/2000.

LA0009FP831811.001. Compilation and Summaries of Data Supporting Computation of Volcanic Event Intersection Frequencies. Submittal date: 09/01/2000.

LA0302GH831811.003. Lithic Clasts Measured at Lathrop Wells Cone, Nevada. Submittal date: 02/25/2003.

LA0307BY831811.001. Characterize Igneous Framework Additional Output. Submittal date: 06/29/2003.

LAFP831811AQ97.001. Chemical and Geochronology Data for the Revision and Final Publication of the Volcanism Synthesis Report. Submittal date: 08/29/1997.

MO0002PVHA0082.000. Probabilistic Volcanic Hazard Analysis for Yucca Mountain, Nevada. Submittal date: 02/17/2000.

MO0003YMP98126.001. Quaternary and Pliocene Basalt. Submittal date: 03/02/2000.

SN0311T0503303.003. Updated Number of Waste Packages Hit by Igneous Intrusion. Submittal date: 11/06/2003.

6.3 CODES, STANDARDS, AND REGULATIONS

10 CFR Part 63. Energy: Disposal of High-Level Radioactive Wastes in a Geologic Repository at Yucca Mountain, Nevada. Readily available.

40 CFR Part 197. Protection of Environment: Public Health and Environmental Radiation Protection Standards for Yucca Mountain, Nevada. Readily available.

INTENTIONALLY LEFT BLANK

APPENDIX A

LIKELY RANGE OF TEPHRA VOLUMES (RESPONSE TO IA 2.03 AIN-1)

Note Regarding the Status of Supporting Technical Information

This document was prepared using the most current information available at the time of its development. This Technical Basis Document and its appendices providing Key Technical Issue Agreement responses that were prepared using preliminary or draft information reflect the status of the Yucca Mountain Project's scientific and design bases at the time of submittal. In some cases this involved the use of draft Analysis and Model Reports (AMRs) and other draft references whose contents may change with time. Information that evolves through subsequent revisions of the AMRs and other references will be reflected in the License Application (LA) as the approved analyses of record at the time of LA submittal. Consequently, the Project will not routinely update either this Technical Basis Document or its Key Technical Issue Agreement appendices to reflect changes in the supporting references prior to submittal of the LA.

APPENDIX A

LIKELY RANGE OF TEPHRA VOLUMES (RESPONSE TO IA 2.03 AIN-1)

This appendix provides a response to Key Technical Issue (KTI) agreement Igneous Activity (IA) 2.03 additional information needed (AIN-1). This KTI agreement relates to the likely range of tephra volumes from Yucca Mountain region volcanoes and is related to U.S. Nuclear Regulatory Commission (NRC) concerns with the Project's use of ASHPLUME V1.4LV-dll (ASHPLUME V1.4LV-dll, STN: 10022-1.4LV-dll-00).

A.1 KEY TECHNICAL ISSUE AGREEMENTS

A.1.1 IA 2.03 AIN-1

Agreement IA 2.03 was reached during the NRC/U.S. Department of Energy (DOE) Technical Exchange and Management Meeting on Igneous Activity held August 29 to 31, 2000, in Las Vegas, Nevada (Reamer and Williams 2000). This agreement was later revised during the NRC/DOE Technical Exchange and Management Meeting on Igneous Activity held June 21 to 22, 2001 (Reamer 2001).

The wording of the revised agreement is as follows:

IA 2.03

> Document how the tephra volumes from analog volcanoes represent the likely range of tephra volumes from Yucca Mountain Region (YMR) volcanoes. DOE agreed and will document the basis for determining the range of tephra volumes that is likely from possible future volcanoes in the YMR in the Eruptive Processes AMR (ANL-MGR-GS-000002). This will be available to the NRC in FY 2002.

For the total system performance assessment for the site recommendation, ASHPLUME V1.4LV-dll was used to model the direct release of radionuclides that could result from a volcanic eruption through the repository. ASHPLUME V1.4LV.dll used erupted volume as a proxy for eruptive power to calculate plume height. The range of erupted volume based on analogs in the Yucca Mountain Region was documented in *Characterize Framework for Igneous Activity at Yucca Mountain, Nevada* (CRWMS M&O 2000a, Table 4). The range of volumes used in the total system performance assessment for the site recommendation was documented in *Igneous Consequence Modeling for the TSPA-SR* (BSC 2001a).

Agreement IA 2.03 was addressed in a letter report (Ziegler 2002) by describing the range of erupted volumes that had been documented in *Characterize Framework for Igneous Activity at Yucca Mountain, Nevada* (CRWMS M&O 2000a, Table 4) and *Igneous Consequence Modeling for the TSPA-SR* (BSC 2001a). In addition, the letter report described the sensitivity of mean annual eruptive dose rate to variations in the volume of erupted material, as documented in *Total System Performance Assessment for the Site Recommendation* (CRWMS M&O 2000b, Section 5.2.9.5). Results of the analysis showed that the total mean annual igneous dose rate was insensitive to the range of values selected for erupted volume. The letter report also noted that

the DOE intended to document the range of tephra volumes and the basis for the range used to support total system performance assessment for the license application (TSPA-LA) calculations in an update of *Characterize Eruptive Processes at Yucca Mountain, Nevada* (BSC 2001b).

The ASHPLUME code (ASHPLUME V1.4LV-dll, STN: 10022-1.4LV-dll-00) utilized in the *Total System Performance Assessment for the Site Recommendation* (CRWMS-M&O 2000b) used erupted volume as a proxy for eruptive power in the computation of plume height estimates. Consistent with their concerns about this code, the NRC issued an additional information need (IA 2.03 AIN-1) (Schlueter 2002) based on the review of the DOE letter report (Ziegler 2002). Completion of the model report *Atmospheric Dispersal and Deposition of Tephra from a Potential Volcanic Eruption at Yucca Mountain, Nevad*a (BSC 2003a) provides the NRC with the information needed to close IA 2.03 AIN-1.

The wording of the additional information need is as follows:

IA 2.03 AIN-1

> DOE needs to: (a) Provide a technical basis for demonstrating how tephra volumes have been calculated based on eroded deposits in the YMR, (b) Provide a technical basis for the inclusion of analog information, and (c) Demonstrate how buried deposits, such as the flows from Little Cones, has been incorporated into the calculation of tephra volumes. In addition, the apparent lack of sensitivity of tephra volume in performance assessment calculations should be demonstrated under appropriate wind conditions. The staff notes that in the letter report "Range of Tephra Volumes," the DOE stated that "DOE intends to document the range of tephra volumes and the basis for the range used to support TSPA-License Application (LA) in an update of the AMR, Characterize Eruptive Processes at Yucca Mountain, Nevada [ANL-MGR-GS-000002]." Completion of this report should provide the NRC with the information needed to close this open item.

A.1.2 Related Key Technical Issue Agreements

None.

A.2 RELEVANCE TO REPOSITORY PERFORMANCE

Tephra (volcanic fallout) deposits represent a potential dispersal mechanism for small particles of radioactive material that could be produced if an eruption through the repository disrupted waste packages. Volcanism during the postclosure period is unlikely, but in the types of basaltic eruptions considered to be representative of possible future volcanoes in the Yucca Mountain region, small particles are produced during moderately energetic explosions at the vent ("Strombolian" eruptions) ranging up to more violent and sustained jets of particles and gas from the vent, which can support an eruption column up to several kilometers in height ("violent Strombolian"). Analyses based on the geologic evidence of regional volcanism over the past 5 m.y. indicate that a small volume, basaltic eruption exhibiting Strombolian to violent Strombolian activity is the form of possible volcanism in the Yucca Mountain region that is most credible within the postclosure performance period of 10,000 years.

The dispersal of ash and lapilli, mostly by winds active during eruption, serves as a first-order proxy for waste particle dispersal. The volume of tephra from a future Yucca Mountain region volcano is important to modeling of the downwind dispersal of ash + waste and in calculating the potential exposure to a reasonably maximally exposed individual at a specified distance from the eruption site. Tephra volume is difficult to determine because most basaltic volcanoes in the Yucca Mountain region are eroded remnants of former scoria cones and their associated tephra sheets and provide only a partial picture of eruption history. The exception is the Lathrop Wells volcano. The approximately 80,000-year-old Lathrop Wells Cone and tephra sheet are the youngest and best preserved in the Yucca Mountain region and currently serve as the principal basis for evaluating future eruption scenarios.

NRC concerns about the range of tephra volumes and the representativeness of that range are related to the use of ASHPLUME V1.4LV-dll for total system performance assessment for the Viability Assessment and the total system performance assessment for the site recommendation. That version of ASHPLUME used erupted volume as a proxy for eruptive power to calculate plume height. Hence, uncertainties in erupted volume could affect plume height estimates, ash-dispersal patterns, and the resulting dose to the reasonably maximally exposed individual.

A.3 RESPONSE

The use of ash volume as a proxy for eruptive power can be traced back to total system performance assessment for the Viability Assessment, when the use of ASHPLUME V1.4LV-dll prompted the NRC to require additional information on the calculation of ash volumes and the basis upon which information from analogs had been incorporated into estimates of the range of erupted volume. Analysis of the volcanic direct release scenario in the total system performance assessment for the site recommendation used a version of the ASHPLUME code (ASHPLUME V1.4LV-dll, STN: 10022-1.4LV-dll-00) that used erupted volume as a proxy for eruptive power to calculate eruption column height. However, for TSPA-LA, ASHPLUME V2.0 (ASHPLUME V2.0, STN: 10022-2.0-00) will be used. ASHPLUME V2.0 is consistent with the original formulation of the ASHPLUME code (Jarzemba et al. 1997) and uses eruptive power to calculate column height. Results of preliminary studies indicate that the use of ASHPLUME V2.0 will result in greater column heights than those that were produced by ASHPLUME V1.4LV-dll. The basis for use of ASHPLUME V2.0 and descriptions of model inputs and outputs have been documented in *Atmospheric Dispersal and Deposition of Tephra from a Potential Volcanic Eruption at Yucca Mountain, Nevada* (BSC 2003a).

The information need IA 2.03 AIN-1 incorporates three elements: (a) provide a technical basis for demonstrating how tephra volumes have been calculated based on eroded deposits in the Yucca Mountain region, (b) provide a technical basis for the inclusion of analog information, and (c) demonstrate how buried deposits, such as the flows from Little Cones, have been incorporated into the calculation of tephra volume.

Provide a Technical Basis for Demonstrating How Tephra Volumes Have Been Calculated Based on Eroded Deposits in the Yucca Mountain Region–Tephra volumes for eroded cones in Crater Flat have been estimated based on information from analog systems and by comparing the apparent levels of erosion at the analog sites with levels observed at the Crater Flat cones. Based on the comparisons, the original tephra volumes have been estimated at five times the

cone volume (Perry et al. 1998) and are listed in *Characterize Eruptive Processes at Yucca Mountain, Nevada* (BSC 2003b, Section 6.3.3.4.2).

Provide a Technical Basis for the Inclusion of Analog Information–The technical basis for inclusion of volume information from analog volcanoes is described in *Characterize Eruptive Processes at Yucca Mountain, Nevada* (BSC 2003b, Section 6.3.3.4.2). A set of analog volcanoes was established based on the results of searches of the technical literature. Then for erupted volume comparisons, the set was reviewed and reduced based on considerations of similarity of tectonic setting to that of the Lathrop Wells Cone (BSC 2003b, Section 6.3.3.4.2). The comparisons suggested that the smaller scoria cones are most appropriate to characterize disruptive volcanic events at Yucca Mountain. The technical basis for the selection of Lathrop Wells as an analog for a future eruption at the repository is described in *Characterize Eruptive Processes at Yucca Mountain, Nevada* (BSC 2003b, Sections 6.3.3 and 6.4). The choice of Lathrop Wells Cone as an analog for a potential disruptive volcano at the repository is based on geologic setting, its proximity to the repository, its composition, and its youth (approximately 80,000 years).

Demonstrate How Buried Deposits, Such as the Flows From Little Cones, Have Been Incorporated into the Calculation of Tephra Volume–Lava volume is not included in DOE estimates of tephra volume. Lava volume is estimated separately from tephra volume (e.g., BSC 2003b, Table 34) because lava is considered to be a separate eruptive phase and to reflect different eruption parameters than tephra deposits. A sensitivity study that examined the effect of including the lava from Little Cones in the tephra volume estimate showed that the volume increased from 0.23 km^3 to 0.26 km^3 (Brocoum 1997, Enclosure 1, page 2). The 13 percent increase was considered not significant.

While eruptive volume is still important for documenting the diminishing volumes of basaltic eruptions over the past 5 m.y. in the Yucca Mountain region, it becomes irrelevant to the calculation of column height because ASHPLUME V2.0 will be used for TSPA-LA. To support the use of ASHPLUME V2.0, eruptive power for several historical eruptions has been calculated from estimations of time-averaged mass fluxes, heat capacities, and temperatures, and documentation has been provided in the update of *Characterize Eruptive Processes at Yucca Mountain, Nevada* (BSC 2003b).

The information in this report is responsive to agreement IA 2.03 and the associated additional information needed (AIN-1). The report contains the information that the DOE considers necessary for NRC review for closure of this agreement.

A.4 BASIS FOR THE RESPONSE

During the development of information for the model report describing the ASHPLUME V1.4LV-dll code, the use of eruptive volume as a proxy for eruptive power was determined to be inappropriate. As a result, ASHPLUME V2.0 will be used for TSPA-LA analysis of the volcanism direct-release scenario. ASHPLUME V2.0 is consistent with ASHPLUME V1.0 code (Jarzemba et al. 1997) because it uses parameters for eruptive power to compute column height. Scoping calculations have shown that ASHPLUME V2.0 produces greater column heights than those obtained for the total system performance assessment for the site recommendation using

ASHPLUME V1.4LV-dll. Validation of the ASHPLUME model and its enumeration in ASHPLUME V2.0 have been documented in a new model report, *Atmospheric Dispersal and Deposition of Tephra from a Potential Volcanic Eruption at Yucca Mountain, Nevada* (BSC 2003a). The model report documents the qualification and validation of the ASHPLUME code from V1.4LV-dll to V2.0.

Documentation of the erupted volumes of the scoria cone, lava flows, and tephra estimated for the Lathrop Wells Cone has been included in the revision of *Characterize Eruptive Processes at Yucca Mountain, Nevada* (BSC 2003b). The documentation also discusses the eruptive history of the volcano, deduced from analysis of the tephra deposits. Based on review of well-documented historical and older volcanoes, the report discusses the relevance of the Lathrop Wells Cone eruptive history to a potential volcanic eruption at the repository. The volumes of older, eroded volcanoes in Crater Flat (Perry et al. 1998) have not been updated because of the extensive erosion of the scoria cones, and erosion or burial of their respective tephra sheets; effort was instead focused upon the Lathrop Wells Cone due to the better preservation of the volcanic products there.

Documentation of the total system performance assessment sensitivity to uncertainties in erupted volume was provided in the *Total System Performance Assessment for the Site Recommendation* (CRWMS M&O 2000b, Section 5.2.9.5). Because TSPA-LA analyses related to the direct-release (eruption) scenario will use ASHPLUME V2.0 rather than ASHPLUME V1.4LV-dll, it is no longer necessary to document the lack of sensitivity of repository performance to uncertainties in the range of tephra volumes used during simulations. It is also not necessary to justify the use of erupted volume as a proxy for eruptive power in the computation of column height. Hence, these analyses will not be included in the license application documentation.

The technical basis for this response is the decision to use ASHPLUME V2.0-dll, which uses eruptive power (rather than erupted ash volume) to calculate eruptive column height. Because the range of calculated column heights will now include the higher altitudes that the NRC considers are possible in violent Strombolian phases of a volcanic eruption, the issues raised in the information need should be satisfied with the documentation provided in the new model report *Atmospheric Dispersal and Deposition of Tephra from a Potential Volcanic Eruption at Yucca Mountain, Nevada* (BSC 2003a). The ash-dispersal pattern resulting from advection and winds acting on the ash column will reflect the higher elevations expected with this approach and provide a better technical basis for evaluation of the potential dose to the reasonably maximally exposed individual.

A.5 REFERENCES

A.5.1 Documents Cited

Brocoum, S.J. 1997. "Evaluation of Data Provided at U.S. Department of Energy (DOE) and U.S. Nuclear Regulatory Commission (NRC) Igneous Activity Technical Exchange, February 25-26, 1997." Letter from S.J. Brocoum (DOE/YMSCO) to J.T. Greeves (NRC), June 4, 1997, with enclosure. ACC: MOL.19970722.0276; MOL.19970722.0277; MOL.19970722.0278.

BSC (Bechtel SAIC Company) 2001a. *Igneous Consequence Modeling for the TSPA-SR.* ANL-WIS-MD-000017 REV 00 ICN 02. Las Vegas, Nevada: Bechtel SAIC Company. ACC: MOL.20011107.0005.

BSC 2001b. *Characterize Eruptive Processes at Yucca Mountain, Nevada.* ANL-MGR-GS-000002 REV 00 ICN 01. Las Vegas, Nevada: Bechtel SAIC Company. ACC: MOL.20020327.0498.

BSC 2003a. *Atmospheric Dispersal and Deposition of Tephra from a Potential Volcanic Eruption at Yucca Mountain, Nevada.* MDL-MGR-GS-000002 REV 00D. Las Vegas, Nevada: Bechtel SAIC Company. ACC: MOL.20030922.0197.

BSC 2003b. *Characterize Eruptive Processes at Yucca Mountain, Nevada.* ANL-MGR-GS-000002 REV 01C. Las Vegas, Nevada: Bechtel SAIC Company. ACC: MOL.20030711.0107.

CRWMS M&O (Civilian Radioactive Waste Management System Management and Operating Contractor) 2000a. *Characterize Framework for Igneous Activity at Yucca Mountain, Nevada.* ANL-MGR-GS-000001 REV 00 ICN 01. Las Vegas, Nevada: CRWMS M&O. ACC: MOL.20001221.0001.

CRWMS M&O 2000b. *Total System Performance Assessment for the Site Recommendation.* TDR-WIS-PA-000001 REV 00 ICN 01. Las Vegas, Nevada: CRWMS M&O. ACC: MOL.20001220.0045.

Jarzemba, M.S.; LaPlante, P.A.; and Poor, K.J. 1997. *ASHPLUME Version 1.0—A Code for Contaminated Ash Dispersal and Deposition, Technical Description and User's Guide.* CNWRA 97-004, Rev. 1. San Antonio, Texas: Center for Nuclear Waste Regulatory Analyses. ACC: MOL.20010727.0162.

Perry, F.V.; Crowe, B.M.; Valentine, G.A.; and Bowker, L.M., eds. 1998. *Volcanism Studies: Final Report for the Yucca Mountain Project.* LA-13478. Los Alamos, New Mexico: Los Alamos National Laboratory. TIC: 247225.

Reamer, C.W. 2001. "U.S. Nuclear Regulatory Commission/U.S. Department of Energy Technical Exchange and Management Meeting on Igneous Activity (June 21 - 22, 2001)." Letter from C.W. Reamer (NRC) to S. Brocoum (DOE/YMSCO), June 29, 2001, with enclosure. ACC: MOL.20010918.0001.

Reamer, C.W. and Williams, D.R. 2000. Summary Highlights of NRC/DOE Technical Exchange and Management Meeting on Igneous Activity. Meeting held August 29-31, 2000, Las Vegas, Nevada, with attachments. Washington, D.C.: U.S. Nuclear Regulatory Commission. ACC: MOL.20001101.0105 through MOL.20001101.0128.

Schlueter, J.R. 2002. "Igneous Activity Agreement 2.03." Letter from J.R. Schlueter (NRC) to J.D. Ziegler (DOE/YMSCO), November 12, 2002, with enclosure: "NRC Review of DOE Documents Pertaining to Igneous Activity Key Technical Issue Agreement Item 2.03." ACC: MOL.20030922.0139.

Ziegler, J.D. 2002. "Transmittal of Report Addressing Key Technical Issue (KTI) Agreement Item Igneous Activity (IA) 2.03." Letter from J.D. Ziegler (DOE/YMSCO) to J.R. Schlueter (NRC), July 30, 2002, with enclosure (*Range of Tephra Volumes*), OL&RC:TCG-1325. ACC: MOL.20021010.0006.

A.5.2 Software Codes

ASHPLUME V1.4LV-dll. STN: 10022-1.4LV-dll-00.

ASHPLUME V2.0. STN: 10022-2.0-00.

INTENTIONALLY LEFT BLANK

APPENDIX B

WIND SPEEDS FOR VARIOUS HEIGHTS OF ERUPTIVE COLUMNS (RESPONSE TO IA 2.09 AIN-1)

Note Regarding the Status of Supporting Technical Information

This document was prepared using the most current information available at the time of its development. This Technical Basis Document and its appendices providing Key Technical Issue Agreement responses that were prepared using preliminary or draft information reflect the status of the Yucca Mountain Project's scientific and design bases at the time of submittal. In some cases this involved the use of draft Analysis and Model Reports (AMRs) and other draft references whose contents may change with time. Information that evolves through subsequent revisions of the AMRs and other references will be reflected in the License Application as the approved analyses of record at the time of its submittal. Consequently, the DOE will not routinely update either this Technical Basis Document or its Key Technical Issue Agreement appendices to reflect changes in the supporting references prior to submittal of the License Application.

APPENDIX B

WIND SPEEDS FOR VARIOUS HEIGHTS OF ERUPTIVE COLUMNS (RESPONSE TO IA 2.09 AIN-1)

This appendix provides a response to Key Technical Issue (KTI) agreement Igneous Activity (IA) 2.09 additional information needed (AIN)-1. This KTI agreement relates to the wind speeds selected for analysis of the dispersal of various heights of volcanic eruptive columns.

B.1 KEY TECHNICAL ISSUE AGREEMENT

B.1.1 IA 2.09 AIN-1

Agreement IA 2.09 was reached during the U.S. Nuclear Regulatory Commission (NRC)/U.S. Department of Energy (DOE) Technical Exchange and Management Meeting on IA, held August 29 to 31, 2000, in Las Vegas, Nevada (Reamer and Williams 2000). This agreement was later revised during the NRC/DOE technical exchange and management meeting on igneous activity held June 21 to 22, 2001 (Reamer 2001).

For the total system performance assessment for site recommendation (TSPA-SR), the DOE used wind speed data described in *Igneous Consequence Modeling for the TSPA-SR* (BSC 2001a, Section 5.1.1). The NRC was concerned that modeling of a volcanic eruption through the repository had underestimated eruptive column heights. In general, wind speed increases with altitude, and underestimating column heights could lead to selection of wind speed data that is inappropriately biased toward lower wind speeds, which result in less dispersal of contaminated ash. Use of low wind speeds in the direct release scenario (volcanic eruption through Yucca Mountain) could underestimate the dose to the reasonably maximally exposed individual (RMEI). The result of this series of concerns was KTI agreement IA 2.09.

The wording of the revised agreement is as follows:

IA 2.09

> Use the appropriate wind speeds for the various heights of eruption columns being modeled. DOE agreed and will evaluate the wind speed data appropriate for the height of the eruptive columns being modeled. This will be documented in a calculation document. This will be available to the NRC in FY 2002.

The agreement was addressed in a previous report (Ziegler 2002). The report was based on results of analyses of the sensitivity of performance to uncertainties in wind direction and wind speed in the TSPA-SR (CRWMS M&O 2000, Sections 5.2.9.2 and 5.2.9.3).

NRC concerns with the use of wind speed data from altitudes that are less than those associated with columns from a violent Strombolian eruption resulted in the request for specific additional information on this subject (Schlueter 2003). This resulted in IA 2.09 AIN-1.

The wording of the additional information needed is as follows:

IA 2.09 AIN-1

> The DOE needs to demonstrate that the wind speed used in performance assessment is appropriate for the height of the eruption column. The DOE should demonstrate that neglecting the effects of higher velocity winds expressed during particle rise and lateral advection does not underestimate risk. If the DOE chooses to convolve wind-speed data into a single distribution for use in performance assessment, the DOE should document how appropriate weight was given in the distribution to upper altitude winds representative of lateral advection processes typically observed in volcanic eruption plumes. The DOE wind speed parameter distribution also should reflect the characteristics of the parameter distribution used for eruption column height, to avoid potential bias towards lower altitude wind speeds. As this information will be used in the TSPA-LA, the DOE needs to provide this information in a format that meets the requirements of the DOE quality assurance program.

B.1.2 Related Key Technical Issue Agreements

None.

B.2 RELEVANCE TO REPOSITORY PERFORMANCE

For the eruptive scenario at Yucca Mountain, an eruption column containing ash and some entrained waste particles may extend up to several kilometers above the growing volcanic cone. For the ASHPLUME model, the problem is one of modeling the distribution of ash/waste particles in the eruption column as it is subjected to a variable wind field and as the particles settle gravitationally onto the ground surface. For TSPA-SR, column height for each realization in ASHPLUME V1.4LV-dll (STN: 10022-1.4LV-dll-00) was calculated using erupted ash volume as a proxy for eruptive power (BSC 2001a, Section 6.1.2.1.8). In addition, column height was calibrated against observed eruptions whose column heights and erupted volumes had been measured (BSC 2001a). The NRC noted that column heights obtained in this manner did not extend to the higher column heights that the NRC considers reasonable (greater than 5 km). Lower column heights are subject to lower wind speeds (as measured with the Quiring 1968 data), resulting in less dispersal of ash/waste particles, thinner deposition of ash/waste with distance, and a potential underestimation of dose to the RMEI.

B.3 RESPONSE

Agreement IA 2.09 was addressed in a report (Ziegler 2002). The report was based on results of analyses of the sensitivity of performance to uncertainties in wind direction and wind speed in the TSPA-SR (CRWMS M&O 2000, Sections 5.2.9.2 and 5.2.9.3). The results of the sensitivity studies showed that when wind directions were sampled, rather than specifying a constant wind blowing toward the RMEI the dose was decreased by about a factor of 5 (CRWMS M&O 2000, Section 5.2.9.2). Results also showed that when higher wind speeds were used, the dose was increased by about a factor of 2 (CRWMS M&O 2000, Section 5.2.9.3). The report also described the results of a separate analysis that used wind speed data from the Desert Rock

airstrip (NOAA n.d.). These data extend to altitudes much higher than those expected for a future basaltic eruption cloud in the Yucca Mountain region (BSC 2001b; BSC 2001c, Section 3.3.1.2.1). The analysis that used the data assumed that the wind blew constantly toward the RMEI. Analysis results showed that the probability-weighted mean annual dose increased by a factor of approximately 2 compared to TSPA-SR values.

For TSPA for the license application (TSPA-LA), two fundamental changes in the DOE approach to modeling eruption columns have been made. These changes better reflect conditions that might be associated with an eruption that includes an ash column with a height in the range of 4-plus kilometers. First, eruption columns from a possible future volcano will be modeled using ASHPLUME V2.0 (STN: 1022-2.0-00), which uses eruptive power and event duration to calculate column height, mass flow rate, and total eruptive ash mass. This approach results in higher eruption columns (up to approximately 13 km) than those that result from calculations using ASHPLUME V.1.4LV dll, and captures uncertainty associated with the eruptive power parameter. Second, the modeling will use wind data (measured at the Desert Rock airstrip) (NOAA n.d.) that encompasses all eruptive column heights expected in a basaltic eruption at Yucca Mountain (BSC 2003, Table IV-7). The technical documentation for column height and wind speed and direction modeling is found in the new model report *Atmospheric Dispersal and Deposition of Tephra from a Potential Volcanic Eruption at Yucca Mountain, Nevada* (BSC 2003), which has been prepared under the requirements of the DOE quality assurance program. The use of these approaches in TSPA-LA and in supporting documentation will provide more realistic modeling of ash column height, ash/waste dispersal by winds, advection, and gravitational settling, and the ability to calculate dose at appropriate distances from a volcano.

The information in this report is responsive to agreement IA 2.09 and the associated additional information needed (AIN-1). The report contains the information that the DOE considers necessary for NRC review for closure of this agreement.

B.4 BASIS FOR THE RESPONSE

The DOE has developed additional information related to ASHPLUME parameters and has determined that ASHPLUME V. 2.0 is more appropriate for modeling atmospheric dispersal of contaminated ash than is ASHPLUME V.1.4LV-dll.

For the Site Recommendation, the dose effects of using higher wind speeds were examined. One analysis documented in TSPA-SR (CRWMS M&O 2000, Section 5.2.9.3) described the effects of using the 95th percentile wind speed rather than the mean wind speed. Another analysis documented in *FY01 Supplemental Science and Performance Analyses, Volume 2: Performance Analyses* (BSC 2001c, Section 3.3.1.2.1) described the effects of using wind speed data collected at higher altitudes above the Desert Rock airstrip. The higher altitudes were consistent with the upper range of column heights proposed as possible for eruptions at Yucca Mountain. The analysis, documented in *FY01 Supplemental Science and Performance Analyses, Volume 2: Performance Analyses* (BSC 2001c, Section 3.3.1.2.1), showed that use of the Desert Rock data increases probability-weighted mean annual doses by a factor of approximately 2 compared to the TSPA-SR values.

The TSPA-LA will use comprehensive wind data from the Desert Rock airstrip that are consistent with the range of potential eruptive column heights (1 km to 13 km). For each realization of the ASHPLUME model, the value selected for wind speed will be appropriate for the column height selected for that realization. The distribution characteristics for wind speeds are described in the new model report *Atmospheric Dispersal and Deposition of Tephra from a Potential Volcanic Eruption at Yucca Mountain, Nevada* (BSC 2003). The documentation will describe the basis for the selection of ASHPLUME v. 2.0, consideration of alternative models, and the parameters that are used as inputs to the code. The model report was developed using the appropriate provisions of the DOE quality assurance program. Hence, NRC concerns about appropriate use of wind speed data consistent with column heights have been addressed.

B.5 REFERENCES

B.5.1 Documents Cited

BSC (Bechtel SAIC Company) 2001a. *Igneous Consequence Modeling for the TSPA-SR.* ANL-WIS-MD-000017 REV 00 ICN 02. Las Vegas, Nevada: Bechtel SAIC Company. ACC: MOL.20011107.0005.

BSC 2001b. *FY01 Supplemental Science and Performance Analyses, Volume 1: Scientific Bases and Analyses.* TDR-MGR-MD-000007 REV 00. Las Vegas, Nevada: Bechtel SAIC Company. ACC: MOL.20010712.0062.

BSC 2001c. *FY01 Supplemental Science and Performance Analyses, Volume 2: Performance Analyses.* TDR-MGR-PA-000001 REV 00. Las Vegas, Nevada: Bechtel SAIC Company. ACC: MOL.20010724.0110.

BSC 2003. *Atmospheric Dispersal and Deposition of Tephra from a Potential Volcanic Eruption at Yucca Mountain, Nevada.* MDL-MGR-GS-000002 REV 00D. Las Vegas, Nevada: Bechtel SAIC Company. ACC: MOL.20030922.0197.

CRWMS M&O (Civilian Radioactive Waste Management System Management and Operating Contractor) 2000. *Total System Performance Assessment for the Site Recommendation.* TDR-WIS-PA-000001 REV 00 ICN 01. Las Vegas, Nevada: CRWMS M&O. ACC: MOL.20001220.0045.

NOAA (National Oceanic and Atmospheric Administration) n.d. *Upper Air Data: Desert Rock, Nevada, 1978-1995.* Reno, Nevada: National Oceanic and Atmospheric Administration, Western Regional Climate Center. TIC: 249335.

Quiring, R.F. 1968. *Climatological Data Nevada Test Site and Nuclear Rocket Development Station.* ESSA Research Laboratories Technical Memorandum - ARL 7. Las Vegas, Nevada: U.S. Department of Commerce, Environmental Science Services Administration Research Laboratories. ACC: NNA.19870406.0047.

Reamer, C.W. 2001. "U.S. Nuclear Regulatory Commission/U.S. Department of Energy Technical Exchange and Management Meeting on Igneous Activity (June 21 to 22, 2001)." Letter from C.W. Reamer (NRC) to S. Brocoum (DOE/YMSCO), June 29, 2001, with enclosure. ACC: MOL.20010918.0001.

Reamer, C.W. and Williams, D.R. 2000. Summary Highlights of NRC/DOE Technical Exchange and Management Meeting on Igneous Activity. Meeting held August 29 to 31, 2000, Las Vegas, Nevada, with attachments. Washington, D.C.: U.S. Nuclear Regulatory Commission. ACC: MOL.20001101.0105 through MOL.20001101.0128.

Schlueter, J.R. 2003. Igneous Activity Agreement 2.09, Additional Information Needed. Letter from J.R. Schlueter to J.D. Ziegler, February 13, 2003. Washington, D.C., U.S. Nuclear Regulatory Commission, 2 pages with 4-page enclosure: NRC Review of DOE Letter Pertaining to Igneous Activity Key Technical Issue Agreement Item 2.09. BSC Correspondence Log #0319036515. ACC: MOL.20030918.0112.

Ziegler, J.D. 2002. Transmittal of Report Addressing Igneous Activity (IA) Key Technical Issue (KTI) Agreement Items 2.02 and 2.09. Letter from J.D. Ziegler, DOE to J.R. Schlueter, NRC. Las Vegas, Nevada, U.S. Department of Energy, June 27, 2002, 4 pages with 2 enclosures: (1) Particle Size Sensitivity and (2) Wind Speed Data Appropriate for the Height of the Eruptive Columns Being Modeled. BSC Correspondence Log 0628023159. ACC: MOL.20020822.0149.

B.5.2 Software Codes

ASHPLUME V1.4lV-dll. STN: 10022-1.4lV-dll-00.

ASHPLUME V2.0. STN: 10022-2.0-00.

INTENTIONALLY LEFT BLANK

APPENDIX C

WASTE PACKAGE RESPONSE TO STRESSES FROM THERMAL AND MECHANICAL EFFECTS ASSOCIATED WITH EXPOSURE TO BASALTIC MAGMA (RESPONSE TO IA 2.19)

Note Regarding the Status of Supporting Technical Information

This document was prepared using the most current information available at the time of its development. This Technical Basis Document and its appendices providing Key Technical Issue Agreement responses that were prepared using preliminary or draft information reflect the status of the Yucca Mountain Project's scientific and design bases at the time of submittal. In some cases this involved the use of draft Analysis and Model Reports (AMRs) and other draft references whose contents may change with time. Information that evolves through subsequent revisions of the AMRs and other references will be reflected in the License Application as the approved analyses of record at the time of License Application submittal. Consequently, the Project will not routinely update either this Technical Basis Document or its Key Technical Issue Agreement appendices to reflect changes in the supporting references prior to submittal of the License Application.

APPENDIX C

WASTE PACKAGE RESPONSE TO STRESSES FROM THERMAL AND MECHANICAL EFFECTS ASSOCIATED WITH EXPOSURE TO BASALTIC MAGMA (RESPONSE TO IA 2.19)

This appendix provides a response to Key Technical Issue (KTI) agreement Igneous Activity (IA) 2.19. This KTI agreement relates to the evaluation of waste package response to stresses from thermal and mechanical effects associated with exposure to basaltic magma.

C.1 KEY TECHNICAL ISSUE AGREEMENT

C.1.1 IA 2.19

Agreement IA 2.19 was reached during the U.S. Nuclear Regulatory Commission (NRC)/U.S. Department of Energy (DOE) Technical Exchange and Management Meeting on Igneous Activity held September 5, 2001, in Las Vegas, Nevada (Reamer 2001).

The wording of the agreement is as follows:

IA 2.19

> DOE will evaluate waste package response to stresses from thermal and mechanical effects associated with exposure to basaltic magma, considering the results of evaluations attendant to IA Agreement 2.18. As currently planned, the evaluation, if implemented, would include (1) appropriate at-condition strength properties and magma flow paths, for duration of an igneous event; and (2) aging effects on materials strength properties when exposed to basaltic magmatic conditions for the duration of an igneous event, which will include the potential effects of subsequent seismically induced stresses on substantially intact waste packages. DOE will also evaluate the response of Zone 3 waste packages, or waste packages covered by backfill or rockfall, if exposed to magmatic gasses at conditions appropriate for an igneous event, considering the results of evaluation attendant to IA Agreement 2.18. If models take credit for engineered barriers providing delay in radionuclide release, DOE will evaluate barrier performance for the duration of the hypothetical igneous event. The results of this investigation would be documented in an update to the technical product *Waste Package Behavior in Magma* CAL-EBS-ME-000002, which would be available by the end of FY 2003, or other appropriate technical document.

For total system performance assessment for the site recommendation (TSPA-SR), modeling of magma-waste package interactions was based on varying levels of damage that defined three damage zones in the repository. Waste packages in the path of an ascending dike (in Zone 1) were assumed to be damaged to the extent that they would provide no further protection for waste forms. Damage to waste packages in intersected drifts, but not in the path of the dike (Zone 2; three waste packages on either side of the point of intersection), was assumed limited to end-cap failure by fissuring. The final damage zone, Zone 3, was defined as repository areas proximal to Zone 2 and containing waste packages exposed to magmatic products but not

directly exposed to magma. Models relied on assumptions about the durability of the waste package when exposed to magma or a magmatic environment.

Analyses by the NRC indicated that intersection of the repository by an ascending basaltic dike could result in magma flow through the repository that would be sufficient to involve the entire inventory of waste. Other analyses (e.g., Reamer 2001, p. 5) indicated that insufficient technical information existed to constrain the extent of damage to waste packages exposed to thermal and gas effects from an intrusion. To address concerns associated with the effects on the waste package from interactions with magma and magmatic products, DOE agreed to evaluate the waste package response to stresses from thermal and mechanical effects associated with exposure to basaltic magma (Reamer 2001, p. 4).

Waste package and waste form effects for TSPA for the license application (TSPA-LA) will be evaluated in the waste package and waste form impacts submodel of the TSPA-LA model. The effects analysis is based on the definition of two damage zones. Zone 1 includes all waste packages in drifts intersected by a dike, regardless of location relative to the ascent path of the dike. Zone 2 includes waste packages in drifts not directly intersected by a dike but potentially exposed to magmatic gases and thermal effects. Documentation of the submodel is provided in *Igneous Intrusion Impacts on Waste Packages and Waste Forms* (BSC 2003a).

C.1.2 Related Key Technical Issue Agreements

There are two KTI agreements related to IA 2.19. Agreements IA 2.18 and IA 2.20, respectively, are to provide inputs for the analysis of magma-waste package interactions and continue the analysis of effects on waste forms of exposure to magma and magmatic components. Agreement IA 2.18 is to ensure that information was obtained about the effects of repository structures on dike propagation and magma flow, exsolution of volatiles, and cooling and solidification of magma. These results could be incorporated in the analysis of effects on components of the engineered barrier system. Agreement IA 2.20 is to carry the analysis forward to the waste form and identify magma-waste form interaction effects that could increase the incorporation of waste in magma and potentially alter the waste chemistry in ways that could increase the mobility of the waste.

C.2 RELEVANCE TO REPOSITORY PERFORMANCE

For the igneous intrusion–groundwater release scenario, the risk of radiological dose is directly related to the number of waste packages contacted by the intrusion. The TSPA-LA approach to implementing the models for waste package and waste form response during igneous intrusion is based on identification of damage zones. Zone 1, which includes all emplacement drifts intruded by the basalt dike and Zone 2, which includes all other emplacement drifts in the repository that are not in Zone 1. *Igneous Intrusion Impacts on Waste Packages and Waste Forms* (BSC 2003a) documents the following model assessments:

- **Zone 1**–Impacts of magma intrusion on the drip shields, waste packages, and cladding directly contacted by magma and the fate of waste forms. Impacts of intrusion on Zone 1 in-drift thermal and geochemical environments, including seepage hydrochemistry.

- **Zone 2**–Impacts of conducted magmatic heat and diffused magmatic gases on the drip shields, waste packages, cladding, and waste packages adjacent to the intruded drifts

Section 5.3 describes a variety of literature studies regarding the potential for enhanced corrosion in magmatic environments in *Igneous Intrusion Impacts on Waste Packages and Waste Forms* (BSC 2003a). These studies indicate that high temperatures and corrosive geochemical environments, which could accompany dike intrusion, can measurably increase the corrosion rates of steel and other metal alloys.

Although none of the analyses indicate that the metallic engineered barriers would be destroyed or fail instantaneously, it appears that the effects would be rapid compared to the 10,000-year regulatory period for the repository. Therefore, because of the uncertainty associated with analyzing the effects of enhanced corrosion rates, performance assessment analyses for Yucca Mountain conservatively assume that any engineered materials contacted by magmas (e.g., drip shields, waste packages and cladding) during an intrusion will no longer provide any waste isolation function.

For waste packages in drifts that are not directly intersected by a dike (Zone 2), model results indicate that significant thermal and volatile effects do not extend to the Zone 2 drifts. The model results indicate that thermal and chemical conditions that would adversely affect Zone 2 waste packages do not develop. Hence, for TSPA-LA, waste package damage is limited by the analysis to the number of waste packages in Zone 1.

C.3 RESPONSE

The current model approach to be implemented for TSPA-LA features significant conservatisms in terms of volcanic process parameters associated with magma flow in drifts and effects on engineered barrier system components, specifically waste packages in drifts that are intersected by a dike. Alternative approaches are being reviewed, and the alternatives would feature less conservatism than the approach being implemented for TSPA-LA.

Igneous Intrusion Impacts on Waste Packages and Waste Forms (BSC 2003a) defines two damage zones for the igneous activity scenarios. Zone 1 is characterized by intersection of the drifts by an ascending basaltic dike accompanied by waste package damage to the extent that waste packages in Zone 1 provide no further protection for the waste (BSC 2003a, Section 6.3). Zone 2 includes drifts not directly intersected by a dike but are adjacent to the intersected drifts (Zone 1) that waste packages and other engineered barrier system components could be exposed to heat and gases migrating from Zone 1. The TSPA-LA assumes that waste packages in Zone 1 offer no protection from disruption by and interaction with the magma, and that all waste material is available for chemical interaction, between the fuel and metal/alloys of damaged waste canisters/assemblies and claddings, and transport. Simulations of heat conduction indicate that the maximum temperature rise in a drift that is not intersected by a dike, but that is adjacent to an intersected drift (Zone 2), is less than 10°C (simulated maximum magma temperatures in an intersected drift was 1,150°C) (BSC 2003a, Section 6.5.2.1.1). The rock provides an effective barrier to the thermal effects associated with the intrusion. The spatial and temporal heat conduction simulation results indicate that waste packages in Zone 2 emplacement drifts would

not be affected by the heat conducting from the magma intruded into Zone 1 emplacement drifts (BSC 2003a, Section 6.5.2.1.1).

Results of magma gas-flow simulations show that the gas-flow velocity decreases to near zero in about a year. The gas front in the wall rock (e.g., pillars) stops at about 3.6 m from the drift wall, and the gas front in the assumed backfill used in main drifts and turnouts of the repository stops at about 1.4 m into the backfill. Simulations of gas transport caused by diffusion, however, show that concentrations of gases entering Zone 2 drifts would be low (a maximum of 100 moles of gas) and would decrease after about 2 years. The concentrations of corrosive gas species in the volatile components could be expected to be significantly less than the concentration of water in the volatiles. These results indicate that waste packages in Zone 2 emplacement drifts would not be affected by the volatile gases exsolving from the basalt magma intruded into Zone 1 drifts (BSC 2003a, Section 6.5.2.2.3).

The information in this report is responsive to agreement IA 2.19 made between the DOE and NRC. The report contains the information that DOE considers necessary for NRC review for closure of this agreement.

C.4 BASIS FOR THE RESPONSE

Discussions of each element of the agreements are provided in the following paragraphs.

Evaluate Appropriate At-Condition Strength Properties and Magma Flow Paths, for Duration of an Igneous Event–Limited analyses of the effects on waste packages to thermal and mechanical effects associated with exposure to basaltic magma have been completed. The results (BSC 2003a, Section 6.5.1.1) indicate that stresses associated with temperatures that are typical of basaltic magma could exceed the tensile strength of the waste package materials. In addition, as the magma cools, the volatile components of the magma could increase corrosion rates. The net result is that the analyses support the conservative assumption that waste packages in drifts intersected by an ascending basaltic dike (Zone 1) provide no further protection for the waste. This assumption makes it unnecessary to evaluate the at-condition strength properties for waste packages in intersected drifts. Evaluation of the effects of prolonged exposure to conditions in intersected drifts is also unnecessary.

Results of numerical simulations of heat flow from Zone 1 emplacement drifts show that temperatures in the tuff wall rock decrease rapidly with distance from the intersected drift(s) (BSC 2003a, Section 6.5.2.1.1). The simulation results also show that the maximum temperature rise is less than 10°C in a drift that is not intersected by a dike (Zone 2) but is adjacent to an intersected drift, and the rock provides an effective barrier to the thermal effects associated with the intrusion. The spatial and temporal heat conduction simulation results indicate that waste packages in Zone 2 emplacement drifts would not be affected by the heat conducting from the magma intruded into Zone 1 emplacement drifts (BSC 2003a, Section 6.5.2.1.1).

Results of gas-flow simulations show that the gas-flow velocity decreases to near zero in about a year. The gas front in the wall rock stops at about 3.6 m from the drift wall, and the gas front in the backfill stops at about 1.4 m into the backfill. Simulations of diffusive gas flow show that concentrations of gas entering Zone 2 drifts would be low and would decrease after about

2 years, and the concentrations of corrosive gases in the volatile components is expected to be significantly less than the concentration of water in the volatiles. These results indicate that waste packages in Zone 2 emplacement drifts would not be affected by the volatile gases exsolving from the basalt magma intruded into Zone 1 drifts (BSC 2003a, Section 6.5.2.2.3).

Numerical simulations reported in *Dike/Drift Interactions* (BSC 2003b, Section 6.5.1.6) differ in detail but reach a similar conclusion that waste packages in unintruded drifts will not be exposed to adverse temperatures or gases. Results show a smaller increase in temperature and indicate that volcanic gases may be absorbed by host rock or diluted by air and backfill in connecting drifts before reaching Zone 2 drifts.

Aging Effects on Materials Strength Properties when Exposed to Basaltic Magmatic Conditions for the Duration of an Igneous Event–Aging effects on strength properties of materials exposed to basaltic magmatic conditions have been evaluated in terms of effects of enhanced corrosion from heat and gases associated with a basaltic intrusion. As noted above, the analyses support the conservative TSPA assumption that waste packages in drifts intersected by an ascending basaltic dike (Zone 1) provide no further protection for the waste. On the other hand, heat or volatiles migrating from Zone 1 drifts are expected to produce no adverse effects on waste packages in Zone 2. Given that waste packages in Zone 1 are assumed compromised, and because simulation results indicate that Zone 2 packages will not be adversely affected by heat or volatiles, there is no need to evaluate aging effects beyond those considered in the nominal case.

Potential Effects of Subsequent Seismically Induced Stresses on Substantially Intact Waste Packages–It is not necessary to evaluate the effects of postintrusion seismically induced stresses on substantially intact waste packages. Waste packages in Zone 1 are already assumed to be compromised and to provide no further protection for the waste; so additional analyses to evaluate seismic effects for Zone 1 waste packages is unnecessary. Seismic effects on waste packages are being included in TSPA-LA, but Zone 2 waste packages are not expected to be damaged by effects from heat and/or gases migrating from Zone 1 drifts (BSC 2003a, Sections 6.5.2.1.1 and 6.5.2.2.3). The seismic analyses being included in TSPA-LA should be, therefore, adequate to address the concern. Hence, there is no need to further evaluate postintrusion seismic effects on Zone 2 packages.

For additional information, see the discussion on the following page under the heading, "Evaluate Barrier Performance for the Duration of the Hypothetical Igneous Event, If Credit Is Taken for Barrier Performance during an Igneous Event."

Response of Zone 3 Waste Packages–For TSPA-LA, no damage Zone 3 has been defined. TSPA-LA Zone 1 now includes all waste packages that were in Zones 1 and 2 for the TSPA-SR, and TSPA-LA Zone 2 includes waste packages that were in Zone 3 for TSPA-SR.

Waste Packages Covered by Backfill or Rockfall, If Exposed to Magmatic Gases at Conditions Appropriate for an Igneous Event–For waste packages in Zone 1, the analyses support the conservative TSPA assumption that waste packages in Zone 1 provide no further protection for the waste. No credit is taken for presence of backfill (natural or man-made) in Zone 1 drifts. This assumption makes it unnecessary to evaluate the effects on waste packages

covered by backfill or rockfall and exposed to magma or magmatic conditions in intersected drifts. For waste packages in Zone 2, results of gas flow simulations show that the gas flow velocity decreases to near zero in about a year. The gas front in the wall rock stops at about 3.6 m from the drift wall, and the gas front in the backfill stops at about 1.4 m into the backfill. Simulations of diffusive gas flow show that concentrations of gas entering Zone 2 drifts would be low and would decrease after about 2 years, and the concentrations of corrosive gases in the volatile components is expected to be significantly less than the concentration of water in the volatiles. These results indicate that waste packages in Zone 2 emplacement drifts would not be affected by the volatile gases exsolving from the basalt magma intruded into Zone 1 drifts (BSC 2003a, Section 6.5.2.2.3).

Evaluate Barrier Performance for the Duration of the Hypothetical Igneous Event, If Credit Is Taken for Barrier Performance during an Igneous Event–No credit for barrier performance will be claimed for emplacement drifts intersected by a dike (Zone 1). All waste packages and drip shields in Zone 1 drifts will be assumed to be damaged to the extent that they provide no further protection for the waste. Simulation results show that the maximum temperature in drifts not intersected by a dike (Zone 2) would be less than 1°C (BSC 2003b, Section 8.1.3). The rock provides an effective barrier to the thermal effects associated with the intrusion.

Results of gas flow simulations show that the gas flow velocity decreases to near zero in about a year. The gas front in the wall rock stops at about 3.6 m from the drift wall, and the gas front in the backfill stops at about 1.4 m into the backfill. Simulations of diffusive gas flow show that concentrations of gas entering Zone 2 drifts would be low and would decrease after about 2 years, and the concentrations of corrosive gases in the volatile components is expected to be significantly less than the concentration of water in the volatiles. These results indicate that waste packages in Zone 2 emplacement drifts would not be affected by the volatile gases exsolving from the basalt magma intruded into Zone 1 drifts (BSC 2003a, Section 6.5.2.2.3).

Thermal and gas flow calculations show that the effects of intrusions on Zone 2 would be negligible (BSC 2003a, Section 6.7.2). Simulation results documented in the model report, *Dike/Drift Interactions* (BSC 2003b, Section 8.1.3) indicate that the maximum temperature increase in Zone 2 drifts would be less than 1°C. This result is consistent with results documented in model report *Igneous Intrusion Impacts on Waste Packages and Waste Forms* (BSC 2003a, Section 6.5.2.1.1) that describe the maximum temperature in Zone 2 drifts as less than 10°C.

If the rise of the surface temperature of the affected waste packages in Zone 2 is less than 10°C, and there is no impact on the chemistry of water in contact with the affected waste packages (BSC 2003a, Sections 6.5.2.1.1 and 5.5.2.2.3), the potential impact on localized corrosion susceptibility of the affected waste packages from the temperature rise is within the uncertainty of the localized corrosion initiation model for the waste packages for nondisrupted conditions (BSC 2003c, Sections 6.4.4.6). For nondisrupted conditions, the uncertainty range in the threshold temperature for initiation of waste package localized corrosion for a given water chemistry is approximately 30°C, which is much larger than the potential temperature rises at the surface of the affected waste packages in Zone 2 (BSC 2003c, Sections 6.4.4.6). Hence, even the

maximum increase in temperature of 10°C is not expected to initiate localized corrosion of waste packages in Zone 2 drifts.

For igneous effects on the invert, the current plan for revision of *Igneous Intrusion Impacts on the Waste Packages and Waste Forms* (BSC 2003a) includes describing disruption of the invert at the point of intersection of a dike with a drift. Outside the zone of intersection/disruption, the model report will show that the invert remains intact because magma is expected to enter a drift at the point of intersection and simply flow over the invert and down the drift. The update of the model report is expected to be ready in the second quarter of fiscal year 2004. For TSPA-LA, the invert nominal-case model will be used because, based on scoping analyses, the area of the invert disrupted by a basaltic dike compared to the total invert area is small. Because of the small disruption, explicit consideration of the disrupted invert for TSPA-LA analysis of the igneous intrusion groundwater-release scenario will likely have a negligible performance effect.

C.5 REFERENCES

BSC (Bechtel SAIC Company) 2003a. *Igneous Intrusion Impacts on Waste Packages and Waste Forms*. MDL-EBS-GS-000002 REV 00. Las Vegas, Nevada: Bechtel SAIC Company. ACC: DOC.20030819.0003.

BSC 2003b. *Dike/Drift Interactions.* MDL-MGR-GS-000005 REV 00E. Las Vegas, Nevada: Bechtel SAIC Company. ACC: MOL.20030916.0259.

BSC 2003c. *General Corrosion and Localized Corrosion of Waste Package Outer Barrier.* ANL-EBS-MD-000003 REV 01. Las Vegas, Nevada: Bechtel SAIC Company. ACC: DOC.20030916.0010.

Reamer, C.W. 2001. "U.S. Nuclear Regulatory Commission/U.S. Department of Energy Technical Exchange and Management Meeting on Igneous Activity (September 5, 2001)." Letter from C.W. Reamer (NRC) to S. Brocoum (DOE/YMSCO), September 12, 2001, with enclosure. ACC: MOL.20011114.0008.

INTENTIONALLY LEFT BLANK

APPENDIX D

POTENTIAL FOR BASALTIC MAGMA TO INCORPORATE HIGH-LEVEL RADIOACTIVE WASTE (RESPONSE TO IA 2.20)

Note Regarding the Status of Supporting Technical Information

This document was prepared using the most current information available at the time of its development. This Technical Basis Document and its appendices providing Key Technical Issue Agreement responses that were prepared using preliminary or draft information reflect the status of the Yucca Mountain Project's scientific and design bases at the time of submittal. In some cases this involved the use of draft Analysis and Model Reports (AMRs) and other draft references whose contents may change with time. Information that evolves through subsequent revisions of the AMRs and other references will be reflected in the License Application as the approved analyses of record at the time of License Application submittal. Consequently, the Project will not routinely update either this Technical Basis Document or its Key Technical Issue Agreement appendices to reflect changes in the supporting references prior to submittal of the License Application.

APPENDIX D

POTENTIAL FOR BASALTIC MAGMA TO INCORPORATE HIGH-LEVEL RADIOACTIVE WASTE (RESPONSE TO IA 2.20)

This appendix provides a response to Key Technical Issue (KTI) agreement igneous activity (IA) 2.20. This KTI agreement relates to the evaluation of the potential for basaltic magma to incorporate high-level radioactive waste.

D.1 KEY TECHNICAL ISSUE AGREEMENT

D.1.1 IA 2.20

Agreement IA 2.20 was reached during the U.S. Nuclear Regulatory Commission (NRC)/U.S. Department of Energy (DOE) Technical Exchange and Management Meeting on Igneous Activity held September 5, 2001, in Las Vegas, Nevada (Reamer 2001).

The wording of the agreement is as follows:

IA 2.20

> DOE will evaluate how ascent and flow of basaltic magma through repository structures could result in processes that might incorporate HLW, considering the results of evaluations attendant to IA Agreements 2.18 and 2.19. As currently planned, the evaluation, if implemented, would include the potential for HLW incorporation along reasonable potential flow paths that could develop during an igneous event. The evaluation would also include the physical and chemical response of HLW and cladding after heating and potential disruption of waste package and contents, for waste packages remaining in drifts. The evaluation would examine effects that may result in increased solubility potential relative to undisturbed HLW forms. The results of this investigation would be documented in a new AMR to document the waste form response to magmatic conditions, which is expected to be available by the end of FY 2003. DOE will describe the method of HLW incorporation used in DOE models, including consideration of particle aggregation and the effect on waste transport. If models take credit for engineered barriers providing delay in radionuclide release, DOE will evaluate barrier performance for the duration of the hypothetical igneous event. This will be documented in an update to the igneous consequences AMR, ANL-WIS-MD-000017, which is expected to be available in FY 2003, or another appropriate technical document.

Analyses by the NRC indicated that intersection of the repository by an ascending basaltic dike could result in magma flow through parts of the repository and migration of heat and volatiles into drifts not directly intersected by a dike. The NRC questioned the extent of potential effects on the waste forms either from direct exposure to magma or from exposure to heat and exsolved volatiles. NRC was concerned that changes in the waste form and/or cladding, specifically changes that would increase solubility of the waste form, could occur, and that the changes could

enhance the mobility of the radionuclides. To address concerns associated with the effects on the waste form from interactions with magma and magmatic products, DOE agreed to describe the method of high-level radioactive waste incorporation that will be used for total system performance assessment for the license application (TSPA-LA) (Reamer 2001).

Waste package and waste form effects for TSPA-LA will be evaluated in the waste package and waste form impacts submodel of the TSPA-LA model. Documentation of the submodel is provided in *Igneous Intrusion Impacts on Waste Packages and Waste Forms* (BSC 2003).

D.1.2 Related Key Technical Issue Agreements

There are two KTI agreements related to IA 2.20. Agreements IA 2.18 and IA 2.19, respectively, are intended to provide inputs for the analysis of magma-drift and magma–waste package interactions to support the analysis of effects on waste forms of exposure to magma and magmatic components. Agreement IA 2.18 is intended to ensure that information was obtained about the effects of repository structures on dike propagation and magma flow, exsolution of volatiles, and cooling and solidification of magma so that the results could be incorporated in the analysis of effects on components of the engineered barrier system. Agreement IA 2.19 is intended to evaluate the damage to waste packages that could result from direct contact with magma (Zone 1) or from exposure to heat and gases that had exsolved from the magma and migrated to adjacent drifts (Zone 2). The analyses of effects of repository structures on dike propagation and magma flow and cooling and of magma and magmatic products on waste package durability determine the potential nature of the effects of igneous intrusion on the waste.

D.2 RELEVANCE TO REPOSITORY PERFORMANCE

Changes in the thermal, mechanical, or chemical properties of waste forms from exposure to magmatic conditions could increase the mobility of radionuclides and increase the resulting dose to the reasonably maximally exposed individual for the igneous intrusion–groundwater release case. However, studies indicate that, even if changes in the waste could occur, the mobility of radionuclides is not increased (BSC 2003, Section 6.5.1.2).

The TSPA-LA approach to implementing the models for waste package and waste form response during igneous intrusion is based on identification of damage zones. Zone 1 includes all emplacement drifts intersected by the basalt dike. Zone 2 includes all emplacement drifts in the repository that are not in Zone 1. *Igneous Intrusion Impacts on Waste Packages and Waste Forms* (BSC 2003) documents the following model assessments:

- **Zone 1**–Impacts of magma intrusion on the drip shields, waste packages and cladding directly contacted by magma, and the fate of waste forms. Impacts of intrusion on Zone 1 in-drift thermal and geochemical environments, including seepage hydrochemistry.

- **Zone 2**–Impacts of conducted magmatic heat and diffused magmatic gases on the drip shields, waste packages, cladding and waste packages adjacent to the intruded drifts.

The current version of the model indicates that spent nuclear fuel in drifts intersected by a dike (Zone 1) would be assimilated by the magma, but the minerals or phases that are likely to result

would be refractory. However, the specific properties of these refractory minerals or phases are unknown. While spent nuclear fuel in Zone 1 is expected be less soluble after exposure to magma and magmatic components, the spent nuclear fuel in Zone 1 is considered, in the base-case model, to be chemically unaffected by the magma intrusion. Because waste packages in Zone 2 will not be damaged by the effects of heat and volatiles migrating from Zone 1, spent nuclear fuel in Zone 2 will be treated the same as in the nominal scenario.

D.3 RESPONSE

The base-case conceptual model for damage to waste packages and waste forms from igneous intrusion include the following components (BSC 2003, Section 6.3):

- Intrusion of basaltic magma (as a dike) into Zone 1 emplacement drifts (without surface eruption)
- Damage to drip shields, waste packages and cladding in Zone 1 results in these components providing no further protection for the waste forms
- Embedding or assimilation of waste materials into magma intruded into Zone 1 drifts
- Postintrusion perturbations to the in-drift environmental conditions from cooling magma include heat loss by conduction, degassing, and fracturing of the intrusion. Following intrusion, the magma would cool, and the deleterious volatile gases that would exsolve from the magma would diffuse through the host rock (with the assumption of no chemical interactions to reduce their concentrations) and reach waste packages in drifts not intersected by the dike (Zone 2).
- Reversion to normal in-drift environmental conditions would follow cooling of the magma. Seepage water entering the Zone 1 drifts would react and equilibrate with the cooled and fractured basalt. Seepage entering the Zone 2 drifts would not be equilibrated with basalt.

The base-case model does not consider the effects of reactions between the waste forms and the basalt and any reactive exudates. For waste in Zone 1, TSPA-LA assumes that radionuclides in the waste forms will be available for dissolution immediately after water flow resumes in the cooled intrusion. The water is assumed to equilibrate with the basalt. Waste packages in Zone 2 are unaffected by migrating heat and volatiles and must be breached before the waste is available for dissolution. When the waste reacts with water, the same solubility model is used for the radionuclides in Zone 1 and Zone 2.

Section 5.3 describes a variety of literature studies regarding the potential for enhanced corrosion in magmatic environments, which are summarized in *Igneous Intrusion Impacts on Waste Packages and Waste Forms* (BSC 2003). These studies indicate that high temperatures and corrosive geochemical environments, which could accompany dike intrusion, could measurably increase the corrosion rates of steel and other metal alloys.

Although none of the analyses indicate that the metallic engineered barriers would be destroyed or fail instantaneously, it appears that the effects would be rapid compared to the 10,000-year regulatory period. Therefore, because of the uncertainty associated with analyzing the effects of enhanced corrosion rates, performance assessment analyses for Yucca Mountain conservatively assume that any engineered materials contacted by magmas (e.g., drip shields, waste packages, cladding) during an intrusion will no longer provide any waste isolation function. However, the natural and engineered features and processes that act as barriers to limit dose will be documented in the license application.

The alternative conceptual model described in *Igneous Intrusion Impacts on Waste Packages and Waste Forms* (BSC 2003, Section 6.4.1) indicates that spent nuclear fuel would be less mobile after exposure to magma and magmatic components. Oxidation of UO_2 fuel would produce minerals that are less soluble than the phase that controls concentration of uranium in fluids transiting the repository. The results also indicate that some portion of the waste in drifts intersected by an ascending basaltic dike (Zone 1) would be assimilated in the magma. However, the alternative conceptual model indicates that mineral phases, which could result from interaction between magma and dispersed waste and waste package materials, would be refractory and of limited solubility (BSC 2003, Section 6.4.1). In addition, radionuclides in the waste could be incorporated into crystallizing silicate mineral phases, such as soddyite $[(UO_2)_2(SiO_4) \cdot 2\ H_2O]$, which would limit the concentration of uranium in fluids transiting the repository under the nominal scenario (BSC 2003, Section 6.4.1). Finally, the spent nuclear fuel is a hard ceramic material with a high melting point temperature of 2,800°C. The commercial spent nuclear fuel and defense spent nuclear fuel wastes exposed to hot magma are not, therefore, expected to melt under temperatures no higher than the maximum magma temperature of 1,169°C (BSC 2003, Section 6.4.1). The net effect is that the mobility of uranium would be reduced by exposure to magma or magmatic conditions.

Conversely, in drifts that are not intersected by a dike (Zone 2), the effects of heat conduction and volatile migration are not expected to perturb the environment in these drifts to the extent that waste package integrity is compromised (BSC 2003, Section 6.7.2). If Zone 2 waste packages are not compromised, waste will not be exposed to the in-drift environmental conditions, and there are no mechanisms available to incorporate waste from Zone 2 drifts. Hence, for TSPA-LA, waste packages and waste in Zone 2 emplacement drifts will be treated the same as in the nominal scenario (BSC 2003, Section 6.7.2).

The information in this report is responsive to agreement IA 2.20 made between the DOE and NRC. The report contains the information that DOE considers necessary for NRC review for closure of this agreement.

D.4 BASIS FOR THE RESPONSE

The technical basis for the response addresses the elements of the agreement, which are identified below in bold type.

Evaluate Methods of High-Level Radioactive Waste Incorporation Used in U.S. Department of Energy Models, Including Consideration of Particle Aggregation and the Effect on Waste Transport–The DOE base-case conceptual model for magma-waste form

interactions is described in *Igneous Intrusion Impacts on Waste Packages and Waste Forms* (BSC 2003, Section 6.3). Damage to drip shields, waste packages, and cladding in Zone 1 results in these components providing no further protection for the waste forms followed by embedding or assimilation of waste materials into magma intruded into Zone 1 drifts. The model includes assimilation of material into magma intruded into Zone 1 drifts, but specific mechanisms have not been identified. Spent nuclear fuel is a hard ceramic material with a high melting point temperature of 2,800°C. The commercial spent nuclear fuel and defense spent nuclear fuel wastes exposed to hot magma are not, therefore, expected to melt under temperatures no higher than the maximum magma temperature of 1,169°C (BSC 2003, Section 6.4.1). The base-case model (BSC 2003) indicates that when the waste canisters/assemblies and fuel claddings are damaged, the fuel pellets/rods would be assimilated into the cooling basalt magma. Under this scenario, the alternative conceptual model (BSC 2003, Section 6.4.1) indicates that two types of processes are expected: (a) interaction between waste forms and the magma and (b) interaction between the waste forms and the metal of waste canisters/assemblies and cladding in the presence of hot magma.

In the first case, (a), the model shows that oxidation of some UO_2 fuel would occur in the presence of water-rich volatiles exuding from cooling basalt magma. In addition, some radionuclides in the waste would be incorporated into crystallizing silicate mineral phases, such as soddyite [$(UO_2)_2(SiO_4) \cdot 2\ H_2O$]. The solubility of soddyite is less than that of schoepite, which is considered to be the phase that controls concentration of uranium in fluids transiting the repository under the nominal scenario. This solubility information indicates that actinide concentrations in water passing through basalt-filled drifts would be decreased relative to actinide concentrations in the nominal case (BSC 2003, Sections 6.5.1.6 and 6.5.2.6).

In the second case, (b), the model shows chemical interactions would occur between some of the fuel and metals/alloys of damaged waste canisters/assemblies and claddings in the presence of the cooling magma that would result in the formation of new phases. The alternative model indicates that these new phases would be refractory and of limited solubility (BSC 2003, Section 6.4.1). Hence, particle aggregation effects that could increase local radionuclide concentrations in magma would likely be offset by the refractory nature and reduced solubilities of the mineral phases.

In drifts that are not intersected by a dike (Zone 2), base-case model results (BSC 2003, Sections 6.5.2.1.1 and 6.5.2.2.3) show that the effects of heat conduction and volatile migration would not perturb the environment in Zone 2 drifts to the extent that waste package integrity is compromised (BSC 2003, Section 6.7.2). If Zone 2 waste packages are not compromised, waste will not be exposed to the in-drift environmental conditions, and there are no mechanisms available to incorporate waste from Zone 2 drifts. Hence, for TSPA-LA, waste packages and waste in Zone 2 emplacement drifts will be treated the same as in the nominal scenario.

Evaluate the Potential for High-Level Radioactive Waste Incorporation along Reasonable Potential Flow Paths That Could Develop during an Igneous Event–Study results indicate that some portion of the waste in drifts intersected by an ascending basaltic dike (Zone 1) would be assimilated in the magma. Properties of assimilated waste phases and reactions of assimilated waste with magma are not known at this time. Therefore, the base-case model does not address

details of reactions between assimilated waste and magma. Rather, depictions of selected reactions are used (BSC 2003, Section 6.4.1) until test results are available.

Evaluate the Physical and Chemical Response of High-Level Radioactive Waste and Cladding after Heating and Potential Disruption of Waste Package and Contents–Study results indicate that some portion of the waste in drifts intersected by an ascending basaltic dike (Zone 1) would be assimilated in the magma. However, the alternative conceptual model indicates that mineral phases, which could result from interaction between magma and dispersed waste and waste package materials, would be refractory and of limited solubility (BSC 2003, Section 6.4.1). In addition, radionuclides in the waste could be incorporated into crystallizing silicate mineral phases, such as soddyite [$(UO_2)_2(SiO_4) \bullet 2\ H_2O$]. Development of soddyite would limit actinide concentrations in fluids exiting the repository.

The spent nuclear fuel is a hard ceramic material with a high melting point temperature of 2,800°C; therefore, the commercial spent nuclear fuel and defense spent nuclear fuel wastes exposed to hot magma are not expected to melt under temperatures no higher than the maximum magma temperature of 1,169°C (BSC 2003, Section 6.4.1). The alternative conceptual model presented in *Igneous Intrusion Impacts on Waste Packages and Waste Forms* (BSC 2003, Section 6.4.4) indicates that fracturing, fragmentation, and granulation of the waste form could result from thermal shock effects associated with exposure of waste to basaltic magma. For TSPA-LA, the waste is assumed to be exposed, and the radionuclides are assumed to be available for transport, but no explicit assumptions about conditions applicable to the waste form are made.

For glass waste exposed to magma, even though magma temperatures could exceed the melting temperature of glass waste forms, the glass waste forms are likely to be minimally affected by exposure to magmatic thermal conditions because the thermal environment during an intrusion would be similar to that in which the glass was produced (BSC 2003, Section 6.4.4; Lichtner et al. 1999).

Evaluate Effects That May Result in Increased Solubility Potential Relative to Undisturbed High-Level Radioactive Waste Forms–Alternative conceptual models indicate that mineral phases, which could result from interaction between magma and dispersed waste and waste package materials, would be refractory and of limited solubility (BSC 2003, Section 6.4.1). In addition, radionuclides from the waste could be incorporated into crystallizing silicate mineral phases, such as soddyite [$(UO_2)_2\ (SiO_4) \bullet 2\ H_2O$]. Development of soddyite would limit actinide concentrations in fluids exiting the repository. Since the properties of these phases have not been determined, the TSPA-LA base case will apply the assumption that the waste is refractory and chemically unaffected by exposure to the intruding magma (BSC 2003, Sections 6.5.1.3 and 6.7.1).

D.5 REFERENCES

BSC (Bechtel SAIC Company) 2003. *Igneous Intrusion Impacts on Waste Packages and Waste Forms.* MDL-EBS-GS-000002 REV 00. Las Vegas, Nevada: Bechtel SAIC Company. ACC: DOC.20030819.0003.

Lichtner, P.C.; Keating, G.; and Carey, B. 1999. *A Natural Analogue for Thermal-Hydrological-Chemical Coupled Processes at the Proposed Nuclear Waste Repository at Yucca Mountain, Nevada.* LA-13610-MS. Los Alamos, New Mexico: Los Alamos National Laboratory. TIC: 246032.

Reamer, C.W. 2001. "U.S. Nuclear Regulatory Commission/U.S. Department of Energy Technical Exchange and Management Meeting on Igneous Activity (September 5, 2001)." Letter from C.W. Reamer (NRC) to S. Brocoum (DOE/YMSCO), September 12, 2001, with enclosure. ACC: MOL.20011114.0008.

INTENTIONALLY LEFT BLANK